Hepatic steatosis and cancer development: Role of insulin-like growth factor 2 mRNA binding protein p62 / IGF2BP2-2 / IMP2-2 and fatty acid elongase ELOVL6

Kumulative Dissertation
zur Erlangung des Grades
des Doktors der Naturwissenschaften
der Naturwissenschaftlich-Technischen Fakultät III
Chemie, Pharmazie, Bio- und Werkstoffwissenschaften
der Universität des Saarlandes

von
Stephan Laggai

Saarbrücken
Juli 2014

Tag des Kolloquiums:	29.09.2014
Dekan:	Prof. Dr. Volkhard Helms
1. Berichterstatter:	Prof. Dr. Alexandra K. Kiemer
2. Berichterstatter:	Prof. Dr. Rolf Müller
Vorsitz:	Prof. Dr. Christian Ducho
Akad. Mitarbeiter:	Dr. Stefan Boettcher

Contents

Abbreviations

1D	one dimensional
3D	three dimensional
AASLD	American Association for the Study of the Liver
AB	antibody
ACC/ACACA	acetyl-CoA carboxylase alpha
AFLD	alcoholic fatty liver disease
AFP	alpha-fetoprotein
AIRE	autoimmune regulator
ALT	alanine aminotransferase
ANA	antinuclear antibody
ASMA	anti-smooth muscle antibody
Asp	aspartic acid
AST	aspartate aminotransferase
BCLCS	Barcelona Clinic Liver Cancer System
bp	base pair
BSA	bovine serum albumin
C16	fatty acid with 16 carbon atoms
C18	fatty acid with 18 carbon atoms
cDNA	complementary desoxyribonucleic acid
CE	ceramide
CH	cholesterol
CHREBP/MLXIPL	carbohydrate response element binding protein/MLX interacting protein-like
co	untreated control
Co-A	coenzyme A
co-v	control vector
CPT1A	carnitine palmitoyltransferase 1A
CT	computerized tomography
DCF	2’,7’-dichlorofluorescein

°C	degree Celsius
DEN	diethylnitrosamine
DG	diglyceride
DLK1	delta-like 1 homologue (*Drosophila*)
DNA	desoxyribunucleic acid
DTT	dithiothreitol
EDTA	ethylenediaminetetraacetic acid
EGTA	ethylene glycol tetraacetic acid
ELISA	enzyme linked immunosorbent assay
ELOVL6	ELOVL fatty acid elongase 6
ER	endoplasmatic reticulum
ERK	extracellular-signal regulated kinase
ESI	electrospray ionization
FABP	liver type fatty acid binding protein
FAME	fatty acid methyl ester
FASN	fatty acid synthase
FCS	fetal calf serum
FFA	free fatty acid
FFPE	formalin-fixed, paraffin-embedded (tissue)
Fig.	figure
g	gramm
GC-MS	gas chromatography-mass spectrometry
GIR	glucose infusion rate
Glu	glutamic acid
Gtl2/MEG3	gene-trap locus 2 (mouse), maternally expressed gene 3 (human)
GTP	guanosine triphosphate
h	hour
HBV	hepatitis B virus
HCC	hepatocellular carcinoma
HCV	hepatitis C virus

HE	hematoxylin / eosin
Hepatol.	Hepatology
HEPES	4-(2-hydroxyethyl)-1-piperazineethanesulfonic acid
HGP	hepatic glucose production
HIPS	Helmholtz Institute for Pharmaceutical Research Saarland
HZI	Helmholtz Centre for Infection Research
IGF2	insulin-like growth factor 2
IGF2BP2-2	*IGF2* mRNA binding protein 2 splice variant 2
Ig-G	immunoglobulin-G
IMP	*IGF2* mRNA binding protein
ISTD	internal standard
J.	journal
k-	kilo [10^3]
l	litre
LC-MS	liquid chromatography-mass spectrometry
LDLR	low density lipoprotein receptor
log	logarithm
LPC	lysophosphatidylcholine
L-PK, PKLR	pyruvate kinase, liver and red blood cell
LXR-α/NR1H3	liver-X-receptor alpha/nuclear receptor subfamily 1, group H, member 3
-m	metre
m-	milli [10^{-3}]
M	molar [mol/litre]
ma	mature
MAPK	mitogen activated protein kinase
MCD	methionine choline deficient
MCS	methionine choline supplemented
m/z	mass per charge
min	minutes

µ-	micro [10^{-6}]
microRNA	micro ribonucleic acid
miR	micro ribonucleic acid
MRI	magnetic resonance imaging
mRNA	messenger ribonucleic acid
NAFLD	non-alcoholic fatty liver disease
n-	nano [10^{-9}]
NASH	non-alcoholic steatohepatitis
NCCN	National Comprehensive Cancer Network
n.d.	not detected
p-	pico [10^{-12}]
p62 tg	*p62* trangenic mice
Pa	Pascal
PBS	phosphate buffered saline
PBST	phosphate buffered saline + Tween® 20
PC	phosphatidylcholine
PE	phosphatidylethanolamine
%	percent
pERK	phosphorylated ERK
PI-3K	phosphoinositid-3-kinase
PKB	protein kinase B
PPARA	peroxisome proliferator activated receptor alpha
pre	precursor
PS	phosphatidylserine
RAC1	ras-related C3 botulinum toxin substrate 1
RBB	Rockland blocking buffer
Real-time RT-PCR	real-time reverse transcription polymerase chain reaction
Ref. Nr.	reference number
Res.	research
RNA	ribonucleic acid

ROS	reactive oxygen species
RP	reverse phase
RT	room temperature
s	seconds
SCD	stearoyl CoA desaturase
SDS-PAGE	sodium dodecyl sulfate polyacrylamide gel electrophoresis
SE	standard error of mean
SEM	standard error of mean
si co	random siRNA
si p62	p62 siRNA
siRNA	small interfering ribonucleic acid
SREBF1/SREBP1	sterol regulatory element binding transcription factor 1
Suppl.	supplemental
tERK	total ERK
tg	transgenic
TG	triglyceride
TLC	thin layer chromatography
TO	glucose turnover
TRE-CMV_{min}	transrepressive responsive element cytomegaly virus
UHPLC	ultra high-performance liquid chromatography
US	ultra sonography
V	volt
Val	valine
vs.	versus
v/v	volume per volume
VLDL	very low density lipoprotein
Wo	wortmannin
wt	wild-typ
x *g*	fold gravitational force

Abstract

The *IGF2* mRNA binding protein p62/IGF2B2-2/IMP2-2 induces hepatic steatosis in mice, is overexpressed in HCC patients, and is associated with the overexpression of the tumorigenic growth factor IGF2.

The underlying mechanisms involved in p62's actions during liver disease are poorly characterized. Therefore, the aim of this study was to elucidate the mechanisms of p62 on lipogenesis and tumorigenesis.

Since alterations in hepatic lipid and fatty acid composition are linked to liver pathogenesis, we analyzed liver lipids and fatty acid composition of *p62* transgenic animals, and found that almost all lipid classes and fatty acids were elevated. The elevated ratio of C18 to C16 fatty acids was attributed to IGF2-mediated SREBF1 and ELOVL6 activation, and was shown to be responsible for steatosis development. Elevated levels of inflammatory markers provided evidence that *p62* transgenic animals are susceptible to hepatic inflammation.

Therefore, these results demonstrate an important role of p62 and ELOVL6 in the development of steatosis and steatohepatitis.

Interestingly, though, ELOVL6 was downregulated in HCC patients and in a murine HCC model. It therefore seems unlikely that ELOVL6 has a pathophysiological role in HCC.

Still, p62 amplifies HCC development, which might be attributed to DLK1/RAC1 mediated activation of the antiapoptotic ERK pathway.

Taken together, our data underline the role of p62 in liver pathologies and provide evidence for p62 as a prognostic marker or therapeutic target.

Zusammenfassung

Das *IGF2* mRNA bindende Protein p62/IGF2B2-2/IMP2-2 induziert im Mausmodell eine Fettleber, ist in HCC Patienten überexprimiert und erhöht die Expression des Wachstumsfaktors IGF2.

Die Mechanismen, über die p62 die Leber-Pathophysiologie beeinflusst, sind weitgehend unbekannt. Ziel dieser Studie war die Aufklärung der Rolle von p62 in der Lipogenese und Karzinogenese.

Veränderte Lipidstoffwechsel können zur Leberpathogenese beitragen. Die Untersuchung der hepatischen Fette aus den Lebern von *p62* transgenen Tieren ergab, dass fast alle Lipide und Fettsäuren akkumuliert vorlagen. Das erhöhte Verhältnis von C18 zu C16 Fettsäuren, das durch eine IGF2-vermittelte Aktivierung von SREBF1 und ELOVL6 verursacht wurde, führte zur Steatose in diesen Tieren. Erhöhte inflammatorische Marker in den transgenen Lebern ließen auf eine verstärkte Entzündungsneigung schließen.

Somit scheinen p62 und ELOVL6 eine wichtige Rolle in der Steatose- und der Steatohepatitis-Entstehung zu spielen.

Interessanterweise war ELOVL6 aber im humanen und murinen HCC herrunterreguliert. Somit ist eine pathophysiologische Rolle von ELOVL6 in der Hepatokarzinogenese unwahrscheinlich.

Die kanzerogenen Effekte von p62 scheinen durch die verstärkte Expression von DLK1 und RAC1, die den antiapoptotischen ERK Signalweg aktivieren, vermittelt zu werden.

Unsere Daten belegen eine wichtige Rolle von p62 in der Leberpathophysiologie. Somit könnte p62 als Biomarker oder therapeutisches Target von Interesse sein.

1. Introduction

1.1 Steatosis, the first step in liver disease

Steatosis is described as the accumulation of lipids within hepatocytes (Day and Yeaman, 1994) and is associated with an imbalance between synthesis, transport, oxidation, and storage of hepatic lipids (Koteish and Diehl, 2001). Since also normal livers sometimes exhibit lipid containing hepatocytes, steatosis has been defined either as more than 5% of cells containing fat droplets (Underwood Ground, 1984) or total lipids exceeding 5% of liver weight (Hoyumpa et al., 1975).

Alcoholic fatty liver disease (AFLD) develops in about 90% of individuals who drink more than 60 g alcohol per day (Crabb, 1999).

Non-alcoholic fatty liver disease (NAFLD) is a form of fatty liver, which is not due to chronic alcohol abuse and covers a histological spectrum from simple steatosis to non-alcoholic steatohepatitis (NASH) with or without fibrosis and cirrhosis (Neuschwander-Tetri and Caldwell, 2003).

In a large cohort (2,766 subjects, 45-74 years) of Finnish subjects the prevalence of NAFLD (21%) was three times higher than the prevalence of AFLD (7%) (Kotronen et al., 2010). Similar observations could also be found in China, where the prevalence of NAFLD (15%) was also threefold compared to AFLD (4.5%) (Fan, 2013).

Several risk factors for the development of steatosis have been well described in the literature. A wide variety of therapeutic drugs (Fromenty and Pessayre, 1995), obesity (Anderson et al., 2014), the metabolic syndrome (Kotronen and Yki-Jarvinen, 2008) / type 2 diabetes (Targher et al., 2007), and chronic hepatitis B/C virus infections (Nascimento et al., 2012) are implicated in steatosis development. For example, patients infected with hepatitis C virus develop chronic hepatitis in 60-80% of cases, and up to 20% may progress to cirrhosis (Lonardo et al., 2004).

The prevalence of NAFLD increased in the recent years, which has reached up to 14-34% of the general population in Europe, Asia, and America (Armstrong et al., 2012)(Fig. 1.1) and is mainly attributed to obesity, overweight, and metabolic disorders in industrialized countries (Kopec and Burns, 2011). Since NAFLD is increasing globally and is set to become the predominant cause of chronic liver disease, NAFLD is regarded as a global epidemic (Loomba and Sanyal, 2013; Ray, 2013).

The progression from simple steatosis to NASH is best described by the ‘two-hit hypothesis’. This hypothesis suggests that a simple steatosis stands for the first hit, which mediates further hits by inflammation, lipid peroxidation, and the generation of reactive oxygen species (ROS). Persistent oxidative stress leads to the release of pro-inflammatory and pro-fibrogenic

cytokines and can thereby induce a progressive hepatic fibrosis or even hepatic cirrhosis (Day and James, 1998).

Hepatocyte injury (hepatocyte ballooning and cell death), inflammatory infiltrates, and / or collagen deposition (fibrosis) are characteristics that allow differentiation between simple steatosis and NASH (Cohen et al., 2011). ROS and products from lipid peroxidation induce fibrosis by activating collagen producing hepatic stellate cells (Browning and Horton, 2004).

Between 10-20% of patients with simple steatosis develop NASH (Schattenberg and Schuppan, 2011)(Fig. 1.1).

Whereas simple steatosis mostly follows a benign course, NASH might progress to cirrhosis in 20-25% of cases over a ten year period (Ratziu et al., 2010)(Fig. 1.1). Liver cirrhosis is characterized by the hyper-accumulation of connective tissue components in the liver and can finally lead to hepatic failure or hepatocellular carcinoma (HCC) (Matsuda et al., 1997). Accordingly, cirrhosis is responsible for around 170,000 deaths / year in Europe (Blachier et al., 2013), and could be found in 80% - 90% of the autopsies from HCC patients, therefore only 10% to 20% of the HCC cases develop in patients without cirrhosis (Fattovich et al., 2004). Approximately 7% of cirrhosis patients develop HCC (Shimada et al., 2002)(Fig. 1.1). Recently, Ganapathy-Kanniappan et al. presented an interesting hypothesis that early stage cirrhotic hepatocytes, which are characterized by metabolic alterations (e.g. increased glycolysis), could be linked to the origin of hepatic tumorigenesis and that endstage cirrhotic hepatocytes further undergo metabolic adaptation leading to HCC (Ganapathy-Kanniappan et al., 2014; Nagrath and Soto-Gutierrez, 2014; Nishikawa et al., 2014).

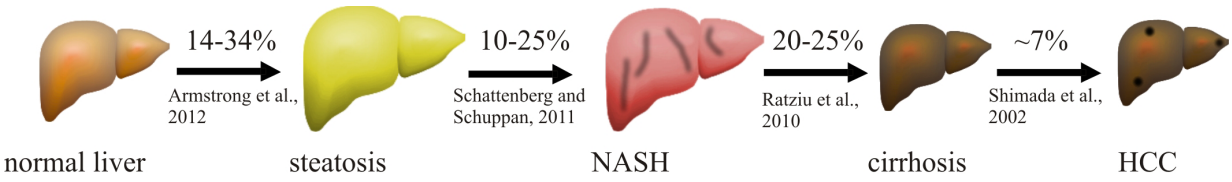

Fig. 1.1: Prevalence of liver disease progression.

The incidence for liver cancer has strongly increased in Germany in the last decades (Fig. 1.2) and HCC is responsible for approximately 47,000 deaths per year in Europe (Blachier et al., 2013). Late diagnosis and inadequate treatment options lead to a high lethality of HCC.

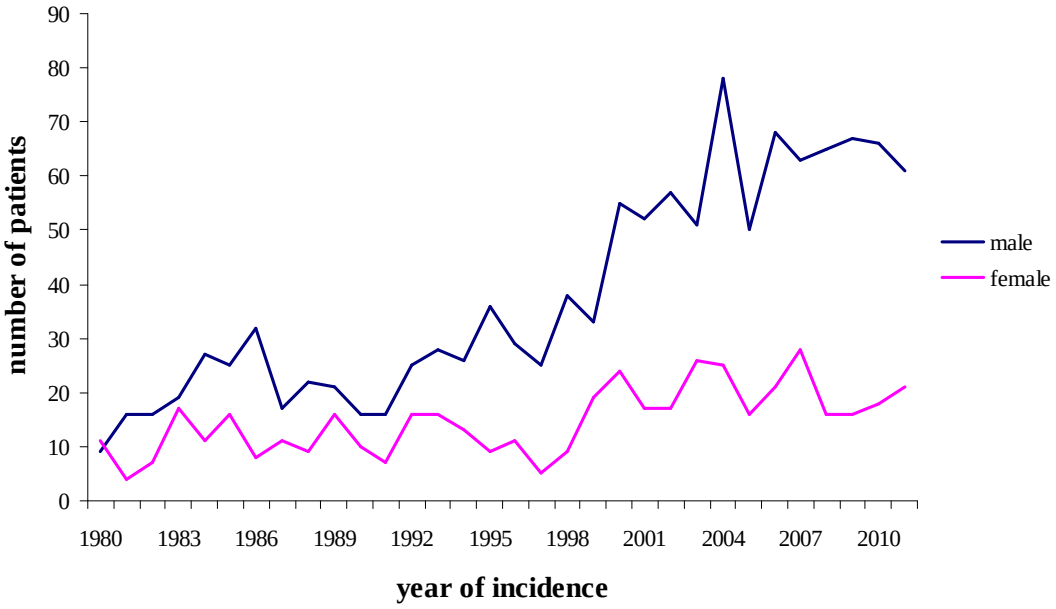

Fig. 1.2: Incidence of liver cancer in Germany (Krebsregister Saarland, 2011)

1.2 Pathways involved in the development of NAFLD

As mentioned above, steatosis occurs when lipid homeostasis linking lipid synthesis, degradation, and transport is disturbed. Interestingly, not only the amount of lipids, but also the lipid composition of the liver is important in NAFLD (Puri et al., 2007; Puri et al., 2009).

Lipid synthesis is regulated by a complex network of transcription factors, which are either transcriptionally or post-translationally regulated and dependent on metabolic factors like insulin, glucose, sterol, and fatty acid levels (Foufelle and Ferre, 2002). The most important ones are liver X receptors (LXRs), sterol regulatory element binding transcription factors (SREBFs), and carbohydrate element-binding transcription factors (MLXIPLs). They lead to a transcriptional activation of a large set of lipogenic genes, including acetyl-CoA carboxylase (ACC), fatty acid synthase (FASN), ELOVL fatty acid elongase 6 (ELOVL6), and stearoyl CoA desaturase (SCD) as the most important ones (Postic and Girard, 2008).

Lipid degradation is mainly attributed to peroxisomal oxidation induced by activation of the peroxisome proliferator activated receptor alpha (PPARA)(Reddy, 2001) or mitochondrial oxidation regulated by carnitine palmitoyl transferase 1 (CPT1)(Reddy and Rao, 2006).

Lipid trafficking involves export and import of lipids within hepatocytes. Processed lipids are bound to apolipoprotein B 100 in hepatocytes and are secreted as very low density lipoprotein (VLDL). Lipids can be incorporated into hepatocytes either by a transmembranous flip-flop

mechanism, e.g. fatty acid translocase, or by mechanisms involving the liver type fatty acid binding proteins (FABPs)(Anderson and Borlak, 2008).

Interference with these pathways is linked to pathophysiological processes. In this context hepatitis (B/C) virus has been described to induce steatosis and to strongly alter hepatic lipid content by activation of lipogenic pathways (Kim et al., 2007; Miyoshi et al., 2011; Moriya et al., 2001).

Due to their pathophysiological role directed interference with these pathways may also exhibit potential targets for treatment options. For example, inhibition of the lipogenic genes SREBF1 and MLXIPL in the liver of obese ob/ob mice (Dentin et al., 2006; Yahagi et al., 2002) and PPARA agonists, like Fenofibrate as inducer of peroxisomal fatty acid oxidation, can ameliorate steatosis (Harano et al., 2006; Kostapanos et al., 2013). Therefore, investigation of these pathways may provide excellent targets for the treatment of liver pathogenesis.

1.3 Diagnosis and therapy of NAFLD: state of the art

NAFLD and specifically NASH are underdiagnosed since most of the affected patients are symptom free and screenings are inadequate and not performed routinely. Non-invasive diagnostics are not sensitive enough in diagnosis or staging of the severity of disease. Therefore, liver biopsy is the gold standard for diagnosis but also exhibits some severe risks like bleeding, bile leak, and even death (Kopec and Burns, 2011). Laboratory serum analytic is limited to some key markers described in the following section.

Aspartate aminotransferase (AST) and alanine aminotransferase (ALT) are typically mildly elevated, ranging from 1-4 times of the normal levels. The ALT/AST ratio is rarely higher than 2. The ALT/AST ratio is often the first evidence for liver pathogenesis and therefore the gold standard in laboratory serum analysis (Fracanzani et al., 2008; Kopec and Burns, 2011; Wong et al., 2009). Pathophysiological markers like bilirubin and albumin tend to be normal and alkaline phosphatase and gamma-glutamyltransferse are only sometimes slightly elevated (Kopec and Burns, 2011). Other biomarkers like antinuclear antibody (ANA) and anti-smooth muscle antibody (ASMA) have been found to be elevated in only 21% of NAFLD patients (Cotler et al., 2004; Vuppalanchi et al., 2012).

In addition to serological screening, ultra sonography (US) is commonly employed as the initial visual tool for diagnosis and has been demonstrated to have a sensitivity of 73% for detection of steatosis (Bohte et al., 2011). Newer methods for non-invasive imaging are

computerized tomography (CT) and magnetic resonance imaging (MRI), which show only a slightly improved sensitivity (Bohte et al., 2011).

According to the American Association for the Study of the Liver guidelines (AASLD, from the year 2012), it is mandatory to treat the liver disease as well as the associated co-morbidities resulting from the metabolic syndrome (Chalasani et al., 2012). The most important recommendation is lifestyle intervention, e.g. weight loss, which can also be achieved by bariatric surgery. A reduction of at least 3-5% of body weight in obese patients is necessary to improve steatosis, and up to 10% is necessary to improve signs of inflammation.

Medical treatment is rare and only recommended in biopsy-proven NASH patients with some limitations. Pioglitazone, a thiazolidindione and peroxisome proliferator receptor gamma agonist, and Vitamin E (alpha-tocopherol, 800 IU/day) are recommended to treat NASH. Statins, as 3-hydroxy-3methyl-glutaryl-CoA reductase inhibitors, can be used to reduce dyslipidemia in NAFLD and NASH (Chalasani et al., 2012). Other tested substances, i.e. Metformin and ursodeoxycholic acid, have no significant effect on liver histology and are not recommended for the treatment of liver disease (Chalasani et al., 2012).

1.4 Diagnosis and therapy of HCC: state of the art

Early detection of HCC is important, because the appearance of symptoms reflects an advanced stage where cure is no longer an option. The optimal profile for a curable stage is when the HCC is smaller than 2 cm (de Lope et al., 2012). Detection of HCC by imaging technologies are identical with those used in NAFLD/NASH diagnostics like US, CT, and MRI, and exhibit similar problems in sensitivity (Bruix and Sherman, 2011).

Serum markers for HCC are only of limited usefulness. Even alpha-fetoprotein (AFP) as the most widely used serological marker for HCC, has a limited sensitivity, is not specific for HCC, and is only detected in patients with advanced tumors (Sherman, 2010).

HCC is commonly classified by the Barcelona Clinic Liver Cancer (BCLC) system. The BCLC system links the size and number of tumors and liver function to the best treatment option (de Lope et al., 2012). Curative treatments are advised only in the very early and early stage and are realised by ablation, resection, and in some suitable cases by liver transplantation. In the intermediate and advanced stage palliative treatments like chemoembolization and treatment with the potent multi-kinase inhibitor sorafenib are recommended (Forner et al., 2012).

To summarize, there is a lack of diagnostic markers and treatment options in NAFLD and HCC. Since NASH and cirrhosis are discussed as risk factors for the development of HCC, it is mandatory to develop improved methods to detect and cure hepatic diseases at the earliest time before progression to a more severe type.

1.5 The insulin-like growth factor 2 (*IGF2*) mRNA binding protein p62: a potential biomarker and therapeutic target?

p62 is a splice variant of the *IGF2* mRNA binding protein (IMP) 2 IMP2/IGF2BP2 lacking exon 10 (Christiansen et al., 2009). The IMP family consists of three different members, which share two RNA recognition motives and four hnRNP K homology domains as characteristic features, which can bind the 5'-untranslated region of the *IGF2*-leader 3 mRNA (Nielsen et al., 1999) and are implicated in RNA processing (Christiansen et al., 2009; Nielsen et al., 2001). p62 was first identified in 1999 as an auto-antigen found in an HCC patient (Zhang et al., 1999). In following studies p62 was shown to be overexpressed in HCC (33-67.5%) (Kessler et al., 2013; Lu et al., 2001; Qian et al., 2005). Furthermore, p62 was suggested as a fetal protein that is re-expressed in cirrhotic tissues and showed strongest expression in HCC (Lu et al., 2001). A recent study showed that analysis of a combination of 14 tumor-associated antigens, among which p62 was one of the important ones, allowed a sensitivity of HCC detection up to 69.7%. Furthermore, this array identified 43.8% HCC cases, where AFP serum levels were unremarkable (Dai et al., 2014). Liu et al. postulated p62/IMP2 also as potential biomarker in diagnosis of ovarian cancer, since 29.4% of ovarian cancer patients revealed higher autoantibody response compared to normal individuals (Liu et al., 2014).

Nevertheless, p62 expression levels in NAFLD progression from simple steatosis to HCC are rarely characterized. Within the last years the group among Prof. Kiemer was able to unravel important pathophysiological features of p62. p62 overexpression induced a steatotic phenotype and strongly elevated levels of the tumorigenic growth factor *Igf2* in a murine model (Tybl et al., 2011), exerts antiapoptotic effects, correlates with *IGF2* in human HCC samples, and is increased in HCC patients with poor outcome (Kessler et al., 2013). Furthermore, p62 was suggested as a pathophysiological regulator in all stages of NAFLD, as found in a *p62* transgenic mouse model fed a methionine-choline deficient diet (Simon et al., 2014a; Simon et al., 2014b).

Therefore, the pathophysiological role and overexpression in cancer and recurrence of p62 expression in cirrhosis strongly suggest p62 as a marker and promoter of liver disease progression.

2. Publications I-IV:

The results of this work are described in the following **publications I-IV**.

Each publication should be considered as a ‘stand alone version’ with own figures and references.

2.1 Rapid chromatographic method to decipher distinct alterations in lipid classes in NAFLD/NASH.

I

p62 transgenic animals spontaneously develop a fatty liver phenotype (Tybl et al., 2011). Since both the amount of lipids but also the lipid composition plays an important role in liver disease (Puri et al., 2007; Puri et al., 2009), the following work was performed to establish an easy to use method for qualitative and quantitative analyis of lipid classes and to determine alterations in the lipid composition of *p62* transgenic livers.

Rapid chromatographic method to decipher distinct alterations in lipid classes in NAFLD/NASH

Stephan Laggai, Yvette Simon, Theo Ranssweiler, Alexandra K. Kiemer and Sonja M. Kessler.

This research was originally published in the World Journal of Hepatology. Laggai, S., Simon, Y., Ranssweiler, T., Kiemer, A.K. and Kessler, S.M. Rapid chromatographic method to decipher distinct alterations in lipid classes in NAFLD/NASH. *World J Hepatol.* 2013; 5(10):558 -567. doi:10.4254/wjh.v5.i10.558. Copyright ©2013, Baishideng Publishing Group Co., Limited. All rights reserved.

The full text article can also be found at:
http://www.wjgnet.com/1948-5182/pdf/v5/i10/558.pdf

2.1.1 Author Contribution

World J Hepatol 5(10):558-567. Published online 2013 October 27. doi:10.4254/wjh.v5.i10.558.

Rapid chromatographic method to decipher distinct alterations in lipid classes in NAFLD/NASH

Laggai S, Simon Y, Ranssweiler T, Kiemer AK and Kessler SM.

Laggai S:
Performed sample preparation.
Performed TLC analysis.
Designed experiments, performed data acquisition and statistical analysis.
Wrote and revised the manuscript.

Simon Y:
Performed MCS/MCD animal procedures.
Performed histochemistry in MCS/MCD animals.
Participated in manuscript revision.

Ranssweiler T:
Assisted in sample preparation.
Assisted in TLC analysis.
Participated in manuscript revision.

Kiemer AK:
Initiated and directed the study.
Wrote and revised the manuscript.

Kessler SM:
Performed *p62* transgenic animal procedures.
Performed histochemistry in *p62* transgenic animals.
Initiated and directed the study.
Wrote and revised the manuscript.

2.1.2 Title page

Rapid chromatographic method to decipher distinct alterations in lipid classes in NAFLD/NASH

Rapid chromatography for lipids in NAFLD/NASH

Stephan Laggai, Yvette Simon, Theo Ranssweiler, Alexandra K. Kiemer, Sonja M. Kessler, Department of Pharmacy, Pharmaceutical Biology, Saarland University, Saarbruecken 66123, Germany

Author contribution: Laggai S, Kiemer AK and Kessler SM designed experiments, analysed data and wrote the manuscript. Kessler SM and Kiemer AK initiated and directed the study. Simon Y and Ranssweiler T designed experiments and participated in data acquisition.

Supportive foundations: The project was funded, in part, by the Graduiertenförderung of Saarland University (Laggai S), an EASL Dame Sheila Sherlock Fellowship (Kessler SM), and by the research committee of Saarland University (61-cl/Anschub2012).

There are no conflicts of interest to disclose.

Correspondence to: Dr. Alexandra K. Kiemer, PhD, Professor of Pharmaceutical Biology, Department of Pharmacy, Pharmaceutical Biology, Saarland University, Campus C2.2, Saarbruecken, 66123, Germany. pharm.bio.kiemer@mx.uni-saarland.de

Telephone: +49-681-302- 57301 **Fax:** +49-681-302-57302

Received: July 17, 2013 Revised: September 23, 2013
Accepted: October 11, 2013
Published online: October 27, 2013

2.1.3 Abstract and core tip

Aim: To establish a simple method to quantify lipid classes in liver diseases and to decipher the lipid profile in *p62/IMP2-2/IGF2BP2* transgenic mice.

Methods: Liver-specific overexpression of the insulin-like growth factor 2 mRNA binding protein p62/IMP2-2/IGF2BP2 was used as a model for steatosis. Steatohepatitis was induced by feeding a methionine-choline deficient diet. Steatosis was assessed histologically. For thin layer chromatographic analysis, lipids were extracted from the freeze dried tissues by hexane / 2-propanol, dried, redissolved and chromatographically separated by a two solvent system. Dilution series of lipid standards were chromatographed, detected, and quantified. The detection was performed by either dichlorofluorescein or sulfuric acid / ethanol.

Results: Histological analyses confirmed steatosis and steatohepatitis development. The extraction, chromatographic and detection method showed high inter-assay reproducibility and allowed quantification of the different lipid classes. The analyses confirmed an increase of triglycerides and phosphatidyletanolamine and a decrease in phosphatidylcholine in the methionine-choline deficient diet.
The method was used for the first time to asses the lipid classes induced in the p62-overexpressing mouse model and showed a significant increase in all detected lipid species with a prominent increase of triglycerides by 2-fold. Interestingly the ratio of phosphatidylcholine to phosphatidyletanolamine was decreased, as previously suggested as a marker in the progression from steatosis to steatohepatitis.

Conclusion: The TLC analysis allows a reliable quantification of lipid classes and provides detailed insight into the lipogenic effect of p62.

Key words: NASH, NAFLD, TLC, IMP2, p62, MCD, polar lipids, neutral lipids, PC/PE ratio, triglycerides

List of abbreviations: NAFLD, non-alcoholic fatty liver disease; NASH, non-alcoholic steatohepatitis; HCC, hepatocellular carcinoma; VLDL, very low density lipoprotein; Igf2, insulin-like growth factor 2; LC-MS, liquid chromatography-mass spectrometry; TLC, thin layer chromatography; HE, hemotoxylin / eosin; DCF, 2',7'-dichlorofluorescein; TG,

triglyceride; FFA, free fatty acid; CH, cholesterol; CE, ceramide; PE, phosphatidylethanolamine; PC, phosphatidylcholine; PS, phosphatidylserine; LPC, lysophosphatidylcholine; DG, diglyceride.

Core tip

We describe a new method to quantify lipid classes in steatosis/steatohepatitis having advantages over both histology and classical analytical methods. Since lipid classes exert differential pathophysiological actions our method should be of interest for all researchers dealing with mechanisms of steatosis and steatohepatitis.

We employ our method to investigate the lipid profile in the steatosis *p62* transgenic mouse model. p62 was originally identified as an autoantigen overexpressed in hepatocellular carcinoma patients, its expression correlates with poor prognosis, and it induces steatosis. The interesting lipid profile in *p62* transgenic animals suggests that it might advance the step from steatosis towards steatohepatitis.

2.1.4 Introduction

The incidence of non-alcoholic fatty liver disease (NAFLD) and non-alcoholic steatohepatitis (NASH) has dramatically increased in Western countries during the last decades[1-3]. Still, the diagnosis of NAFLD displays a problem since there is a known heterogeneity in the histological staging of lipid accumulation in the liver[4, 5]. This problem is equally relevant for research laboratories studying mechanistic and therapeutic aspects of NAFLD and NASH.

A commonly used model for the investigation of NASH is the methionine choline deficient (MCD) mouse model, which is histologically similar to human NASH regarding steatohepatitis and fibrosis[6]. The MCD model is well characterized regarding its effect on the expression of lipid regulators, such as lipogenic transcription factors and lipogenic enzymes[7, 8]. The development of steatosis in the MCD model is attributable in part to impaired very low density lipoprotein (VLDL) secretion due to the deficiency of methionine and choline, which are the precursors for phosphatidylcholine, the main phospholipid coating VLDL particles[9].

An interesting but as yet less characterized steatosis model is the insulin-like growth factor 2 (*Igf2*) mRNA binding protein *p62*/IMP2-2/IGF2BP2-2 transgenic mouse model[10]. p62 was originally identified as an autoantigen in an HCC patient[11] and its expression correlates with poor prognosis in HCC[12]. Hepatic p62 overexpression induces a microvesicular fatty liver [10], which is characterized by an absence of inflammatory processes and liver damage[10]. Still p62 overexpression amplifies murine NASH and fibrosis[13].

NAFLD, even in the absence of cirrhosis, can progress to hepatocellular carcinoma (HCC)[14]. Increasing knowledge suggests that not only the increase in lipid accumulation itself but rather the hepatic lipid composition plays a dominant role in the development of both simple steatosis and steatohepatitis[15]. Lipid composition has in fact been shown to have a pathophysiological relevance in different metabolic diseases[15-18] as well as in cancer[19]. Accordingly, the pharmacologically reduced production of cholesterol by inhibition of hydroxy-methyl-glutaryl-coenzyme A reductase is discussed as a strategy for the chemoprevention and a slower progression of HCC[20]. The comparison of the lipidome of a murine NASH and HCC model with the human NASH and HCC lipidome found significant changes within several fatty acid signatures between the normal, NASH, and HCC lipidome[21]. Therefore, a more comprehensive characterization and understanding of pathophysiological lipidomic changes in liver diseases and common disease models seems mandatory.

For the investigation of lipid composition liquid chromatography–mass spectrometry (LC-MS) is state-of-the-art. However, due to high costs for the equipment and maintenance, the method is not suitable for routine analyses in clinical and research laboratories. Furthermore, the results obtained by LC-MS contain information in a level of detail too complex for most of the studies, in which rather general alterations in lipid classes are of interest. Thin layer chromatography (TLC) offers some advantages over LC-MS. For example, the possibility to apply many different samples on a single TLC plate is in practice often faster than LC[22]. 3D TLC was developed in the 1960s as a reliable method for lipid separation. However, a major limitation of the technique is the fact that it is possible to test only one sample per plate[23]. Since 3D TLC has a very low inter-plate reproducibility it is only suitable for qualitative measurements.

We herein present a rapid and low-cost quantitative 1D TLC, which can detect major lipid classes and can be used to quantitatively compare up to 12 samples per plate. Furthermore, we provide insight into changes of lipid composition in the *p62* transgenic mouse model for the first time[13].

2.1.5 Materials and Methods

Materials

Standard substances 1,3-diolein (D3627), L-α-lysophosphatidylcholine from egg yolk (L4129), cholesterol (C8667), glyceryl trioleate (T7140), 3-*sn*-phosphatidylethanolamine from bovine brain (P7693), L-α-phosphatidylcholine (P3556), 1,2-diacyl-*sn*-glycero-3-phospho-L-serine (P7769), non-hydroxy fatty acid ceramide from bovine brain (C2137), and stearic acid (85679) were purchased from Sigma-Aldrich (Taufkirchen, Germany). The standard substances were dissolved in chloroform/methanol (1:1 [v/v]) at a concentration of 1 mg/ml, aliquoted, and stored at -80°C. TLC silica gel 60 F_{254} glass plates were purchased from Merck (105715, Merck, Darmstadt, Germany). All solvents were distilled prior to utilization.

Animal models

All animal procedures were performed in accordance with the local animal welfare committee. Mice were kept under stable conditions regarding temperature, humidity, food delivery, and 12 h day/night rhythm.

Steatosis model

p62 transgenic mice were established as described previously[10]. Mice carrying a liver enriched activator protein promoter under tetracycline transactivator control[24] were crossed with *p62* transgenic mice, in which the human *p62* is under the control of the transrepressive responsive element cytomegaly virus (TRE-CMV_{min}). The double positive offspring expresses p62 liver-specifically. The mice were sacrificed at an age between 2.5 and 5 weeks.

Steatohepatitis model

Wild-type mice were fed either a methionine choline deficient (MCD, 960439, MP Biomedicals, Illkirch Cedex, France) or a methionine choline supplemented control diet (co, 960441, MP Biomedicals, Illkirch Cedex, France) for 3 weeks.

Histology

For hematoxylin / eosin (HE) staining 5 µm paraffin slides were rehydrated in a xylol/alcohol series, incubated for 10 min in hematoxylin, washed for 5 min under running water, and incubated for 2 min in eosin.

Extraction of bovine and murine liver lipids

Bovine liver was bought from a local butchery and directly freeze dried and stored at -80°C. Lipids from snap-frozen murine or bovine liver samples were extracted by a modified version of a published method[25]. Briefly, 60 mg liver samples were lyophilized, 15 mg of the freeze-dried tissue was dispersed with 18 volumes of a mixture of hexane / 2-propanol (3:2 [v/v]) for 10 minutes, and centrifuged at 4°C and 10,000 *g* for 10 minutes. The supernatant was transferred to a new vial and dried under a nitrogen stream, redissolved in an appropriate volume of chloroform / methanol (1:1 [v/v]), and applied in equal amounts onto the TLC plates.

1D TLC with two solvent system

The TLC plates were prewashed with a mixture of chloroform / methanol (2:1 [v/v]) to remove any contaminants and afterwards activated at 110°C for 1 hour. The samples and standard substances were applied onto the TLC plates and chromatographically separated with the first solvent system containing chloroform / methanol / acetic acid / water (50:30:8:3 [v/v/v/v])[26] to half of the plate. The TLC was dried and subjected to chromatography in a

second solvent system consisting of heptane / diethyl ether / acetic acid (70:30:2 [v/v/v])[27] to the top of the plate[28].

Detection and quantification

The TLC plates were dried for 30 minutes under a nitrogen stream and first sprayed with 0.1% 2',7'-dichlorofluorescein (DCF, 109676, Merck, Darmstadt, Germany) in methanol and afterwards with sulfuric acid / ethanol (1:1 [v/v]) followed by heating at 160 °C[23]. After drying the plates one UV image at 312 nm for DCF and one white top light image for sulfuric acid / ethanol was captured using the Biostep (Jahnsdorf, Germany) dark hood dh-4050 with transilluminator Biostep bioview (excitation 312 nm, UST-20M-8E) and an stationary fixed olympus digital camera (Hamburg, Germany) in combination with the Biostep argus X1 software (version 4.1.10). The unprocessed images in tiff format were quantified using the ImageJ 1.47i software[29].

Statistical analysis

Results are expressed as means +/- SE. The statistical significance was determined by independent two-sample *t*-test and was considered as statistically significant when *p* values were less than 0.05. The Microsoft® Office Excel 2003 software (Microsoft Coperation, Redmond, USA) was used for statistical analyses.

2.1.6 Results

Quantification of lipids on the TLC plate

In order to check the linearity of the method used, lipid standards for triglyceride (TG), free fatty acid (FFA), cholesterol (CH), ceramide (CE), phosphatidylethanolamine (PE), phosphatidylcholine (PC), phosphatidylserine (PS), lysophosphatidylcholine (LPC), and diglyceride (DG) (2.5, 5, 7.5, 10, 12.5, 15, 20 µg, each) were chromatographed, stained, and quantified according to our newly developed method described in the methods section. The DCF spray reagent was susceptible to all subjected lipids, the sulfuric acid / ethanol spray reagent was susceptible to almost all substances except for the FFA stearic acid and LPC (Figure 1A). As expected the band intensities increased with higher amount of the standard substances (Figure 1A). The quantification revealed a strong correlation with R^2 values close to one for all substances (Figure 1B).

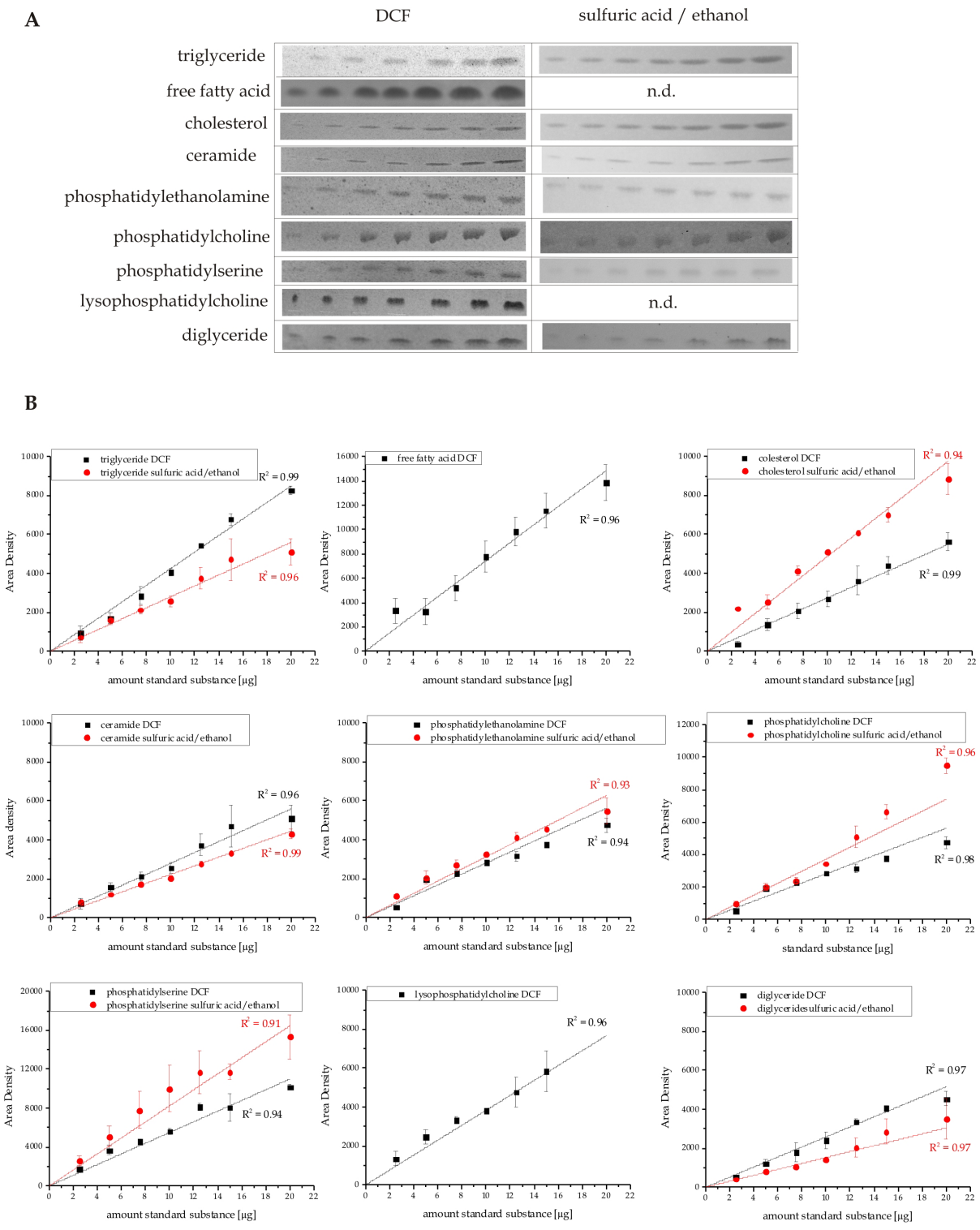

Figure 1 Quantification of lipids on the TLC plate. (A) Representative lipid dilution series (range: 2.5, 5, 7.5, 10, 12.5, 15, 20 µg) detected with DCF or sulfuric acid / ethanol. **(B)** Quantification of the standard dilution series detected with DCF or sulfuric acid / ethanol and quantified with ImageJ. Results represent the mean ± SE from at least two independent TLC plates. FFA: free fatty acids.

Validation of the lipid extraction procedure

For validation of the reproducibility of the extraction procedure, freeze-dried tissue from bovine liver was extracted in seven independent extraction procedures and subjected to chromatography. The extraction procedure revealed a high reproducibility in all lipid classes investigated (Figure 2A, B). PC, PE, TG and CH were most prominent in bovine liver (Figure 2A, B).

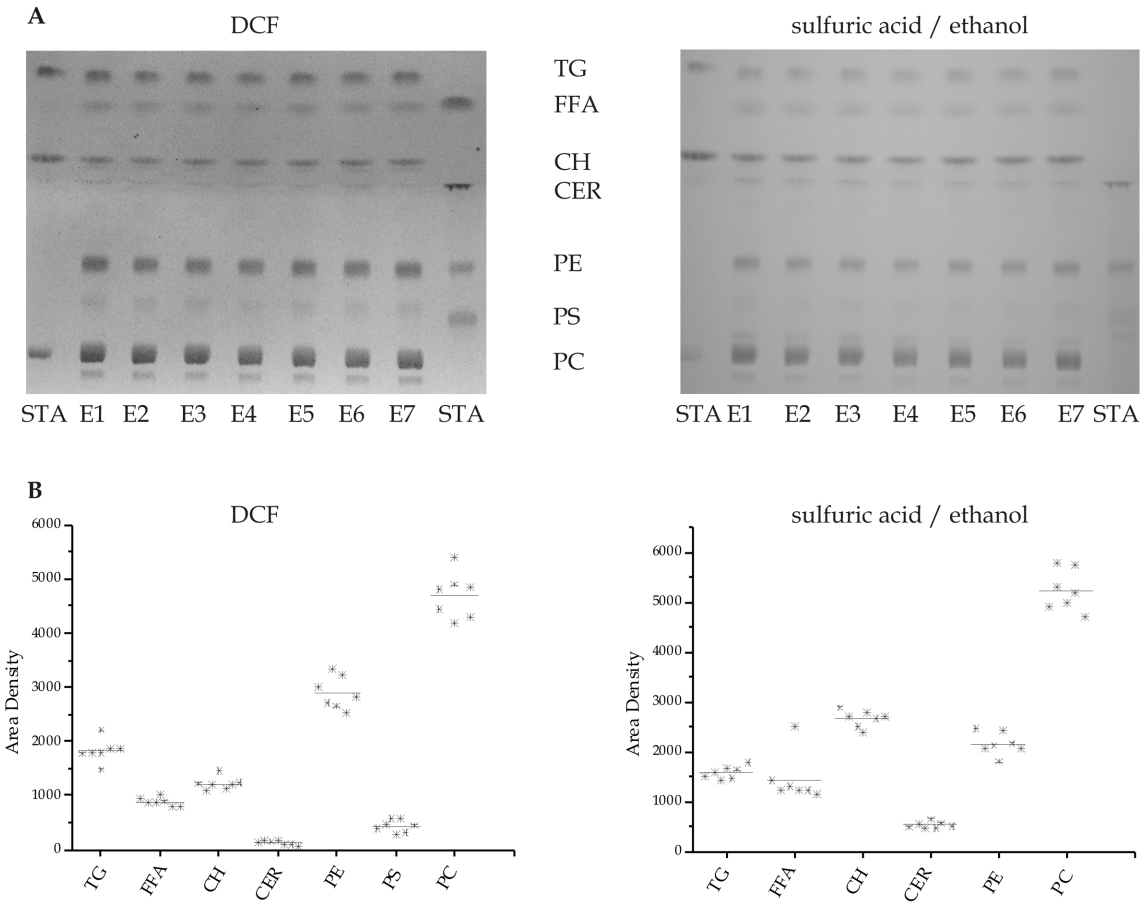

Figure 2 Validation of the lipid extraction procedure. (A) Freeze-dried bovine liver was extracted in seven independent extraction procedures (E1-E7). STA: standard substances co-chromatographed with the samples. left: detection with DCF; right: detection with sulfuric acid / ethanol. **(B)** Quantification of TLC with ImageJ detected with DCF (left) or sulfuric acid / ethanol (right).

Lipid quantification in different mouse models

Steatohepatitis / MCD mouse model

In order to test whether altered lipid composition can be determined reliably we used a well established murine steatohepatitis model, for which altered lipid classes are known[30]. Livers from control and MCD fed mice were processed, extracted, and lipids were chromatographed and detected as mentioned above. Two independent TLC plates revealed a strong increase in TG with DCF and sulfuric acid / ethanol (Figure 3B, C). As the MCD model is characterized by choline deficiency, the levels of PC were significantly decreased, whereas the levels of PE were significantly increased (Figure 3B, C). We consequently observed a reduced PC/PE ratio by approximately one third (p = 0.003) with both detection methods. The other lipid classes investigated were not significantly changed (data not shown). Due to the high amount of TG in this model, the routinely subjected amount of lipid extract had to be reduced by five folds compared to normal tissues. Routinely used amounts led to overloading of the plates (data not shown).

Steatosis / p62 transgenic mouse model

Since our method confirmed changes in lipid classes in the MCD steatohepatitis mouse model, we used it to characterize changes in lipid classes in the p62 steatosis model. The model shows distinct histologically proven microvesicular lipid incorporation in up to 58% of the animals[10] when specific lipid staining is performed. Accordingly, HE staining revealed a milder extent of steatosis compared to the MCD diet (Figure 3A, D). Two independent TLC plates revealed that all detected lipid classes were significantly increased in the livers of *p62* transgenic animals (Figure 3E, F). FFA, DG and LPC were not detectable (Figure 3E). The strongest effect was observed for TG, which were increased approximately two folds in *p62* trangenic animals compared to wildtype controls (Figure 3F). Interestingly, although the levels of both PC and PE were significantly increased, the PC/PE ratio was significantly decreased by about 10% (p = 0.05) with both detection methods. The same was true for the ratio of CH/PC, which was increased by approximately 23%, as validated by the DCF detection (p = 0.05).

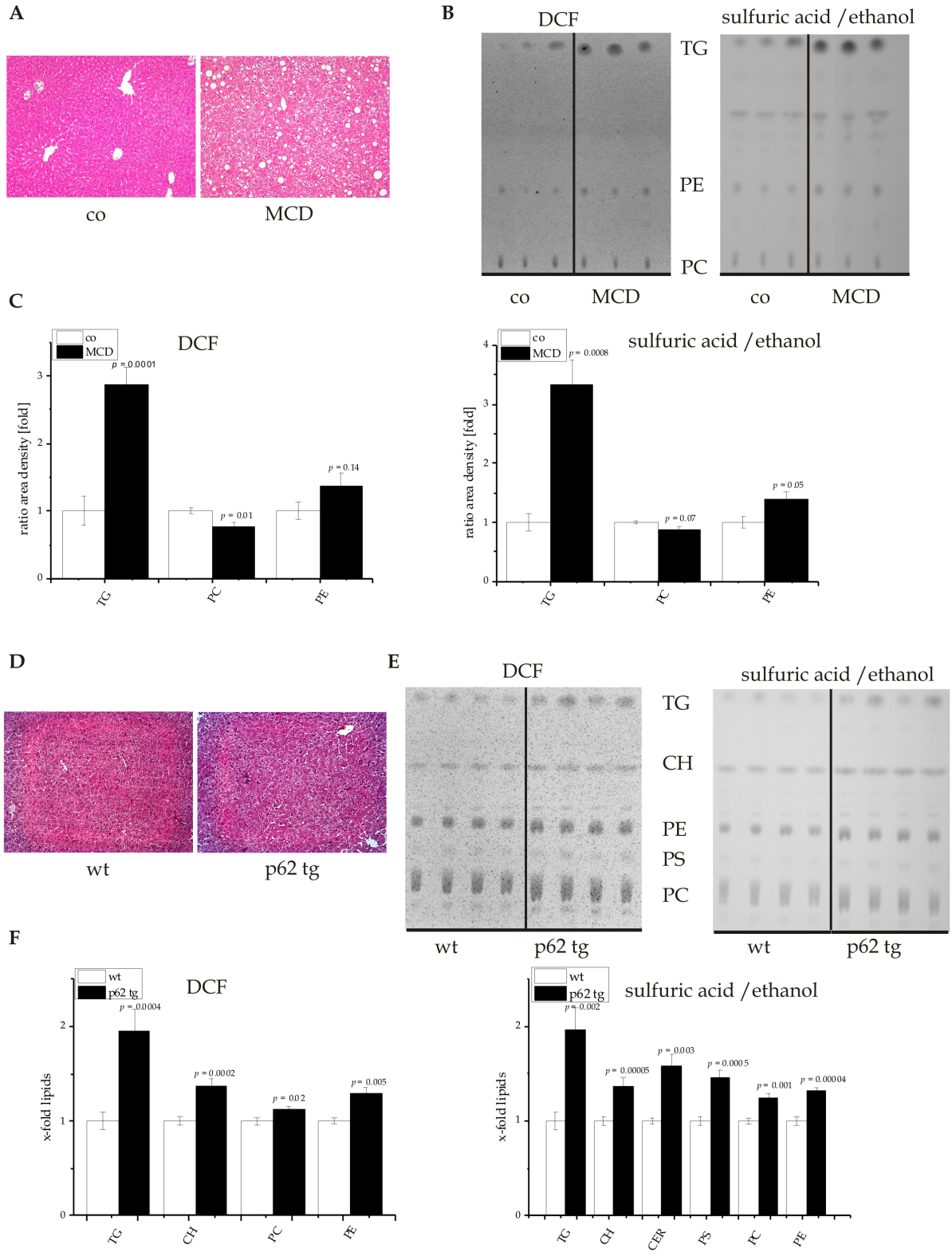

Figure 3 Lipid quantification in different mouse models. (A) Representative HE staining of control (co) or MCD fed mice (200x). **(B)** Representative TLC detected with DCF (left) or sulfuric acid / ethanol (right). **(C)** Quantification of TLC with ImageJ, detected with DCF (left) or sulfuric acid / ethanol (right). Results represent the mean ± SE from at least two independent TLC plates with *n* = 7 in each group. **(D)** representative HE staining of wildtype (wt) and *p62* transgenic mice (p62 tg)(200x). **(E)** Representative TLC detected with DCF (left) or sulfuric acid / ethanol (right). **(F)** Quantification of TLC with ImageJ detected with

DCF (left) or sulfuric acid / ethanol (right). Results represent the mean ± SE from at least two independent TLC plates and $n = 4$ in each group.

2.1.7 Discussion

Within this work we developed a rapid analytical method, which allows to quantify changes in hepatic lipid classes. The newly established method confirmed published findings for the lipid changes in a mouse NASH model and for the first time reports the lipid composition in the *p62* transgenic steatosis model.

TLC method

The one-dimensional TLC with a two-step solvent system and the detection with DCF or sulfuric acid / ethanol was able to separate and to detect the major lipid classes of TG, FFA, CH, CE, PE, PC, PS, LPC, and DG within a time period of 2.5 h (Figure 4). Standard curves revealed a high linearity of the standard substances from 2.5 to 20 µg. The chosen standard substances corresponded with the major lipid classes typically changed in NAFLD/NASH[31]. A lack of reactivity of saturated fatty acids towards a sulfuric acid / ethanol / hexane reagent was reported previously[32] and is in line with our finding that our FFA (the saturated fatty acid stearic acid) and LPC standard (which contains mostly palmitic acid and stearic acid) showed no staining with sulfuric acid / ethanol.

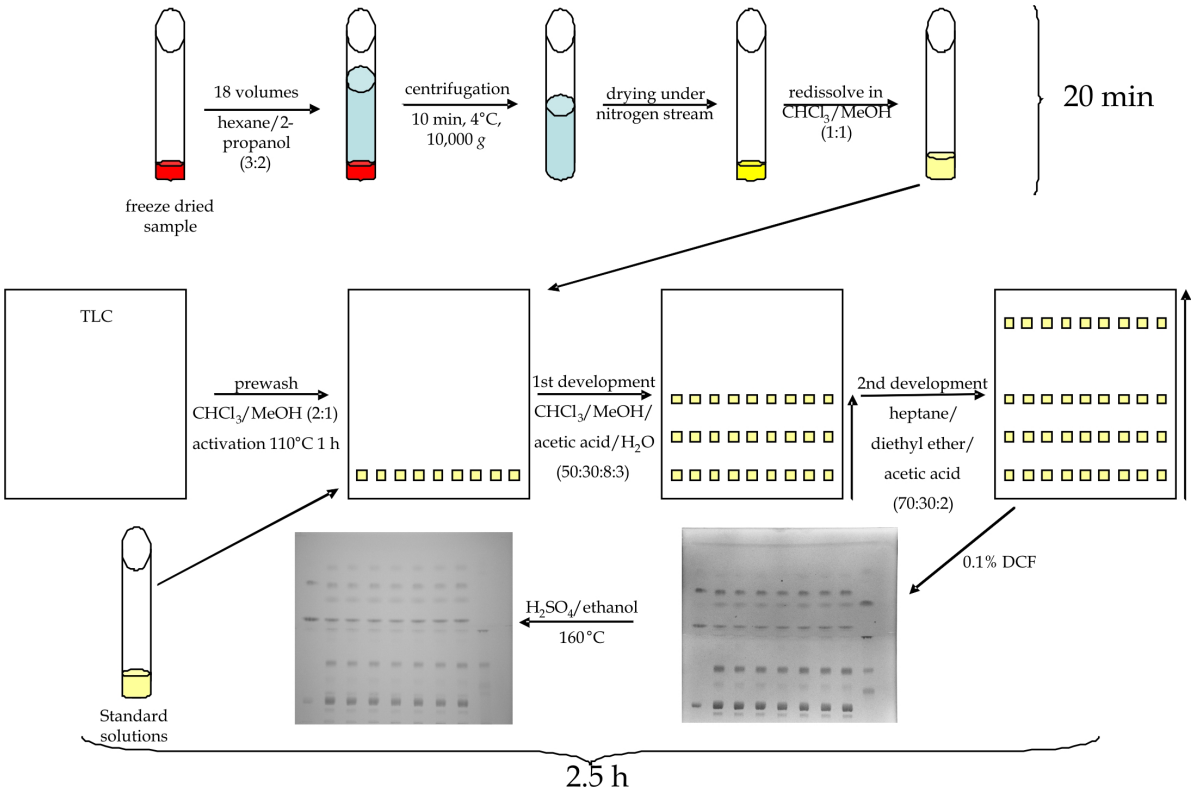

Figure 4 TLC method. Samples were freeze-dried, extracted, centrifuged, and the supernatant was transferred to a new vessel and dried under gaseous nitrogen. In the meantime plates were prewashed and activated. Standard solutions and samples were subjected to the prewashed and activated TLC plates and developed with the first eluant system to half of the plate. After drying the TLC plate was subjected to a second eluant system in the same direction up to the top of the plate. After drying of the plates, lipids were visualised with DCF and afterwards with sulfuric acid / ethanol and heating to 160°C.

Most publications only investigate an assortment of the most important lipids in liver diseases[18, 26, 27, 31]. It is almost impossible to detect all abundant lipid species in tissues within one method, because the physicochemical properties of the broad spectrum of lipid classes are too variable[22]. The lipid class spectrum of the bovine liver extract was quite similar to published studies, which showed that PC and PE are the main components of the bovine liver phospholipids[34, 35].

The extraction procedure has the advantage to be quick and that it requires relatively low amounts of tissue (approximately 70 mg wet weight tissue) compared to other methods[33]. Additional advantages are a low contamination with non-lipids due to the high apolarity of the solvent mixture, a low toxicity, a low phospholipid degradation, and the possibility to use plastic materials[22, 36]. Freeze-drying of the liver tissue samples reduces the enzymatic activity of potential lipid degrading enzymes[37]. Taken together, this method is an easy, cheap, and rapid screening method for up to 12 samples in parallel. In addition, it needs only little

technical equipment. The TLC method allows detection from the applied crude lipid extracts without the need of additional purification steps.

Confirmation of known changes in lipid classes in the MCD NASH model

After establishing a reliable technique we sought to confirm known alterations in lipid classes in the MCD NASH model. The MCD-induced NASH has the advantage of a histological appearance highly similar to human NASH concerning steatosis, i.e. mixed inflammatory cell infiltrates, hepatocellular necrosis, and eventual pericellular fibrosis mimics[38]. We found strongly increased levels of TG, increased levels of PE, and decreased levels of PC, which led to a significantly decreased PC/PE ratio. Yao et al. reported decreased PC levels in choline deficient rat hepatocytes[39]. Since PC biosynthesis is partly due to the methylation of PE by S-adenosyl methionine[40], it is not surprising that the lack of methionine in this model resulted in the accumulation of PE. An increase in TG[30] and a decreased mitochondrial PC/PE ratio[41] in the MCD diet was described previously. Therefore, our one-dimensional TLC method could well confirm known alterations in lipid classes in this dietary model of NASH.

Lipid composition in p62-induced steatosis

This is the first study, which clarifies the lipid composition in p62-induced steatosis. The increase in all detected lipid classes might be due to a p62-mediated activation of lipogenic genes induced by the lipogenic growth factor Igf2[42], which is highly overexpressed in *p62* transgenic animals[10]. The p62-induced microvesicular steatosis is difficult to evaluate with simple histological H/E staining (Figure 3D). Still, our TLC method revealed strongly affected lipid accumulation also in histologically normal tissue and allows more reliable and quantitative statements.

Accumulation of TG in hepatocytes is a hallmark of NAFLD[43]. As expected, TG were the lipid class elevated to the highest degree in p62-induced fatty liver. Interestingly, Yetukuri et al. described a positive correlation between TG and CER in an *ob/ob* steatosis model[44]. The precursor for TG[45], namely DG, were not detectable in our murine models, despite the fact that DG standard series revealed strong signals. A similar observation could be seen for FFA and LPC. Since the age of our investigated transgenic and control animals were 2.5 to 5 weeks, the lack of abundance of some lipid species might be explained by the relatively young age. In this context Rappley et al. reported age-dependent changes in phospholipid levels in mouse brain[46].

An unaltered content of FFA in human NAFLD was described previously[18]. Since we saw weak signals for FFA, which were not elevated in the *p62* transgenics, no elevation by p62 can be assumed.

One of the most complex investigations of the human NAFLD/NASH lipidome found in the literature reports elevated CH levels, and an increased ratio of CH to PC[18]. Accordingly, these results are in line with the findings in our p62 steatotic animals. On the other hand, the literature report also found decreased levels of PC and PE, whereas PS remained unaltered[18]. Since increased CH levels are often associated with enhanced PC synthesis[47], increased PC levels in our *p62* transgenic animals might be explainable. Most notably, a decreased PC/PE ratio was observable in *p62* transgenic animals although PC and PE levels were both increased. The distinct manipulation of the PC/PE ratio performed by Li et al. showed that an elevation of the ratio can in fact reverse steatohepatitis, but not steatosis[48]. This observation strongly suggests that a decreased PC/PE ratio plays a role in the progression from steatosis to steatohepatitis. In fact, NASH patients were found to have decreased PC/PE ratios in the same study[48]. The responsible mechanisms are as yet only speculative and might involve the inhibition of the PE N-methyltransferase[48], which converts PE to PC. Among the lipids, which were elevated in the *p62* transgenics, cholesterol[49] and ceramides[50]are highly cytotoxic. Although p62 overexpression induces a benign steatosis in the absence of inflammatory events, we speculate that the increased levels of CH and CER and the decreased PC/PE ratio might finally promote an inflammatory environment in the livers of *p62* transgenic animals. In fact, p62 overexpression can promote the development of NASH and fibrosis[13].

Taken together, we have established a rapid technique to quantify altered lipid classes in experimental models of steatosis and steatohepatitis. The method confirmed known changes in the well-established MCD NASH model and for the first time revealed a distinctly altered lipid composition in the p62 steatosis model. The knowledge of changes in lipid composition might be helpful for the understanding of pathophysiological mechanisms in NAFLD and NASH.

2.1.8 Comments

1 Background

Non-alcoholic fatty liver disease and non-alcoholic steatohepatitis are mostly of benign appearance, but they are highly discussed as potential risk factors for the development of

hepatocellular carcinoma. Hepatocellular carcinoma is a highly aggressive cancer type with high mortality, which is difficult to detect and to cure. Changes in lipid and fatty acid composition in disease progression to hepatocellular carcinoma are not well characterized, but are suggested to be of major importance. The high impact of these lipidomic changes needs appropriate *in vivo* models, and rapid and reliable methods to quantify the whole spectrum of lipid classes simultaneously.

2 Research frontiers

A state of the art method used for the identification of lipid classes is lipid chromatography coupled with mass spectrometric detection. This method is highly cost intensive, needs a lot of time for the establishment of the method and requires well-educated and experienced staff. Thin layer chromatography on the other hand represents a well-established technique, which allows a fast establishment in each laboratory within a really short time and allows a highly sensitive detection. As already mentioned, the lipidomic changes in the different states of liver disease progression in diverse *in vivo* mouse models and their potential correlation with human liver diseases are rare.

3 Related publications

Simon Y, Kessler SM, Bohle RM, Haybaeck J, Kiemer AK. The insulin-like growth factor 2 (IGF2) mRNA binding protein p62/IGF2BP2-2 as a promoter of NAFLD and HCC? *Gut* 2014; **63**, 861-863.

Kessler SM, Pokorny J, Zimmer V, Laggai S, Lammert F, Bohle RM, Kiemer AK. IGF2 mRNA binding protein p62/IMP2-2 in hepatocellular carcinoma: antiapoptotic action is independent of IGF2/PI3K signaling. *Am J Physiol Gastrointest Liver Physiol* 2013; **304**(4): G328-G336 doi: 10.1152/ajpgi.00005.2012 PMID: 23257922

Laggai S, Kessler SM, Gemperlein K, Haybaeck J, Mueller R, Kiemer AK. 1270 Altered fatty acid profile in livers overexpressing the *Igf2* mRNA binding protein p62: Induction of fatty acid elongase ELOVL6 *via* Igf2-dependent SREBP1 activation. *J Hepatol 2013*; **58**: S514 PMID: S0168-8278(13)61271-4

Bell JL, Wachter K, Muhleck B, Pazaitis N, Kohn M, Lederer M, Huttelmaier S. Insulin-like growth factor 2 mRNA-binding proteins (IGF2BPs): post-transcriptional drivers of cancer progression? *Cell Mol Life Sci* 2013; **70**(15): 2657-2675 doi: 10.1007/s00018-012-1186-z PMID: 23069990

Tybl E, Shi FD, Kessler SM, Tierling S, Walter J, Bohle RM, Wieland S, Zhang J, Tan EM, Kiemer AK. Overexpression of the IGF2-mRNA binding protein p62 in transgenic mice induces a steatotic phenotype. *J Hepatol* 2011; **54**(5): 994-1001 doi: S0168-8278(10)00944-X PMID: 21145819

4 Innovations and breakthroughs

The thin layer chromatography of lipids is normally limited by the requirement to separately analyze either polar lipids or neutral lipids, each on one plate. Another method is the 3D thin layer chromatography, which allows only one sample per plate. Here we describe a fast screening method to chromatograph several samples on one plate, to separate the main polar and neutral lipid classes, to visualize them by two different staining methods, and to quantify them using the freely available ImageJ software within a short time. We proved the reliability of the method by comparing the obtained data from a methionine choline deficient non-alcoholic steatohepatitis mouse model to published data. We investigated the alterations in lipid classes in the *p62*/IMP2-2/IGF2BP2-2 transgenic mouse model for the first time and found interesting changes, which might indicate the progressive character of this steatosis model.

5 Applications

The described method can be used by all research laboratories for the lipidomic analyses of liver samples from the whole array of existing and newly developed experimental models for liver diseases. The method is not restricted to steatosis and steatohepatitis, but should also be useful for the analysis of HCC samples. While the gold standard for lipidomic analyses, i.e. lipid chromatography-mass spectrometry is a quite expensive method, the thin layer chromatographic method can also be used in laboratories, which have no access to respective high-end equipment. The *p62* transgenic mouse model might be a potentially interesting model to investigate mechanisms of steatosis and disease progression. Further characterization and correlation to human data might help to understand the role of lipid changes in pathogenesis.

6 Terminology

Non-alcoholic fatty liver disease: non-alcoholic fatty liver disease is characterized by a strong accumulation of lipids, especially triglycerides, within hepatocytes; non-alcoholic steatohepatitis: non-alcoholic steatohepatitis is a steatotic liver, which is characterized by an

inflammatory environment and might result in fibrosis; hepatocellular carcinoma: hepatocellular carcinoma is an aggressive form of liver cancer; thin layer chromatography: thin layer chromatography is a chromatographic method, glass or aluminium plates are coated mostly with silica gel and allows separation with different solvent systems.

2.1.9 References

1 **Rafiq N,** Bai C, Fang Y, Srishord M, McCullough A, Gramlich T, Younossi ZM. Long-Term Follow-Up of Patients With Nonalcoholic Fatty Liver. *Clin Gastroenterol Hepatol* 2009; **7**(2): 234 doi: 10.1016/j.cgh.2008.11.005 PMID: 19049831

2 **Caldwell SH,** Oelsner DH, Iezzoni JC, Hespenheide EE, Battle EH, Driscoll CJ. Cryptogenic cirrhosis: Clinical characterization and risk factors for underlying disease. *Hepatology* 1999; **29**(3): 664 PMID: 10051466

3 **Agopian VG,** Kaldas FM, Hong JC, Whittaker M, Holt C, Rana A, Zarrinpar A, Petrowsky H, Farmer D, Yersiz H, Xia V, Hiatt JR, Busuttil RW. Liver Transplantation for Nonalcoholic Steatohepatitis: The New Epidemic. *Ann Surg* 2012; **256**(4): 624-633 doi: 10.1097/SLA.0b013e31826b4b7e PMID: 22964732

4 **Bedossa P,** Poitou C, Veyrie N, Bouillot J-L, Basdevant A, Paradis V, Tordjman J, Clement K. Histopathological algorithm and scoring system for evaluation of liver lesions in morbidly obese patients. *Hepatology*; **56**(5): 1751 doi: 10.1002/hep.25889 PMID: 22707395

5 **Kleiner DE,** Brunt EM, Van Natta M, Behling C, Contos MJ, Cummings OW, Ferrell LD, Liu Y-C, Torbenson MS, Unalp-Arida A, Yeh M, McCullough AJ, Sanyal AJ. Design and validation of a histological scoring system for nonalcoholic fatty liver disease. *Hepatology* 2005; **41**(6): 1313 doi: 10.1002/hep.20701 PMID: 15915461

6 **Wasmuth HE,** Zaldivar MM, Beraza N, Trautwein C. Of mice and NASH – from fat to inflammation and fibrosis. *Drug Discov Today Dis Models* 2007; **4**(1): 25 doi: 10.1016/j.ddmod.2007.09.006

7 **Park HS,** Jeon BH, Woo SH, Leem J, Jang JE, Cho MS, Park IS, Lee KU, Koh EH. Time-dependent changes in lipid metabolism in mice with methionine choline deficiency-induced fatty liver disease. *Mol Cells* 2011; **32**(6): 571-577 doi: 10.1007/s10059-011-0184-6 PMID: 22083307

8 **Lee JY,** Moon JH, Park JS, Lee BW, Kang ES, Ahn CW, Lee HC, Cha BS. Dietary oleate has beneficial effects on every step of non-alcoholic Fatty liver disease progression in a methionine- and choline-deficient diet-fed animal model. *Diabetes Metab J* 2011; **35**(5): 489-496 doi: 10.4093/dmj.2011.35.5.489 PMID: 22111040

9 **Rinella ME,** Elias MS, Smolak RR, Fu T, Borensztajn J, Green RM. Mechanisms of hepatic steatosis in mice fed a lipogenic methionine choline-deficient diet. *J Lipid Res* 2008; **49**(5): 1068-1076 doi: M800042-JLR200 PMID: 18227531

10 **Tybl E,** Shi FD, Kessler SM, Tierling S, Walter J, Bohle RM, Wieland S, Zhang J, Tan EM, Kiemer AK. Overexpression of the IGF2-mRNA binding protein p62 in transgenic mice induces a steatotic phenotype. *J Hepatol* 2011; **54**(5): 994-1001 doi: S0168-8278(10)00944-X PMID: 21145819

11 **Zhang J-Y,** Chan EKL, Peng X-X, Tan EM. A Novel Cytoplasmic Protein with RNA-binding Motifs Is an Autoantigen in Human Hepatocellular Carcinoma. *J Exp Med* 1999; **189**(7): 1101-1110 doi: 10.1084/jem.189.7.1101 PMID: 10190901

12 **Kessler SM,** Pokorny J, Zimmer V, Laggai S, Lammert F, Bohle RM, Kiemer AK. IGF2 mRNA binding protein p62/IMP2-2 in hepatocellular carcinoma: antiapoptotic

action is independent of IGF2/PI3K signaling. *Am J Physiol Gastrointest Liver Physiol* 2013; **304**(4): G328-G336 doi: 10.1152/ajpgi.00005.2012 PMID: 23257922

13 **Simon Y,** Kessler SM, Bohle RM, Haybaeck J, Kiemer AK. The insulin-like growth factor 2 (IGF2) mRNA binding protein p62/IGF2BP2-2 as a promoter of NAFLD and HCC? *Gut* 2014, **63**, 861-863.

14 **Baffy G,** Brunt EM, Caldwell SH. Hepatocellular carcinoma in non-alcoholic fatty liver disease: an emerging menace. *J Hepatol* 2012; **56**(6): 1384-1391 doi: S0168-8278(12)00114-6 PMID: 22326465

15 **Puri P,** Wiest MM, Cheung O, Mirshahi F, Sargeant C, Min HK, Contos MJ, Sterling RK, Fuchs M, Zhou H, Watkins SM, Sanyal AJ. The plasma lipidomic signature of nonalcoholic steatohepatitis. *Hepatology* 2009; **50**(6): 1827-1838 doi: 10.1002/hep.23229 PMID: 19937697

16 **Alkhouri N,** Dixon LJ, Feldstein AE. Lipotoxicity in nonalcoholic fatty liver disease: Not all lipids are created equal. Expert Rev Gastroenterol Hepatol. 2009; **3**(4): 445 doi: 10.1586/egh.09.32 PMID:19673631

17 **Ricchi M,** Odoardi MR, Carulli L, Anzivino C, Ballestri S, Pinetti A, Fantoni LI, Marra F, Bertolotti M, Banni S, Lonardo A, Carulli N, Loria P. Differential effect of oleic and palmitic acid on lipid accumulation and apoptosis in cultured hepatocytes. *J Gastroenterol Hepatol* 2009; **24**(5): 830-840 doi: JGH5733 PMID: 19207680

18 **Puri P,** Baillie RA, Wiest MM, Mirshahi F, Choudhury J, Cheung O, Sargeant C, Contos MJ, Sanyal AJ. A lipidomic analysis of nonalcoholic fatty liver disease. *Hepatology* 2007; **46**(4): 1081-1090 doi: 10.1002/hep.21763 PMID: 17654743

19 **Zhang F,** Du G. Dysregulated lipid metabolism in cancer. *World J Biol Chem* 2012; **3**(8): 167-174 doi: 10.4331/wjbc.v3.i8.167 PMID: 22937213

20 **Lonardo A,** Loria P. Potential for statins in the chemoprevention and management of hepatocellular carcinoma. *J Gastroenterol Hepatol* 2012; **27**(11): 1654-1664 doi: 10.1111/j.1440-1746.2012.07232.x PMID: 22849701

21 **Muir K,** Hazim A, He Y, Peyressatre M, Kim DY, Song X, Beretta L. Proteomic and Lipidomic Signatures of Lipid Metabolism in NASH-Associated Hepatocellular Carcinoma. *Cancer Res* 2013; **73**(15): 4722-4731 doi: 0008-5472.CAN-12-3797 PMID: 23749645

22 **Fuchs B,** Suss R, Teuber K, Eibisch M, Schiller J. Lipid analysis by thin-layer chromatography--a review of the current state. *J Chromatogr A* 2011; **1218**(19): 2754-2774 doi: S0021-9673(10)01654-7 PMID: 21167493

23 **Kramer JKG,** Fouchard RC, Farnworth ER. A complete separation of lipids by three-directional thin layer chromatography. *Lipids* 1983; **18**(12): 896-899 doi: 10.1007/BF02534569

24 **Kistner A,** Gossen M, Zimmermann F, Jerecic J, Ullmer C, Lübbert H, Bujard H. Doxycycline-mediated quantitative and tissue-specific control of gene expression in transgenic mice. *Proc Natl Acad Sci USA* 1996; **93**(20): 10933 PMID: 8855286

25 **Hara A,** Radin NS. Lipid extraction of tissues with a low-toxicity solvent. *Anal Biochem* 1978; **90**(1): 420-426 doi: 0003-2697(78)90046-5 PMID: 727482

26 **Pai JK,** Siegel MI, Egan RW, Billah MM. Phospholipase D catalyzes phospholipid metabolism in chemotactic peptide-stimulated HL-60 granulocytes. *J Biol Chem* 1988; **263**(25): 12472-12477 PMID: 3165977

27 **Plekhanov AY.** Rapid staining of lipids on thin-layer chromatograms with amido black 10B and other water-soluble stains. *Anal Biochem* 1999; **271**(2): 186-187 doi: 10.1006/abio.1999.4127S0003-2697(99)94127-1 PMID: 10419634

28 **Schuh TJ.** An Introduction to Lipid Analysis in the Cell Biology Laboratory. *The Am Biol Teach* 2002; **64**(2): 122 doi: 10.1662/0002-7685(2002)064[0122:AITLAI]2.0.CO;2

29 **Schneider CA,** Rasband WS, Eliceiri KW. NIH Image to ImageJ: 25 years of image analysis. *Nat Methods* 2012; **9**(7): 671-675 PMID: 22930834

30 **Larter CZ,** Yeh MM, Haigh WG, Williams J, Brown S, Bell-Anderson KS, Lee SP, Farrell GC. Hepatic free fatty acids accumulate in experimental steatohepatitis: role of adaptive pathways. *J Hepatol* 2008; **48**(4): 638-647 doi: S0168-8278(08)00044-5 PMID: 18280001

31 **Miura K,** Ohnishi H. Nonalcoholic fatty liver disease: from lipid profile to treatment. *Clin J Gastroenterol* 2012; **5**(5): 313-321 doi: 10.1007/s12328-012-0315-4

32 **Kurantz MJ,** Maxwell RJ, Kwoczak R, Taylor F. Rapid and sensitive method for the quantitation of non-polar lipids by high-performance thin-layer chromatography and fluorodensitometry. *J Chromatogr A* 1991; **549**(0): 387 doi: 10.1016/S0021-9673(00)91449-3

33 **Hijona E,** Hijona L, Larzabal M, Sarasqueta C, Aldazabal P, Arenas J, Bujanda L. Biochemical determination of lipid content in hepatic steatosis by the Soxtec method. *World J Gastroenterol* 2010; **16**(12): 1495-1499 doi: 10.3748/wjg.v16.i12.1495 PMID: 20333790

34 **Hidiroglou N,** McDowell LR, Johnson DD. Effect of diet on animal performance, lipid composition of subcutaneous adipose and liver tissue of beef cattle. *Meat Sci* 1987; **20**(3): 195-210 doi: 0309-1740(87)90011-8 PMID: 22054497

35 **Dawson RM,** Hemington N, Davenport JB. Improvements in the method of determining individual phospholipids in a complex mixture by successive chemical hydrolyses. *Biochem J* 1962; **84**: 497-501 PMID: 13884048

36 **Fiori M,** Scintu M, Addis M. Characterization of the Lipid Fraction in Lamb Meat: Comparison of Different Lipid Extraction Methods. *Food Anal Methods* 2013: 1-9 doi: 10.1007/s12161-013-9589-5

37 **Jiang S,** Nail SL. Effect of process conditions on recovery of protein activity after freezing and freeze-drying. *Eur J Pharm Biopharm* 1998; **45**(3): 249-257 doi: S0939-6411(98)00007-1 PMID: 9653629

38 **Leclercq IA,** Farrell GC, Field J, Bell DR, Gonzalez FJ, Robertson GR. CYP2E1 and CYP4A as microsomal catalysts of lipid peroxides in murine nonalcoholic steatohepatitis. *J Clin Invest* 2000; **105**(8): 1067-1075 doi: 10.1172/JCI8814 PMID: 10772651

39 **Yao ZM,** Vance DE. The active synthesis of phosphatidylcholine is required for very low density lipoprotein secretion from rat hepatocytes. *J Biol Chem* 1988; **263**(6): 2998-3004 PMID: 3343237

40 **Sundler R,** Akesson B. Biosynthesis of phosphatidylethanolamines and phosphatidylcholines from ethanolamine and choline in rat liver. *Biochem J* 1975; **146**(2): 309-315 PMID:168873

41 **Caballero F,** Fernandez A, Matias N, Martinez L, Fucho R, Elena M, Caballeria J, Morales A, Fernandez-Checa JC, Garcia-Ruiz C. Specific contribution of methionine and choline in nutritional nonalcoholic steatohepatitis: impact on mitochondrial S-adenosyl-L-methionine and glutathione. *J Biol Chem* 2010; **285**(24): 18528-18536 doi: M109.099333 PMID: 20395294

42 **Chao W,** D'Amore PA. IGF2: epigenetic regulation and role in development and disease. *Cytokine Growth Factor Rev* 2008; **19**(2): 111-120 doi: S1359-6101(08)00007-5 PMID: 18308616

43 **Yamaguchi K,** Yang L, McCall S, Huang J, Yu XX, Pandey SK, Bhanot S, Monia BP, Li YX, Diehl AM. Inhibiting triglyceride synthesis improves hepatic steatosis but exacerbates liver damage and fibrosis in obese mice with nonalcoholic steatohepatitis. *Hepatology* 2007; **45**(6): 1366-1374 doi: 10.1002/hep.21655 PMID: 17476695

44 **Yetukuri L,** Katajamaa M, Medina-Gomez G, Seppanen-Laakso T, Vidal-Puig A, Oresic M. Bioinformatics strategies for lipidomics analysis: characterization of obesity related hepatic steatosis. *BMC Syst Biol* 2007; **1**: 12 doi: 1752-0509-1-12 PMID: 17408502

45 **Gorden DL,** Ivanova PT, Myers DS, McIntyre JO, VanSaun MN, Wright JK, Matrisian LM, Brown HA. Increased diacylglycerols characterize hepatic lipid changes in progression of human nonalcoholic fatty liver disease; comparison to a murine model. *PLoS One* 2011; **6**(8): e22775 doi: 10.1371/journal.pone.0022775PONE-D-11-04361 PMID: 21857953

46 **Rappley I,** Myers DS, Milne SB, Ivanova PT, Lavoie MJ, Brown HA, Selkoe DJ. Lipidomic profiling in mouse brain reveals differences between ages and genders, with smaller changes associated with alpha-synuclein genotype. *J Neurochem* 2009; **111**(1): 15-25 doi: JNC6290 PMID: 19627450

47 **Tabas I.** Cholesterol and phospholipid metabolism in macrophages. *Biochim Biophys Acta* 2000; **1529**(1-3): 164-174 doi: S1388-1981(00)00146-3 PMID: 11111086

48 **Li Z,** Agellon LB, Allen TM, Umeda M, Jewell L, Mason A, Vance DE. The ratio of phosphatidylcholine to phosphatidylethanolamine influences membrane integrity and steatohepatitis. *Cell Metab* 2006; **3**(5): 321-331 doi: S1550-4131(06)00116-1 PMID: 16679290

49 **Yao PM,** Tabas I. Free cholesterol loading of macrophages induces apoptosis involving the fas pathway. *J Biol Chem* 2000; **275**(31): 23807-23813 doi: 10.1074/jbc.M002087200M002087200 PMID: 10791964

50 **Arora AS,** Jones BJ, Patel TC, Bronk SF, Gores GJ. Ceramide induces hepatocyte cell death through disruption of mitochondrial function in the rat. *Hepatology* 1997; **25**(4): 958 doi: 0.1002/hep.510250428 PMID:9096604

P- Reviewers Assy N, Lonardo A, Omata M, Waisberg J
S- Editor Wen LL **L- Editor** A **E- Editor** Yan JL

2.2 The *IGF2* mRNA binding protein p62/IGF2BP2-2 induces fatty acid elongation as a critical feature of steatosis

II

Since the quantity of hepatic lipids was icreased (Tybl et al., 2011) and also the quality of hepatic lipids was altered in the livers of *p62* transgenic animals (Laggai et al., 2013), the aim of this study was to evaluate changes in the fatty acid profile (incorporated in total lipids), to decipher the pathways related to p62-induced steatosis development and to validate these pathways also in the human system.

The *IGF2* mRNA binding protein p62/IGF2BP2-2 induces fatty acid elongation as a critical feature of steatosis

Stephan Laggai, Sonja M Kessler, Stefan Boettcher,Valérie Lebrun, Katja Gemperlein, Eva Lederer, Isabelle A Leclercq, Rolf Mueller, Rolf W Hartmann, Johannes Haybaeck and Alexandra K Kiemer.

This research was originally published in Journal of Lipid Research. Laggai, S., Kessler, S.M., Boettcher, S., Lebrun, V., Gemperlein, K., Lederer, E., Leclercq, I.A., Mueller, R., Hartmann, R.W., Haybaeck, J., and Kiemer, A.K. The *IGF2* mRNA binding protein p62/IGF2BP2-2 induces fatty acid elongation as a critical feature of steatosis. *J Lipid Res.* 2014; 55: 1087-1097. doi: 10.1194/jlr.M045500. Copyright © 2014, the American Society for Biochemistry and Molecular Biology, Inc.

The full text article can also be found at:
http://www.jlr.org/content/55/6/1087.full

2.2.1 Author Contribution

First Published on April 22, 2014, doi: 10.1194/jlr.M045500. June 2014; *The Journal of Lipid Research*, 55, 1087-1097.

The *IGF2* mRNA binding protein p62/IGF2BP2-2 induces fatty acid elongation as a critical feature of steatosis.

Laggai S, Kessler SM, Boettcher S, Lebrun V, Gemperlein K, Lederer E, Leclercq IA, Mueller R, Hartmann RW, Haybaeck J, Kiemer AK.

Laggai S:

Performed cell culture studies.

Performed real-time RT-PCR analysis of cell culture, murine liver and human liver samples.

Performed Western blot analysis of cell culture and murine liver samples.

Performed sample preparation and assisted in GC-MS (in cooperation with Gemperlein K and Mueller R) and UHPLC-MS/MS (in cooperation with Boettcher S and Hartmann RW) analysis.

Designed experiments, performed data acquisition and statistical analysis.

Wrote and revised the manuscript.

Kessler SM:

Performed animal procedures.

Performed immuno/histochemistry.

Participated in hyperinsulinemic euglycemic clamp study in cooperation with Lebrun V and Leclercq IA.

Participated in analysis of human liver samples in cooperation with Lederer E and Haybaeck J.

Designed experiments, performed data acquisition and statistical analysis.

Wrote and revised the manuscript.

Boettcher S and Hartmann RW:

Established, performed and directed UHPLC-MS/MS analysis and wrote the respective methods.

Lebrun V and Leclercq IA:

Performed and directed hyperinsulinemic euglycemic clamp study.

Participated in manuscript revision.

Gemperlein K and Mueller R:
Performed and directed GC-MS/MS analysis.

Lederer E and Haybaeck J:
Provided human liver samples and the respective data on disease etiology.
Performed and directed reverse transcription and real-time RT-PCR of human liver samples.
Participated in manuscript revision.

Kiemer AK:
Initiated and directed the study.
Designed experiments.
Wrote and revised the manuscript.

2.2.2 Title page

The *IGF2* mRNA binding protein p62/IGF2BP2-2 induces fatty acid elongation as a critical feature of steatosis

Stephan Laggai[a], Sonja M. Kessler[a, b, c], Stefan Boettcher[d], Valérie Lebrun[c], Katja Gemperlein[e,f], Eva Lederer[b], Isabelle A. Leclercq[c], Rolf Mueller[e,f], Rolf W. Hartmann[d,f], Johannes Haybaeck[b], Alexandra K. Kiemer[a]*

[a]Department of Pharmacy, Pharmaceutical Biology, Saarland University, Saarbrücken, Germany

[b]Institute of Pathology, Medical University of Graz, Graz, Austria

[c]Laboratory of Hepato-gastroenterology, Institut de Recherche expérimentale et Clinique, Université catholique de Louvain, Brussels, Belgium

[d]Department of Pharmacy, Pharmaceutical and Medicinal Chemistry, Saarland University, Saarbrücken, Germany

[e]Department of Pharmacy, Pharmaceutical Biotechnology, Saarland University, Saarbrücken, Germany

[f]Helmholtz Institute for Pharmaceutical Research Saarland (HIPS), Helmholtz Centre for Infection Research (HZI), Saarbrücken, Germany

*Corresponding Author

Telephone: +49-681-302-57301

Fax: +49-681-302-57302

Email: pharm.bio.kiemer@mx.uni-saarland.de

Running title: p62 induces fatty acid elongation

Abbreviations: acetyl-CoA carboxylase alpha (ACC/ACACA), carbohydrate responsive element-binding protein (CHREBP/MLXIPL), carnitine palmitoyltransferase 1A (CPT1A), ELOVL fatty acid elongase 6 (ELOVL6), fatty acid synthase (FASN), *gas chromatography-mass spectrometry* (GC-MS), glucose infusion rate (GIR), glucose turnover (TO), hepatic glucose production (HGP), hepatocellular carcinoma (HCC), insulin-like growth factor 2 (IGF2), liver-X-receptor alpha (LXR-α/NR1H3), non-alcoholic fatty liver disease (NAFLD), non-alcoholic steatohepatitis (NASH), peroxisome proliferator-activated receptor alpha (PPARA), pyruvate kinase, liver and RBC (L-PK, PKLR), sterol regulatory element binding

transcription factor 1 (SREBF1/SREBP1), ultra high-performance liquid chromatography–mass spectrometry (UHPLC-MS/MS)

2.2.3 Abstract

Liver-specific overexpression of the insulin-like growth factor 2 (*IGF2*) mRNA binding protein p62/IGF2BP2-2 induces a fatty liver, which highly expresses *IGF2*. Since *IGF2* expression is elevated in patients with steatohepatitis, the aim of our study was to elucidate the role and interconnection of p62 and IGF2 in lipid metabolism. Expression of *p62* and *IGF2* highly correlated in human liver disease. *p62* induced an elevated ratio of C18:C16 and increased ELOVL fatty acid elongase 6 (ELOVL6) protein, the enzyme catalyzing the elongation of C16 to C18 fatty acids and promoting non-alcoholic steatohepatitis in mice and humans. p62 overexpression induced the activation of the ELOVL6 transcriptional activator SREBF1. Recombinant IGF2 induced the nuclear translocation of sterol regulatory element binding transcription factor 1 (SREBF1) and a neutralizing IGF2 antibody reduced ELOVL6 and mature SREBF1 protein levels. Concordantly, *p62* and *IGF2* correlated with *ELOVL6* in human livers. Decreased palmitoyl-CoA levels as found in *p62* tg livers can explain the lipogenic action of ELOVL6. Accordingly, p62 represents an inducer of hepatic C18 fatty acid production *via* a SREBF1-dependent induction of ELOVL6. These findings underline the detrimental role of p62 in liver disease.

Supplemental Keywords: ELOVL6, p62/IGF2BP2-2/Imp2-2, SREBF1/SREBP1, IGF2 signalling, Hepatic steatosis

2.2.4 Introduction

Non-alcoholic fatty liver disease (NAFLD) is considered as the most common liver disorder in Western countries with a prevalence of 20-30% of the adult population (1, 2). There is a strong correlation between characteristics of the metabolic syndrome, such as obesity and diabetes mellitus, and NAFLD/non-alcoholic steatohepatitis (NASH) (3).

The 'two-hit' hypothesis represents a common model to describe the development and progression of fatty liver diseases. A simple steatosis can stand for the first step in early liver pathogenesis (4, 5). The progression from simple steatosis to NASH requires a 'second hit' mediated by reactive oxygen species and release of inflammatory cytokines (6). This inflammatory environment can result in hepatic cirrhosis and finally in hepatocellular carcinoma (HCC) (7).

The development of hepatosteatosis can be induced by different mechanisms. The synthesis of lipids is regulated in a complex interplay induced by a set of lipogenic transcription factors, among which liver-X-receptor alpha (LXR-α, NR1H3), sterol regulatory element binding transcription factor 1 (SREBF1, SREBP1), and carbohydrate responsive element-binding protein (ChREBP, MLXIPL) represent the most important ones (8). In this context, the fact that MLXIPL controls 50% of hepatic lipogenesis by regulating glycolytic and lipogenic gene expression (9) illustrates the importance of both insulin- as well as glucose-induced lipogenic pathways. One of the relevant inducers of lipid degradation in the liver is the peroxisome proliferator-activated receptor alpha (PPARA) (10). Most importantly, there is a close interconnection between catabolic and anabolic pathways. In this context it is important to note that the mitochondrial β-oxidation pathway is negatively regulated by high malonyl-CoA levels (11, 12).

Besides the amount of lipids, which are relevant for pathophysiological actions, there is increasing evidence that also the composition of lipids has an impact on pathophysiology. In fact, human NAFLD is characterized by numerous changes in hepatic lipid composition and relative abundance of specific fatty acids (13, 14). Also hepatitis (B/C) has been described to strongly alter hepatic lipid content and composition (15, 16). Recently, the fatty acid elongase 6 (ELOVL6), which catalyzes the elongation of C16 to C18 fatty acids (17) and is a direct target of SREBF1 (18, 19), has been shown to promote NASH in mice and humans and to be overexpressed in a murine NASH model (20, 21). Interestingly, however, there is still a lack of understanding of the upstream signaling pathways being responsible for SREBF1 activation and why elevated ELOVL6 increases total fatty acid production. Also the role of

ELOVL6 in HCC is as yet poorly understood and seems to depend on disease etiology (21-23).

We recently reported that a liver-specific overexpression of the insulin-like growth factor 2 (*IGF2*) mRNA binding protein p62/IGF2BP2-2 induces steatosis in mice, coupled with high *Igf2* expression and activation of the phosphoinositide 3-kinase/AKT-signaling pathway (24). Furthermore, p62 has been shown to promote NASH development (25). Most lipid species are elevated in p62-induced steatosis, with triglycerides showing the strongest increase (26). p62 was originally identified as an autoantigen overexpressed in about one third to two thirds of HCC patients and correlates with poor outcome (27-30). Interestingly, also *IGF2* is overexpressed in NASH and HCC (31, 32), which is linked to p62 overexpression in HCC (27), and might be explained by the involvement of the *IGF2* mRNA-binding proteins in RNA localization, stability and translation (33). p62 is a splice variant of IGF2BP2 lacking exon 10, though exon 10 deletion is not affecting the six characteristic RNA binding motifs (33). Recently, Li et al. reported IGF2BP2 to bind and control the translation of c-Myc, Sp1 transcription factor and insulin-like growth factor 1 receptor (34). Binding affinities of IGF2BP2-2 to the respective mRNAs, however, are not described in the literature.

Aim of our study was to decipher the effects of p62 on lipid metabolism and to elucidate the influence of IGF2.

2.2.5 Materials and Methods

Animals

All animal procedures were performed in accordance with the local animal welfare committee. Mice were kept under stable conditions regarding temperature, humidity, food delivery, and 12 h day/night rhythm. *p62* transgenic mice were established as described by Tybl et al. (24). The mice were sacrificed at an age between 2.5 and 5 weeks.

Hyperinsulinemic euglycemic clamp study

Hepatic insulin sensitivity was determined by the hyperinsulinemic euglycemic clamp technique as described previously (35).

Human liver tissue

35 human liver tissues from patients undergoing surgical resection were analysed in the framework of the project, which was authorized by the ethical committees of the Medical

University of Graz (Ref. Nr. 1.0 24/11/2008) and the University of Heidelberg (Prof. Bannasch). Details on patient data are given in supplemental data Table I (online).

Cell culture and transfection

HepG2 cells were cultured in RPMI-1640 (PAA, Cölbe, Germany) with supplementation of 10% [v/v] FCS (PAA, Cölbe, Germany), 1% [v/v] glutamine (PAA, Cölbe, Germany), and 1% [v/v] penicillin/streptomycin (PAA, Cölbe, Germany) at 37°C and 5% CO_2. HepG2 overexpression and knockdown assays were performed according to Kessler et al. (27). For the detection of IGF2-mediated SREBF1 translocation, cells were treated for the indicated time with rhIGF-II (0.075 µg/ml, 292-G2, R&D Systems, Minneapolis, U.S.A) or with IGF2 antibody (ab9574, Abcam, United Kingdom) as previously described (27).

Fatty acid measurement by gas chromatography-mass spectrometry (GC-MS)

Murine liver samples or HepG2 cells were lyophilized, hydrolyzed by the fatty acid methyl ester (FAME) method and analysed according to Bode et al. (36). Methyl-nonadecanoate (74208, Sigma Aldrich, Taufkirchen, Germany) was used as an internal standard. The method detects both free and bound free fatty acids.

Histochemistry

Hematoxylin / eosin (HE)-staining and immunohistochemical detection of F4/80 of paraffin embedded sections were performed as previously reported (22, 24).

Real-time RT-PCR

Isolation of total RNA and reverse transcription was performed as described previously (37). RNA from human liver samples was isolated as previously described (27). Real-time RT-PCR was performed in an iQ5 cycler (Bio-Rad, Munich, Germany) or in a CFX96 cycler (Bio-Rad, Munich, Germany) with 5 x HOT FIREPol® EvaGreen® qPCR Mix Plus (Solis BioDyne, Tartu, Estonia). All samples were estimated in triplicate. Primers and conditions are listed in supplemental data Table II. Efficiency was determined for each experiment using a cDNA dilution series with a starting concentration equivalent to 0.5 µg RNA or with a standard dilution series as described previously (37). The relative gene expression was normalized to *ACTB* or *18s* mRNA values.

Preparation of nuclear extracts

Nuclear extracts from HepG2 cells were prepared as described previously (38).

Protein isolation and analysis by Western blot

Protein isolation from murine liver tissue was done according to Tybl et al. (24), whereas protein isolation from cells was according to Basirico et al. (39).

Protein separation and detection were peformed as previously described (24). Information on the used antibodies and conditions can be found in the supplemental data Table III. The primary antibodies anti-ELOVL6 and anti-α–tubulin were purchased from Sigma Aldrich (PRS4571, T9026, Taufkirchen, Germany), anti-SREBF1 and anti-PPARA from Abcam (ab3259, ab8934, Cambridge, United Kingdom), anti-FASN, anti-lamin A/C antibody from Cell Signaling Technology (#3180, #2032, Danvers, USA), anti-p62 antibody was kindly provided by Dr. Tan (TSRI, La Jolla, CA, USA) (30, 40).

Palmitoyl-CoA extraction and analyses with ultra high-performance liquid chromatography–mass spectrometry (UHPLC-MS/MS)

Fresh snap-frozen liver tissue was immediately freeze-dried and homogenized and stored at –80°C. 40 mg of freeze-dried tissue was extracted for 30 minutes in 1 ml methanol containing *n*-heptadecanoyl-CoA as internal standard (with a final concentration of 500 nM in 150 µl final volume). The extract was centrifuged at 22,000 *g* for 10 min and 4°C. The supernatant was transferred to a new vial and dried under gaseous nitrogen and reconstituted in 150 µl methanol / water (1:1 [v/v]). The standard dilution series was made in methanol / water (1:1 [v/v]). All steps were performed on ice.

The analyses were performed using a TSQ Access Max mass spectrometer equipped with an ESI source and a triple quadrupole mass detector (Thermo Finnigan, San Jose, CA). The MS detection was carried out in heated ESI mode, at a spray voltage of 4.5 kV, a probe temperature of 400 °C, a nitrogen sheath gas pressure of 3.0×10^5 Pa, an auxiliary gas pressure of 1.0×10^5 Pa, a capillary temperature of 350 °C, and a tube lens voltage of 114 V in negative ionization mode. Palmitoyl coenzyme A lithium salt (P9716-5MG) and *n*-heptadecanoyl coenzyme A lithium salt (H1385-5MG) were purchased from Sigma Aldrich (Taufkirchen, Germany).

Xcalibur software was used for data acquisition and plotting.

The chromatographic separation was carried out on an Accela UPLC, consisting of a quaternary pump, degasser, and autosampler (Thermo Finnigan, San Jose, CA) using a Accucore RP-MS column (150x2.1, 2.6µm), with an injection volume of 25 µl.
The solvent system consisted of 10 mM ammonium acetate (A) and methanol (B).
HPLC-Method: Gradient run of initial 65% of B in A and a flow of 600 µl/min. In 0.6 min the solvent mixture was changed to 100% of B, with a flow of 700 µl/min and kept for 3.4 min.
The amounts of palmitoyl-CoA and the internal standard n-heptadecanoyl-CoA were each determined in single reaction monitoring mode using the following transitions:
Palmitoyl-CoA: precursor ion 1005.992 m/z; product ion 672.075 m/z; scan time 0.5 sec; scan width 3.000 m/z; collision voltage 44 V.
Heptadecanoyl-CoA (ISTD): precursor ion 992.228 m/z; product ion 926.442 m/z; scan time 0.5 sec; scan width 3.000 m/z; collision voltage 42 V.
Palmitoyl-CoA, with a retention time of 2.27 min, was quantified using the chromatographic peak area relative to the internal standard (Retention time 2.17 min). The lower limit of quantitation was 2.1 nM. The measurement was performed with wild-type livers (n=9) and livers of *p62* transgenic animals (n=10). Supplemental data Fig I shows the measurement of a representative Palmitoyl-CoA dilution series. Supplemental data Fig II (online) shows a representative measurement of Palmitoyl-CoA extracted from mouse liver.

Statistical analysis

Results are expressed as means ± SEM. The statistical significance was determined by independent two-sample t-test. Pearson's correlation was used to test the relationship between *p62*, *IGF2*, *ELOVL6*, and *FASN* mRNA in human liver samples.
The results were considered as statistically significant when p value was less than 0.05.

2.2.6 Results

Characterization of steatosis

Liver-specific overexpression of p62 has previously been shown to induce histologically detectable steatotic features in about 60% of the animals (24) (Fig 1A).
Previous data suggested no distinct inflammation in *p62* transgenic animals since we observed no elevated liver damage (24). Still, immunohistochemical staining and real-time RT-PCR revealed elevated levels of the macrophage marker F4/80 in *p62* transgenic livers (Fig 1B, C).

18.2% of *p62* transgenic animals exhibited distinct leukocyte infiltrates (2-3 infiltrates per microscopic field, magnification 100x), which were not observed in wild-type animals.

Our previous data indicated slightly improved glucose tolerance of *p62* transgenic animals (24). We now performed hyperinsulinemic euglycemic clamp analysis: Both, the higher glucose infusion rate and lower hepatic glucose production with unchanged glucose turnover indicated elevated hepatic insulin sensitivity. However, these results were not statistically significant (Fig 1D).

Quantification of fatty acid composition revealed that also transgenic animals, which exhibited a normal histology, showed an increased fatty acid content (Table 1). Still, the fatty acid content was even higher in animals with a histologically proven steatosis (Table 1). Taking all *p62* transgenic animals together, we observed a 1.66 ± 0.12 fold ($p = 0.0007$) increase of the total fatty acid content compared to wild-type animals. Having a closer look at the composition of the fatty acids, we observed that the chain length of fatty acids was different in *p62* transgenic livers compared to wild-type tissue: steatotic livers exhibited an increased ratio of C18 to C16 fatty acids (Fig 1E).

Fatty acid	wt	*p62* tg normal histology		*p62* tg microvesicular steatosis	
	[µg / mg dry tissue]	[µg / mg dry tissue]	p *vs.* wt	[µg / mg dry tissue]	p *vs.* wt
12:0	0.05±0.05	0.26±0.13	0.205	0.81±0.18	0.0016
14:0	0.32±0.11	0.65±0.29	0.344	2.08±0.38	0.0009
16:0	16.7±0.77	21.82±1.99	0.050	28.72±1.75	0.00002
16:1	0.04±0.03	0.10±0.06	0.441	0.69±0.12	0.0003
18:0	11.7±0.20	14.04±0.71	0.018	14.24±0.54	0.0008
18:1	5.54±0.47	9.98±1.84	0.061	19.34±1.76	0.000007
18:2	9.75±0.62	16.69±2.49	0.035	30.12±2.76	0.00002
20:1	n.d.	0.06±0.05	0.351	0.20±0.09	0.0455
20:2	0.34±0.07	0.43±0.14	0.611	1.11±0.17	0.0010
20:3	0.29±0.07	0.61±0.17	0.135	1.47±0.19	0.00006
20:4	10.9±0.26	10.17±0.86	0.461	13.47±0.65	0.0032
20:5	n.d.	n.d.		0.08±0.08	0.3409
22:4	0.11±0.07	0.16±0.11	0.698	0.88±0.21	0.0038
22:5	2.20±0.92	0.98±0.64	0.340	3.31±0.66	0.3781
22:6	1.55±0.52	1.00±0.30	0.413	0.83±0.22	0.2663
sum FA	59.5±2.57	76.94±8.03	0.072	117.3±9.76	0.000028

Table 1. p62-induced changes in murine hepatic fatty acids. Livers of wild-type (wt, n=7) and *p62* transgenic (*p62* tg, n=19, n=8 normal histology, n=11 microvesicular steatotic histology) mice were analyzed by GC-MS. p values indicate differences compared to values in livers of wt animals.

In order to study the mechanisms responsible for hepatic lipid alterations we employed HepG2 cells, which are able to develop cellular steatosis and are frequently used for respective mechanistic studies (15, 41-44). The fatty acid chain length in fact depended on the presence of p62: when p62 was knocked down in HepG2 cells, increased levels of C16 fatty acids were detectable (Table 2), so that the ratio of C18 to C16 fatty acids decreased (Fig 1F). We therefore investigated the effect of p62 on ELOVL6, which catalyses the elongation of C16 to C18 fatty acids (17).

Fatty acid	si co [µg / mg lyophilized cells]	si p62 [µg / mg lyophilized cells]	p
16:0	20.06±0.91	29.21±1.93	0.03
16:1	5.40±1.32	8.01±1.53	0.12
18:0	8.98±1.3	10.04±1.88	0.71
18:1	36.08±5.17	40.58±2.52	0.55
18:2	1.63±0.21	1.31±0.25	0.57

Table 2. p62-induced changes in HepG2 fatty acids. HepG2 cells treated with random siRNA (si co) and p62 siRNA (si p62) were analyzed by GC-MS. p values indicate differences compared to si co treated HepG2 cells (n=3, duplicate).

We observed that ELOVL6 is induced in a p62-dependent fashion: *p62* transgenic animals displayed significantly increased levels of ELOVL6 protein (Fig 1G). *Vice versa*, knockdown of p62 in HepG2 cells exhibited significantly reduced ELOVL6 mRNA and protein levels (Fig 1H). The dependency of ELOVL6 expression on p62 in human livers was supported by a strong correlation of *p62*/*ELOVL6* expression (Fig 1H).

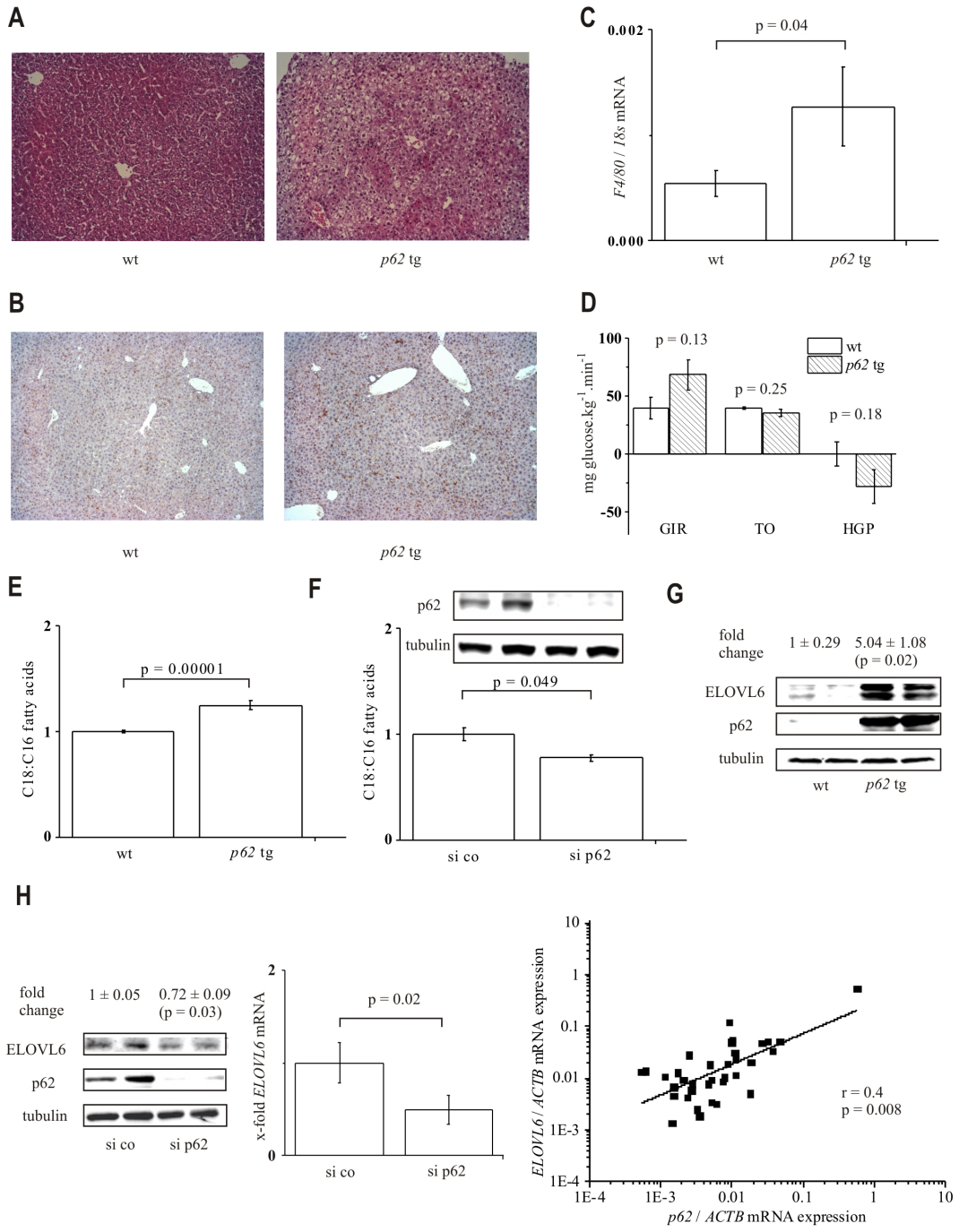

Figure 1. p62-induced steatosis, C18:C16 ratio, and ELOVL6 expression.
A. HE staining of wild-type (wt) and *p62* transgenic liver tissue (*p62* tg) (original magnification 100x).
B. F4/80 staining of wt and *p62* tg liver tissue (original magnification 100x).
C. F4/80 real-time RT-PCR of wild-type (wt) and *p62* transgenic (*p62* tg) livers (n=13, each).
D. Hyperinsulinemic euglycemic clamp study in wt (n=3) and *p62* tg (n=4) mice: glucose infusion rate (GIR), glucose turnover (TO), and hepatic glucose production (HGP). Data show mean ± SEM.
E. Hepatic C18:C16 fatty acid ratio: wt: n=10, *p62* tg: n=19.

F. C18:C16 fatty acid ratio and Western Blot of the transfection control (72 h) in HepG2 cells transfected with random siRNA (si co) or p62 siRNA (si p62) (n=3, duplicate)
G. Representative ELOVL6 Western blot of wt and *p62* tg mice (n=5, each).
H. ELOVL6 Western blot (n=3, duplicate, left) and real-time RT-PCR (n=2, triplicate, middle) of HepG2 transfected with si co or si p62 for ELOVL6, Right: Real-time RT-PCR for *ELOVL6* and *p62* of 35 liver tissues normalized on *ACTB* mRNA levels.

Expression of lipogenic regulators

Surprisingly, *MLXIPL* mRNA expression was significantly upregulated in p62 siRNA-treated HepG2 cells (Fig 2A) and downregulated in cells overexpressing p62 (Fig 2A). We could validate this effect in *p62* tg animals, in which MLXIPL was significantly downregulated (15% ± 8%, p = 0.0497, n = 5 in each group). Looking at *NR1H3* mRNA expression as another lipogenic transcription factor in either p62 overexpressing or p62 siRNA cells, we did not observe any significant difference (Fig 2A). The same was true for *SREBF1c* mRNA (Fig 2A).

In addition to transcriptional regulation (45, 46), SREBF1 can be activated by cleavage from its precursor to its mature form upon insulin treatment (38). Because p62 has been demonstrated to upregulate *IGF2* in both mouse (24) as well as in human livers (27), we hypothesized that p62 regulates SREBF1 on protein level. We observed significantly increased levels of the mature isoform of SREBF1 after overexpression of p62 in HepG2 (Fig 2B). The SREBF1 mature form in *p62* transgenic mice behaved similarly, but quantified values were not statistically significant (Fig 2C). The precursor showed neither an induction in p62 overexpressing HepG2 (Fig 2B) nor in *p62* transgenic mice (Fig 2C). Knockdown of p62 by siRNA resulted in reduced levels of both the SREBF1 precursor as well as the mature form of SREBF1 (Fig 2B).

Suggesting IGF2 to be responsible for SREBF1 activation, we treated HepG2 cells with IGF2, and indeed observed higher amounts of mature SREBF1 in their nuclei (Fig 2D). Antagonization of IGF2 activity with an IGF2 specific antibody in HepG2 reduced the levels of ELOVL6 and the nuclear form of SREBF1 compared to their respective controls (Fig 2E). In human liver tissue, in which p62 and ELOVL6 correlated, we also observed a distinct correlation of IGF2 and ELOVL6 expression levels (Fig 2F). In the same tissues (n = 35) we could confirm a correlation between p62 and IGF2 (r = 0.41, p = 0.02) as recently reported for a cohort of HCC patients (27).

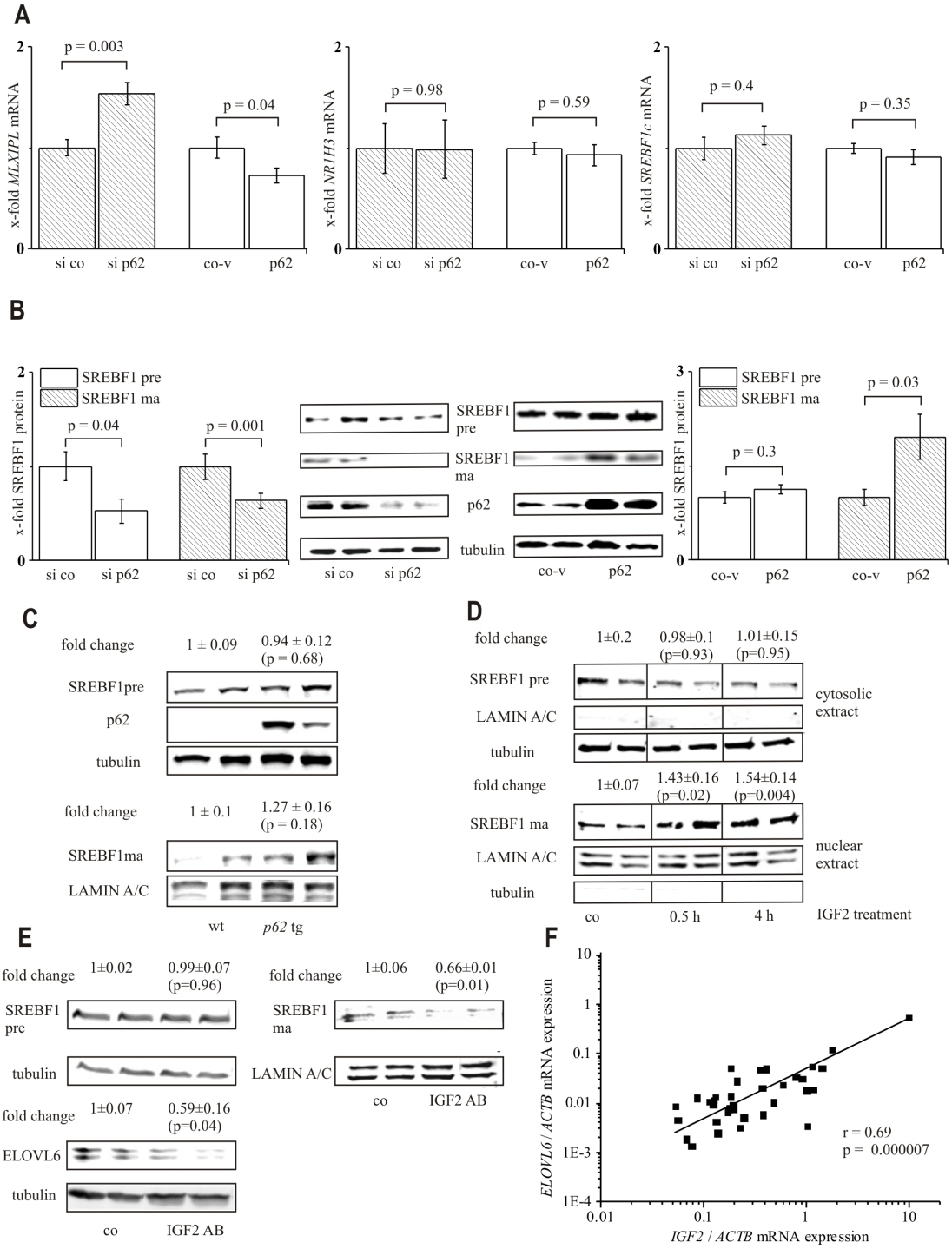

Figure 2. Implications of p62 on lipogenic pathways.
Real-time RT-PCR (n=3-6, triplicate, A) or Western blot (n=3, duplicate, B) of HepG2 transfected with either p62 siRNA (si p62) or p62 overexpression vector (p62) and their respective controls (si co, co-v).
A. *MLXIPL*, *NR1H3*, and *SREBF1c* mRNA.
B. Precursor (SREBF1 pre) and mature SREBF1 (SREBF1 ma).
C. SREBF1 pre and SREBF1 ma Western blot of wild-type (wt) and *p62* transgenic (*p62* tg) livers (n=6).
D. SREBF1 pre and SREBF1 ma Western blot on cytosolic and nuclear proteins of HepG2 treated with IGF2 (n=9, duplicate).

E. SREBF1 pre and SREBF1 ma and ELOVL6 Western blot on cytosolic and nuclear proteins of HepG2 (co) incubated with neutralizing IGF2 antibody (IGF2 AB, 48 h) (n=4, duplicate).
F. Real-time RT-PCR for *ELOVL6* and *p62* of 35 liver tissues normalized on *ACTB* mRNA levels.

The fatty acid synthase (FASN) as an important lipogenic enzyme displays also a target of SREBF1 activation, which is why we hypothesized that p62-induced lipid accumulation might be mediated *via* FASN induction. Interestingly, however, *FASN* mRNA and protein levels were not changed upon p62 overexpression and increased upon p62 knockdown (Fig 3A, B). Concordantly, the *p62* transgenics revealed reduced levels of FASN protein (Fig 3C). The analysis of human liver samples showed no correlation between *p62* and *FASN* mRNA ($r = -0.1$, $p = 0.58$). To reassess the unforeseen behaviour of the direct SREBF1 target FASN, we had a closer look on stearoyl-CoA desaturase (delta-9-desaturase) (*SCD1*, *SCD)* and acetyl-CoA carboxylase alpha (*ACC*, *ACACA*) mRNA, which are SREBF1 targets and important enzymes in lipogenesis. Interestingly, neither p62 knockdown nor p62 overexpression revealed changes in *SCD* or *ACACA* mRNA levels (Fig 3D). Since most lipogenic genes are coordinately regulated by SREBF1 and MLXIPL (47), we speculated that inversely regulated MLXIPL action might reverse the action of activated SREBF1. Therefore, we had a closer look on pyruvate kinase, liver and RBC (L-PK, PKLR) expression, which is exclusively regulated by MLXIPL (48). Indeed, p62 regulation of *PKLR* mRNA exhibited the same expression pattern compared to *MLXIPL* mRNA: *PKLR* mRNA was increased after p62 knockdown and decreased after p62 overexpression (Fig 3E).

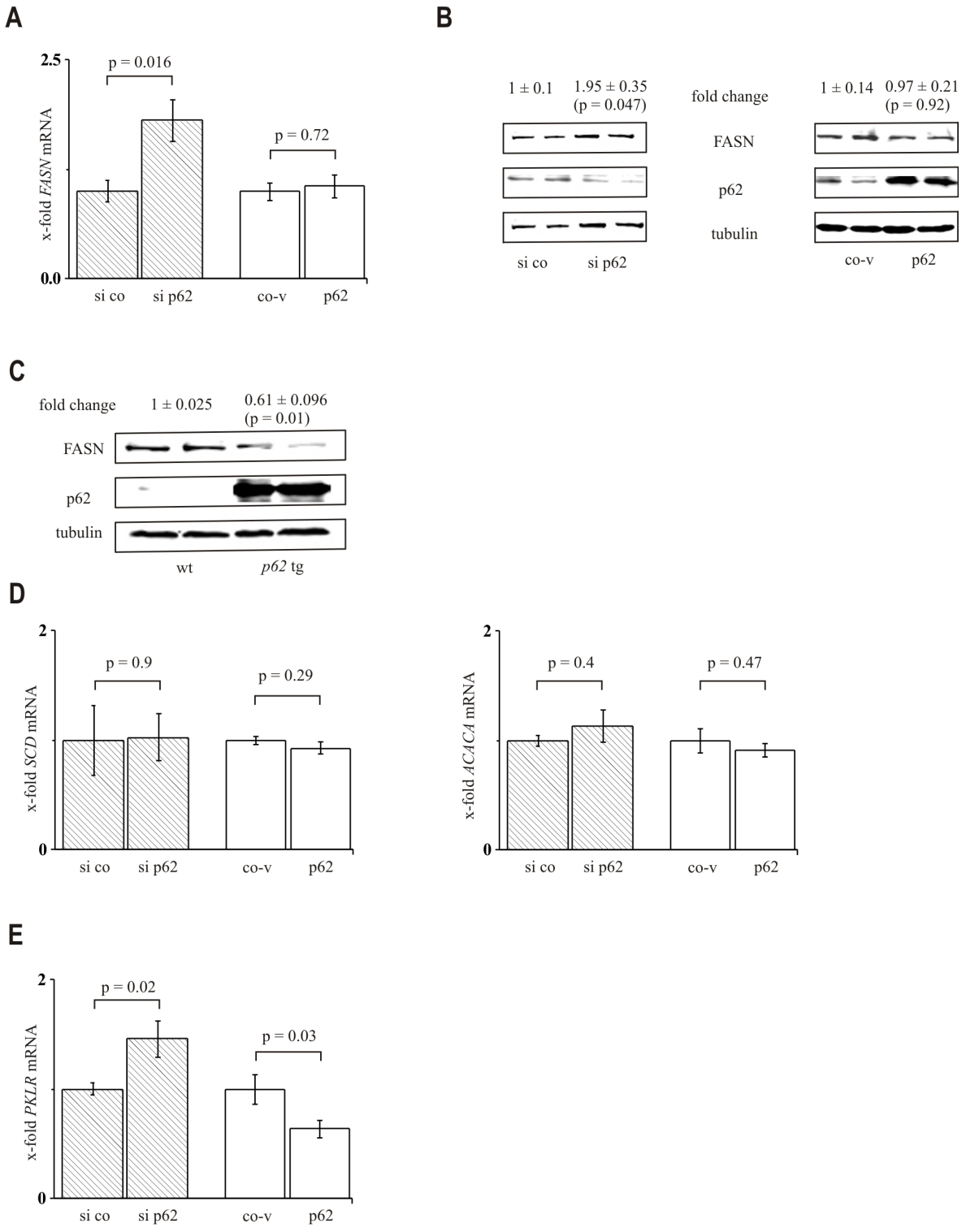

Figure 3. Effect of p62 on lipogenic genes.

A. *FASN* real-time RT-PCR of HepG2 transfected with either p62 siRNA (si p62, n=3, triplicate) or p62 overexpression vector (p62, n=5, triplicate) and their respective controls (si co, co-v).

B. FASN Western blot of HepG2 transfected with si p62 or p62 (n=3, duplicate).

C. Representative FASN Western blot of wild-type (wt) and *p62* transgenic (*p62* tg) livers (n=5, each).

D. *SCD* and *ACACA* real-time RT-PCR of HepG2 transfected with either p62 siRNA (n=3, triplicate) or p62 overexpression vector (n=5, triplicate) and their respective controls.

E. *PKLR* real-time RT-PCR of HepG2 transfected with either p62 siRNA (n=4, triplicate) or p62 overexpression vector (n=5, triplicate) and their respective controls.

Regulation of lipolytic pathways

Our data as yet suggested a distinct action of p62 on fatty acid composition (i.e. chain length), but rather no effect on lipogenic enzymes. We therefore suggested that the elevated levels of lipids in p62 livers might rather be facilitated by a decreased β-oxidation. We therefore tested *PPARA* expression upon both p62 knockdown and overexpression in human hepatoma cells, and in *p62* transgenic mice. The data revealed a downregulation of *PPARA* mRNA after p62 overexpression in cells (Fig 4A) and a lack of effect in the *p62* transgenic mouse model (Fig 4B). Therefore, the investigation of PPARA expression does not provide conclusive data on a potentially decreased β-oxidation due to p62.

Mitochondrial β-oxidation is regulated by carnitine palmitoyltransferase 1A (CPT1A) activity (Fig 4C), which is controlled by malonyl-CoA. Malonyl-CoA levels depend on the palmitoyl-CoA-mediated inhibition of acetyl-CoA carboxylase alpha (ACACA). Malonyl-CoA levels were below the detection limit of UHPLC-MS/MS analysis. Still, reduced palmitoyl-CoA levels (37 ± 12%) as found in *p62* transgenic animals suggested that attenuated mitochondrial β-oxidation is responsible for ELOVL6-induced steatosis.

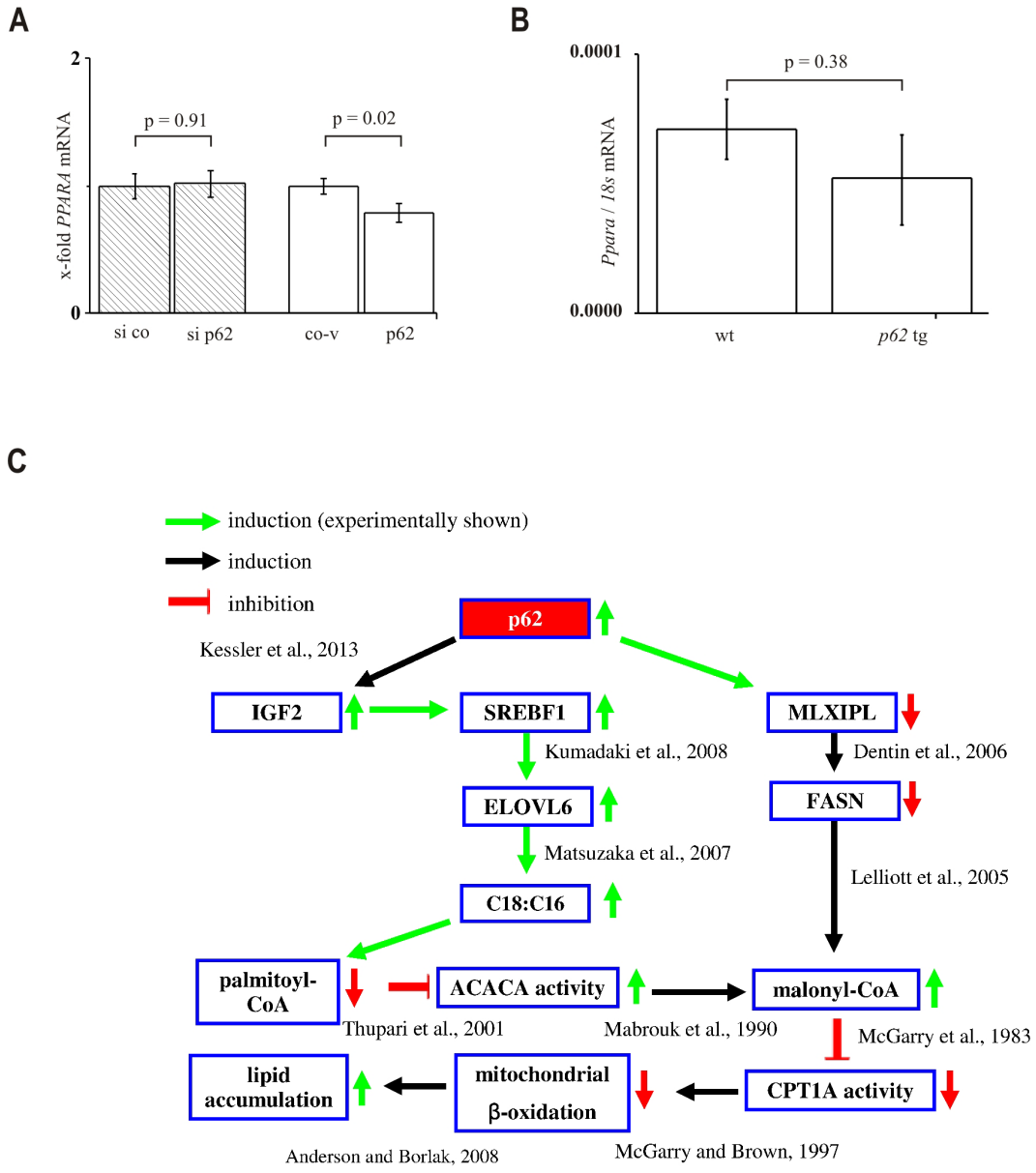

Figure 4. Implications of p62 on lipolytic pathways and summary.
A. *PPARA* real-time RT-PCR of HepG2 transfected with either p62 siRNA (si p62, n=3, triplicate) or p62 overexpression vector (p62, n=5, triplicate) and their respective controls (si co, co-v).
B. *PPARA* real-time RT-PCR of wild-type (wt) and *p62* transgenic (*p62* tg) livers (n=5, each).
C. p62 overexpression decreases FASN expression by MLXIPL depletion and induces IGF2 expression. Reduced FASN levels lead to malonyl-CoA accumulation. IGF2 promotes the maturation of SREBF1, which increases ELOVL6 expression, leading to an increased C18 to C16 ratio. The reduced inhibition of palmitoyl-CoA on ACACA activity elevates malonyl-CoA levels, which inhibit the CPT1A-activity and therefore mitochondrial β-oxidation.

2.2.7 Discussion

The p62-induced steatosis is characterized by an increase in almost all lipid classes with the most distinct effect on triglycerides (26). Accordingly, we here observe an elevated abundance of almost all fatty acids (Table 1). Due to unchanged serum cholesterol and triglyceride levels in *p62* transgenics compared to wild-type animals (24) it is unlikely that hepatic lipid accumulation is due to reduced lipid export from the liver or increased lipid uptake.

Excess hepatic lipid incorporation is often associated with inflammatory events, which link a simple steatosis to NASH (6). We here show that *p62* transgenic mice also display inflammatory signs, as validated by increased F4/80 and leukocyte infiltrates. The inflammation is rather mild, though, and does not result in elevated transaminase levels (24), which might also be linked to cytoprotective actions of p62 (27). Despite lipid accumulation and an inflammatory environment, development of insulin resistance is absent in *p62* transgenic mice confirming our previous data (24), which suggest slightly elevated glucose tolerance.

In addition to the general increase in lipids in *p62* transgenic livers we could observe an increased ratio of C18 to C16 fatty acids. Accordingly, ELOVL6, which catalyzes the elongation of C16 to C18 fatty acids (17), is increased in *p62* transgenic mice. Our results from HepG2 cells and human liver tissues are in line with these findings. Recently, Matsuzaka et al. reported that overexpression of ELOVL6 promotes NASH in mice and humans (20). What is more, ELOVL6 expression specifically characterizes steatotic events being linked to inflammation (21, 22). This is in line with the finding that p62 transgenic mice, which both exhibit increased levels of ELOVL6 and show signs of liver inflammation.

Pathways being responsible for the upregulation of this pathophysiological regulator of liver disease have as yet been unknown. SREBF1 is an important transcription factor that regulates lipid metabolism and contributes to the pathophysiology of the metabolic syndrome (49, 50). Our data demonstrate a p62-dependent cleavage of SREBF1 into its active form. SREBF1 gene expression as well as its cleavage-induced activation is enhanced by insulin, leading to its binding to sterol-response element, which is located in the promoters of its target genes (51). HepG2 cells, in which the transcriptional regulator of SREBF1 NR1H3 was activated, displayed increased *SREBF1c* mRNA levels (52-54), whereas SREBF1a expression, the dominant isoform in cultured hepatocytes (55), was not regulated by NR1H3 activation (54, 56, 57). Since neither p62 knockdown nor p62 overexpression showed any effect on *NR1H3* expression, it is hardly surprising that *SREBF1c* mRNA levels were not affected by p62.

IGF1 and insulin treatment have been shown to induce SREBF1 in sebocytes *via* activation of the insulin- and IGF1-receptor (58). IGF2 binds to insulin receptor, IGF1-receptor, and IGF2-receptor, with moderate to high affinity (45). Human hepatoma cell lines overexpressing p62 and *p62* transgenic animals have been shown to express high levels of *IGF2* mRNA (24, 27). We here report a p62-mediated induction of SREBF1 and ELOVL6, which depends on IGF2 expression. This causal link is supported by the correlation of *p62*, *IGF2*, and *ELOVL6* expression in human liver tissue.

Our data revealed an upregulation of *MLXIPL* by p62 knockdown, while SREBF1 is inactivated. *Vice versa*, a *MLXIPL* downregulation occurs after p62 overexpression, while SREBF1 is activated. In fact, the literature reports that SREBF1 overexpression reduces *MLXIPL* expression (41). Since MLXIPL knockout animals show improved plasma glucose control (48, 59), the improved glucose tolerance exhibited in *p62* transgenic animals (24) can be explained by MLXIPL downregulation and increased Igf2 levels.

Although SREBF1 can induce FASN (41), we observed that p62 decreased FASN levels, while SREBF1 was activated. The effects of p62-induced SREBF1 activation seems to be abrogated by the parallel decreased MLXIPL expression, which is in line with the finding that 50% of lipogenic gene expression is associated to MLXIPL (9). Interestingly, the p62 model is characterized by a higher sensitivity of ELOVL6 towards SREBF1 activation than to MLXIPL depletion. FASN, on the other hand, is stronger affected by attenuated MLXIPL levels. In this context, Yu et al. recently reported that human fibroblasts, in which MLXIPL was knocked down by a lentiviral short hairpin RNA plasmid showed strongly decreased levels of *FASN* mRNA expression, but rather no effect on *ELOVL6* expression (60) suggesting that MLXIPL shows stronger transcriptional activation towards FASN than to ELOVL6. PKLR, which is uniquely induced by MLXIPL (61), is reversely regulated by p62 and is therefore convergent to the *MLXIPL* expression.

Despite the effect of p62 on FASN in HepG2 and in the murine mouse model, we could not detect any correlation between *p62* and *FASN* expression in human liver samples. Also published data showed no elevation of FASN in human NAFLD (62). Concordantly, Donnelly et al. reported that *de novo* lipogenesis only to a minor extent contributes to elevated hepatic lipids as found in human NAFLD (63).

In line with these findings, the literature describes that liver-specific knockout of FASN did not rescue the animals from the development of a fatty liver (64) and Jones et al. recently reported the development of steatosis in TSC22D4 overexpressing mice despite decreased *FASN* mRNA levels (65). Most interestingly, also animals overexpressing ELOVL6 show

increased liver triglycerides and at the same time reduced FASN expression (20). Therefore, fatty acid synthesis appears not to be the pivotal step in p62-mediated steatosis development.

One of the important inducers of peroxisomal and mitochondrial β-oxidation pathways in the liver is PPARA (10). PPARA agonists like fenofibrate reduce steatosis in mice with a hereditary fatty liver (66). PPARA is downregulated in p62 overexpressing HepG2, but not in the *p62* transgenics, suggesting that p62 does not facilitates lipolysis *via* PPARA. We suggest that p62 induces high fatty acid levels due to elevated malonyl-CoA levels. Indeed, the mitochondrial β-oxidation pathway as the central lipolytic pathway is negatively regulated by high malonyl-CoA levels (67). ELOVL6 can elevate malonyl-CoA since it reduces the levels of its substrate palmitoyl-CoA in *p62* transgenic mice (Fig 4C). Since fatty acids in *p62* transgenic mice are mostly bound in triglycerides (26) and only free fatty acids are converted to acyl-CoAs (68), triglyceride-bound palmitic acid can not be converted into palmitoyl-CoA. Whereas high levels of palmitoyl-CoA inhibit the activity of the enzyme responsible for malonyl-CoA synthesis (69), i.e. acetyl-CoA carboxylase alpha (ACACA) (67), low levels promote the generation of malonyl-CoA *via* ACACA. Consequently, the mitochondrial β-oxidation is reduced due to malonyl-CoA-mediated attenuation in CPT1A activity (70) (Fig 4C). Pharmacological inhibition of CPT1A is associated with the development of steatosis and steatohepatitis (71, 72). Furthermore, a tamoxifen-induced steatosis in rats, which strongly inhibited *FASN* expression, was characterised by an accumulation of malonyl-CoA and therefore decreased CPT1A activity (73) (Fig 4C).

In summary, our data provide evidence of p62 as an inducer of ELOVL6, a pathophysiological promoter of NASH. ELOVL6 overexpression results in a subsequent production of a deleterious fatty acid profile, which finally induces hepatic steatosis (Fig 4C). This study underlines the detrimental role of p62 in liver disease.

2.2.8 Acknowledgments

The project was funded, in part, by the Graduiertenförderung of Saarland University (SL), an EASL Dame Sheila Sherlock Fellowship, the Boehringer Ingelheim Fonds, and by the research committee of Saarland University (61-cl/Anschub2012)(to SMK).

2.2.9 References

1. de Alwis, N. M., and C. P. Day. 2008. Non-alcoholic fatty liver disease: the mist gradually clears. *J Hepatol* **48 Suppl 1**: S104-112.
2. Erickson, S. K. 2009. Nonalcoholic fatty liver disease. *J Lipid Res* **50 Suppl**: S412-416.
3. Adams, L. A., O. R. Waters, M. W. Knuiman, R. R. Elliott, and J. K. Olynyk. 2009. NAFLD as a risk factor for the development of diabetes and the metabolic syndrome: an eleven-year follow-up study. *Am J Gastroenterol* **104**: 861-867.
4. Adams, L. A., P. Angulo, and K. D. Lindor. 2005. Nonalcoholic fatty liver disease. *Cmaj* **172**: 899-905.
5. Angulo, P. 2002. Nonalcoholic fatty liver disease. *N Engl J Med* **346**: 1221-1231.
6. Day, C. P. 2006. From fat to inflammation. *Gastroenterology* **130**: 207-210.
7. Malhi, H., and G. J. Gores. 2008. Molecular mechanisms of lipotoxicity in nonalcoholic fatty liver disease. *Semin Liver Dis* **28**: 360-369.
8. Musso, G., R. Gambino, and M. Cassader. 2009. Recent insights into hepatic lipid metabolism in non-alcoholic fatty liver disease (NAFLD). *Prog Lipid Res* **48**: 1-26.
9. Iizuka, K., and Y. Horikawa. 2008. ChREBP: a glucose-activated transcription factor involved in the development of metabolic syndrome. *Endocr J* **55**: 617-624.
10. Lefebvre, P., G. Chinetti, J. C. Fruchart, and B. Staels. 2006. Sorting out the roles of PPAR alpha in energy metabolism and vascular homeostasis. *J Clin Invest* **116**: 571-580.
11. Wakil, S. J., and L. A. Abu-Elheiga. 2009. Fatty acid metabolism: target for metabolic syndrome. *J Lipid Res* **50 Suppl**: S138-143.
12. McGarry, J. D., S. E. Mills, C. S. Long, and D. W. Foster. 1983. Observations on the affinity for carnitine, and malonyl-CoA sensitivity, of carnitine palmitoyltransferase I in animal and human tissues. Demonstration of the presence of malonyl-CoA in non-hepatic tissues of the rat. *Biochem J* **214**: 21-28.
13. Puri, P., M. M. Wiest, O. Cheung, F. Mirshahi, C. Sargeant, H. K. Min, M. J. Contos, R. K. Sterling, M. Fuchs, H. Zhou, S. M. Watkins, and A. J. Sanyal. 2009. The plasma lipidomic signature of nonalcoholic steatohepatitis. *Hepatology* **50**: 1827-1838.
14. Puri, P., R. A. Baillie, M. M. Wiest, F. Mirshahi, J. Choudhury, O. Cheung, C. Sargeant, M. J. Contos, and A. J. Sanyal. 2007. A lipidomic analysis of nonalcoholic fatty liver disease. *Hepatology* **46**: 1081-1090.
15. Miyoshi, H., K. Moriya, T. Tsutsumi, S. Shinzawa, H. Fujie, Y. Shintani, H. Fujinaga, K. Goto, T. Todoroki, T. Suzuki, T. Miyamura, Y. Matsuura, H. Yotsuyanagi, and K. Koike. 2011. Pathogenesis of lipid metabolism disorder in hepatitis C: polyunsaturated fatty acids counteract lipid alterations induced by the core protein. *J Hepatol* **54**: 432-438.
16. Kim, K. H., H. J. Shin, K. Kim, H. M. Choi, S. H. Rhee, H. B. Moon, H. H. Kim, U. S. Yang, D. Y. Yu, and J. Cheong. 2007. Hepatitis B virus X protein induces hepatic steatosis via transcriptional activation of SREBP1 and PPARgamma. *Gastroenterology* **132**: 1955-1967.
17. Matsuzaka, T., H. Shimano, N. Yahagi, T. Kato, A. Atsumi, T. Yamamoto, N. Inoue, M. Ishikawa, S. Okada, N. Ishigaki, H. Iwasaki, Y. Iwasaki, T. Karasawa, S. Kumadaki, T. Matsui, M. Sekiya, K. Ohashi, A. H. Hasty, Y. Nakagawa, A. Takahashi, H. Suzuki, S. Yatoh, H. Sone, H. Toyoshima, J. Osuga, and N. Yamada. 2007. Crucial role of a long-chain fatty acid elongase, Elovl6, in obesity-induced insulin resistance. *Nat Med* **13**: 1193-1202.
18. Kumadaki, S., T. Matsuzaka, T. Kato, N. Yahagi, T. Yamamoto, S. Okada, K. Kobayashi, A. Takahashi, S. Yatoh, H. Suzuki, N. Yamada, and H. Shimano. 2008.

Mouse Elovl-6 promoter is an SREBP target. *Biochem Biophys Res Commun* **368**: 261-266.

19. Wang, C. Y., D. S. Stapleton, K. L. Schueler, M. E. Rabaglia, A. T. Oler, M. P. Keller, C. M. Kendziorski, K. W. Broman, B. S. Yandell, E. E. Schadt, and A. D. Attie. 2012. Tsc2, a positional candidate gene underlying a quantitative trait locus for hepatic steatosis. *J Lipid Res* **53**: 1493-1501.
20. Matsuzaka, T., A. Atsumi, R. Matsumori, T. Nie, H. Shinozaki, N. Suzuki-Kemuriyama, M. Kuba, Y. Nakagawa, K. Ishii, M. Shimada, K. Kobayashi, S. Yatoh, A. Takahashi, K. Takekoshi, H. Sone, N. Yahagi, H. Suzuki, S. Murata, M. Nakamuta, N. Yamada, and H. Shimano. 2012. Elovl6 promotes nonalcoholic steatohepatitis. *Hepatology* **56**: 2199-2208.
21. Muir, K., A. Hazim, Y. He, M. Peyressatre, D. Y. Kim, X. Song, and L. Beretta. 2013. Proteomic and Lipidomic Signatures of Lipid Metabolism in NASH-Associated Hepatocellular Carcinoma. *Cancer Res* **73**: 4722-4731.
22. Kessler, S. M., Y. Simon, K. Gemperlein, K. Gianmoena, C. Cadenas, V. Zimmer, J. Pokorny, A. Barghash, V. Helms, N. van Rooijen, R. M. Bohle, F. Lammert, J. G. Hengstler, R. Mueller, J. Haybaeck, and A. K. Kiemer. 2014. Fatty acid elongation in non-alcoholic steatohepatitis and hepatocellular carcinoma. *Int J Mol Sci in Press*.
23. Kessler, S. M., S. Laggai, A. Barghash, V. Helms, and A. K. Kiemer. 2014. Lipid Metabolism Signatures in NASH-Associated HCC - Letter. *Cancer res in Press* [doi: 10.1158/0008-5472.CAN-13-2852].
24. Tybl, E., F. D. Shi, S. M. Kessler, S. Tierling, J. Walter, R. M. Bohle, S. Wieland, J. Zhang, E. M. Tan, and A. K. Kiemer. 2011. Overexpression of the IGF2-mRNA binding protein p62 in transgenic mice induces a steatotic phenotype. *J Hepatol* **54**: 994-1001.
25. Simon, Y., S. M. Kessler, R. M. Bohle, J. Haybaeck, and A. K. Kiemer. 2013. The insulin-like growth factor 2 (IGF2) mRNA-binding protein p62/IGF2BP2-2 as a promoter of NAFLD and HCC? *Gut, 2014*, **63**, 861-863..
26. Laggai, S., Y. Simon, T. Ranssweiler, A. K. Kiemer, and S. M. Kessler. 2013. Rapid chromatographic method to decipher distinct alterations in lipid classes in NAFLD/NASH. *World J Hepatol* **5**: 558-567.
27. Kessler, S. M., J. Pokorny, V. Zimmer, S. Laggai, F. Lammert, R. M. Bohle, and A. K. Kiemer. 2013. IGF2 mRNA binding protein p62/IMP2-2 in hepatocellular carcinoma: antiapoptotic action is independent of IGF2/PI3K signaling. *Am J Physiol Gastrointest Liver Physiol* **304**: G328-G336.
28. Qian, H. L., X. X. Peng, S. H. Chen, H. M. Ye, and J. H. Qiu. 2005. p62 Expression in primary carcinomas of the digestive system. *World J Gastroenterol* **11**: 1788-1792.
29. Zhang, J., and E. K. Chan. 2002. Autoantibodies to IGF-II mRNA binding protein p62 and overexpression of p62 in human hepatocellular carcinoma. *Autoimmun Rev* **1**: 146-153.
30. Zhang, J. Y., E. K. Chan, X. X. Peng, and E. M. Tan. 1999. A novel cytoplasmic protein with RNA-binding motifs is an autoantigen in human hepatocellular carcinoma. *J Exp Med* **189**: 1101-1110.
31. Tovar, V., C. Alsinet, A. Villanueva, Y. Hoshida, D. Y. Chiang, M. Sole, S. Thung, S. Moyano, S. Toffanin, B. Minguez, L. Cabellos, J. Peix, M. Schwartz, V. Mazzaferro, J. Bruix, and J. M. Llovet. 2010. IGF activation in a molecular subclass of hepatocellular carcinoma and pre-clinical efficacy of IGF-1R blockage. *J Hepatol* **52**: 550-559.
32. Chiappini, F., A. Barrier, R. Saffroy, M. C. Domart, N. Dagues, D. Azoulay, M. Sebagh, B. Franc, S. Chevalier, B. Debuire, S. Dudoit, and A. Lemoine. 2006.

Exploration of global gene expression in human liver steatosis by high-density oligonucleotide microarray. *Lab Invest* **86**: 154-165.

33. Christiansen, J., A. M. Kolte, T. Hansen, and F. C. Nielsen. 2009. IGF2 mRNA-binding protein 2: biological function and putative role in type 2 diabetes. *J Mol Endocrinol* **43**: 187-195.
34. Li, Z., J. A. Gilbert, Y. Zhang, M. Zhang, Q. Qiu, K. Ramanujan, T. Shavlakadze, J. K. Eash, A. Scaramozza, M. M. Goddeeris, D. G. Kirsch, K. P. Campbell, A. S. Brack, and D. J. Glass. 2012. An HMGA2-IGF2BP2 axis regulates myoblast proliferation and myogenesis. *Dev Cell* **23**: 1176-1188.
35. Lanthier, N., O. Molendi-Coste, Y. Horsmans, N. van Rooijen, P. D. Cani, and I. A. Leclercq. 2010. Kupffer cell activation is a causal factor for hepatic insulin resistance. *Am J Physiol Gastrointest Liver Physiol* **298**: G107-116.
36. Bode, H. B., M. W. Ring, G. Schwar, R. M. Kroppenstedt, D. Kaiser, and R. Muller. 2006. 3-Hydroxy-3-methylglutaryl-coenzyme A (CoA) synthase is involved in biosynthesis of isovaleryl-CoA in the myxobacterium Myxococcus xanthus during fruiting body formation. *J Bacteriol* **188**: 6524-6528.
37. Kiemer, A. K., R. H. Senaratne, J. Hoppstadter, B. Diesel, L. W. Riley, K. Tabeta, S. Bauer, B. Beutler, and B. L. Zuraw. 2009. Attenuated activation of macrophage TLR9 by DNA from virulent mycobacteria. *J Innate Immun* **1**: 29-45.
38. Azzout-Marniche, D., D. Becard, C. Guichard, M. Foretz, P. Ferre, and F. Foufelle. 2000. Insulin effects on sterol regulatory-element-binding protein-1c (SREBP-1c) transcriptional activity in rat hepatocytes. *Biochem J* **350 Pt 2**: 389-393.
39. Basirico, L., P. Morera, N. Lacetera, B. Ronchi, A. Nardone, and U. Bernabucci. 2010. Down-regulation of hepatic ApoB100 expression during hot season in transition dairy cows. *Livestock Science* **137**: 49.
40. Lu, M., R. M. Nakamura, E. D. Dent, J. Y. Zhang, F. C. Nielsen, J. Christiansen, E. K. Chan, and E. M. Tan. 2001. Aberrant expression of fetal RNA-binding protein p62 in liver cancer and liver cirrhosis. *Am J Pathol* **159**: 945-953.
41. Dubuquoy, C., C. Robichon, F. Lasnier, C. Langlois, I. Dugail, F. Foufelle, J. Girard, A. F. Burnol, C. Postic, and M. Moldes. 2011. Distinct regulation of adiponutrin/PNPLA3 gene expression by the transcription factors ChREBP and SREBP1c in mouse and human hepatocytes. *J Hepatol* **55**: 145-153.
42. Lee, H., M. T. Park, B. H. Choi, E. T. Oh, M. J. Song, J. Lee, C. Kim, B. U. Lim, and H. J. Park. 2011. Endoplasmic reticulum stress-induced JNK activation is a critical event leading to mitochondria-mediated cell death caused by beta-lapachone treatment. *PLoS One* **6**: e21533.
43. Vinciguerra, M., F. Carrozzino, M. Peyrou, S. Carlone, R. Montesano, R. Benelli, and M. Foti. 2009. Unsaturated fatty acids promote hepatoma proliferation and progression through downregulation of the tumor suppressor PTEN. *J Hepatol* **50**: 1132-1141.
44. Tripathy, S., and D. B. Jump. 2013. Elovl5 regulates the mTORC2-Akt-FOXO1 pathway by controlling hepatic cis-vaccenic acid synthesis in diet-induced obese mice. *J Lipid Res* **54**: 71-84.
45. Chao, W., and P. A. D'Amore. 2008. IGF2: epigenetic regulation and role in development and disease. *Cytokine Growth Factor Rev* **19**: 111-120.
46. Chen, G., G. Liang, J. Ou, J. L. Goldstein, and M. S. Brown. 2004. Central role for liver X receptor in insulin-mediated activation of Srebp-1c transcription and stimulation of fatty acid synthesis in liver. *Proc Natl Acad Sci U S A* **101**: 11245-11250.
47. Postic, C., and J. Girard. 2008. Contribution of de novo fatty acid synthesis to hepatic steatosis and insulin resistance: lessons from genetically engineered mice. *J Clin Invest* **118**: 829-838.

48. Dentin, R., F. Benhamed, I. Hainault, V. Fauveau, F. Foufelle, J. R. Dyck, J. Girard, and C. Postic. 2006. Liver-specific inhibition of ChREBP improves hepatic steatosis and insulin resistance in ob/ob mice. *Diabetes* **55**: 2159-2170.
49. Ahmed, M. H., and C. D. Byrne. 2007. Modulation of sterol regulatory element binding proteins (SREBPs) as potential treatments for non-alcoholic fatty liver disease (NAFLD). *Drug Discov Today* **12**: 740-747.
50. Shimomura, I., Y. Bashmakov, and J. D. Horton. 1999. Increased levels of nuclear SREBP-1c associated with fatty livers in two mouse models of diabetes mellitus. *J Biol Chem* **274**: 30028-30032.
51. Ferre, P., and F. Foufelle. 2007. SREBP-1c transcription factor and lipid homeostasis: clinical perspective. *Horm Res* **68**: 72-82.
52. Kim, K. H., G. Y. Lee, J. I. Kim, M. Ham, J. Won Lee, and J. B. Kim. 2010. Inhibitory effect of LXR activation on cell proliferation and cell cycle progression through lipogenic activity. *J Lipid Res* **51**: 3425-3433.
53. Wang, M., S. Sun, T. Wu, L. Zhang, H. Song, W. Hao, P. Zheng, L. Xing, and G. Ji. 2013. Inhibition of LXRalpha/SREBP-1c-Mediated Hepatic Steatosis by Jiang-Zhi Granule. *Evid Based Complement Alternat Med* **2013**: 584634.
54. Yoshikawa, T., H. Shimano, M. Amemiya-Kudo, N. Yahagi, A. H. Hasty, T. Matsuzaka, H. Okazaki, Y. Tamura, Y. Iizuka, K. Ohashi, J. Osuga, K. Harada, T. Gotoda, S. Kimura, S. Ishibashi, and N. Yamada. 2001. Identification of liver X receptor-retinoid X receptor as an activator of the sterol regulatory element-binding protein 1c gene promoter. *Mol Cell Biol* **21**: 2991-3000.
55. Shimomura, I., H. Shimano, J. D. Horton, J. L. Goldstein, and M. S. Brown. 1997. Differential expression of exons 1a and 1c in mRNAs for sterol regulatory element binding protein-1 in human and mouse organs and cultured cells. *J Clin Invest* **99**: 838-845.
56. DeBose-Boyd, R. A., J. Ou, J. L. Goldstein, and M. S. Brown. 2001. Expression of sterol regulatory element-binding protein 1c (SREBP-1c) mRNA in rat hepatoma cells requires endogenous LXR ligands. *Proc Natl Acad Sci U S A* **98**: 1477-1482.
57. Repa, J. J., G. Liang, J. Ou, Y. Bashmakov, J. M. Lobaccaro, I. Shimomura, B. Shan, M. S. Brown, J. L. Goldstein, and D. J. Mangelsdorf. 2000. Regulation of mouse sterol regulatory element-binding protein-1c gene (SREBP-1c) by oxysterol receptors, LXRalpha and LXRbeta. *Genes Dev* **14**: 2819-2830.
58. Smith, T. M., K. Gilliland, G. A. Clawson, and D. Thiboutot. 2008. IGF-1 induces SREBP-1 expression and lipogenesis in SEB-1 sebocytes via activation of the phosphoinositide 3-kinase/Akt pathway. *J Invest Dermatol* **128**: 1286-1293.
59. Iizuka, K., B. Miller, and K. Uyeda. 2006. Deficiency of carbohydrate-activated transcription factor ChREBP prevents obesity and improves plasma glucose control in leptin-deficient (ob/ob) mice. *Am J Physiol Endocrinol Metab* **291**: E358-364.
60. Yu, Y., T. G. Maguire, and J. C. Alwine. 2014. ChREBP, a glucose-responsive transcriptional factor, enhances glucose metabolism to support biosynthesis in human cytomegalovirus-infected cells. *Proc Natl Acad Sci U S A* **111**: 1951-1956.
61. Denechaud, P. D., P. Bossard, J. M. Lobaccaro, L. Millatt, B. Staels, J. Girard, and C. Postic. 2008. ChREBP, but not LXRs, is required for the induction of glucose-regulated genes in mouse liver. *J Clin Invest* **118**: 956-964.
62. Caballero, F., A. Fernandez, A. M. De Lacy, J. C. Fernandez-Checa, J. Caballeria, and C. Garcia-Ruiz. 2009. Enhanced free cholesterol, SREBP-2 and StAR expression in human NASH. *J Hepatol* **50**: 789-796.
63. Donnelly, K. L., C. I. Smith, S. J. Schwarzenberg, J. Jessurun, M. D. Boldt, and E. J. Parks. 2005. Sources of fatty acids stored in liver and secreted via lipoproteins in patients with nonalcoholic fatty liver disease. *J Clin Invest* **115**: 1343-1351.

64. Chakravarthy, M. V., Z. Pan, Y. Zhu, K. Tordjman, J. G. Schneider, T. Coleman, J. Turk, and C. F. Semenkovich. 2005. "New" hepatic fat activates PPARalpha to maintain glucose, lipid, and cholesterol homeostasis. *Cell Metab* **1**: 309-322.
65. Jones, A., K. Friedrich, M. Rohm, M. Schafer, C. Algire, P. Kulozik, O. Seibert, K. Muller-Decker, T. Sijmonsma, D. Strzoda, C. Sticht, N. Gretz, G. M. Dallinga-Thie, B. Leuchs, M. Kogl, W. Stremmel, M. B. Diaz, and S. Herzig. 2013. TSC22D4 is a molecular output of hepatic wasting metabolism. *EMBO Mol Med*.
66. Harano, Y., K. Yasui, T. Toyama, T. Nakajima, H. Mitsuyoshi, M. Mimani, T. Hirasawa, Y. Itoh, and T. Okanoue. 2006. Fenofibrate, a peroxisome proliferator-activated receptor alpha agonist, reduces hepatic steatosis and lipid peroxidation in fatty liver Shionogi mice with hereditary fatty liver. *Liver Int* **26**: 613-620.
67. Thupari, J. N., M. L. Pinn, and F. P. Kuhajda. 2001. Fatty acid synthase inhibition in human breast cancer cells leads to malonyl-CoA-induced inhibition of fatty acid oxidation and cytotoxicity. *Biochem Biophys Res Commun* **285**: 217-223.
68. Soupene, E., and F. A. Kuypers. 2008. Mammalian long-chain acyl-CoA synthetases. *Exp Biol Med (Maywood)* **233**: 507-521.
69. Mabrouk, G. M., I. M. Helmy, K. G. Thampy, and S. J. Wakil. 1990. Acute hormonal control of acetyl-CoA carboxylase. The roles of insulin, glucagon, and epinephrine. *J Biol Chem* **265**: 6330-6338.
70. McGarry, J. D., and N. F. Brown. 1997. The mitochondrial carnitine palmitoyltransferase system. From concept to molecular analysis. *Eur J Biochem* **244**: 1-14.
71. Anderson, N., and J. Borlak. 2008. Molecular mechanisms and therapeutic targets in steatosis and steatohepatitis. *Pharmacol Rev* **60**: 311-357.
72. Koteish, A., and A. M. Diehl. 2001. Animal models of steatosis. *Semin Liver Dis* **21**: 89-104.
73. Lelliott, C. J., M. Lopez, R. K. Curtis, N. Parker, M. Laudes, G. Yeo, M. Jimenez-Linan, J. Grosse, A. K. Saha, D. Wiggins, D. Hauton, M. D. Brand, S. O'Rahilly, J. L. Griffin, G. F. Gibbons, and A. Vidal-Puig. 2005. Transcript and metabolite analysis of the effects of tamoxifen in rat liver reveals inhibition of fatty acid synthesis in the presence of hepatic steatosis. *FASEB J* **19**: 1108-1119.

2.2.10 Supplement

Supplemental data Figures

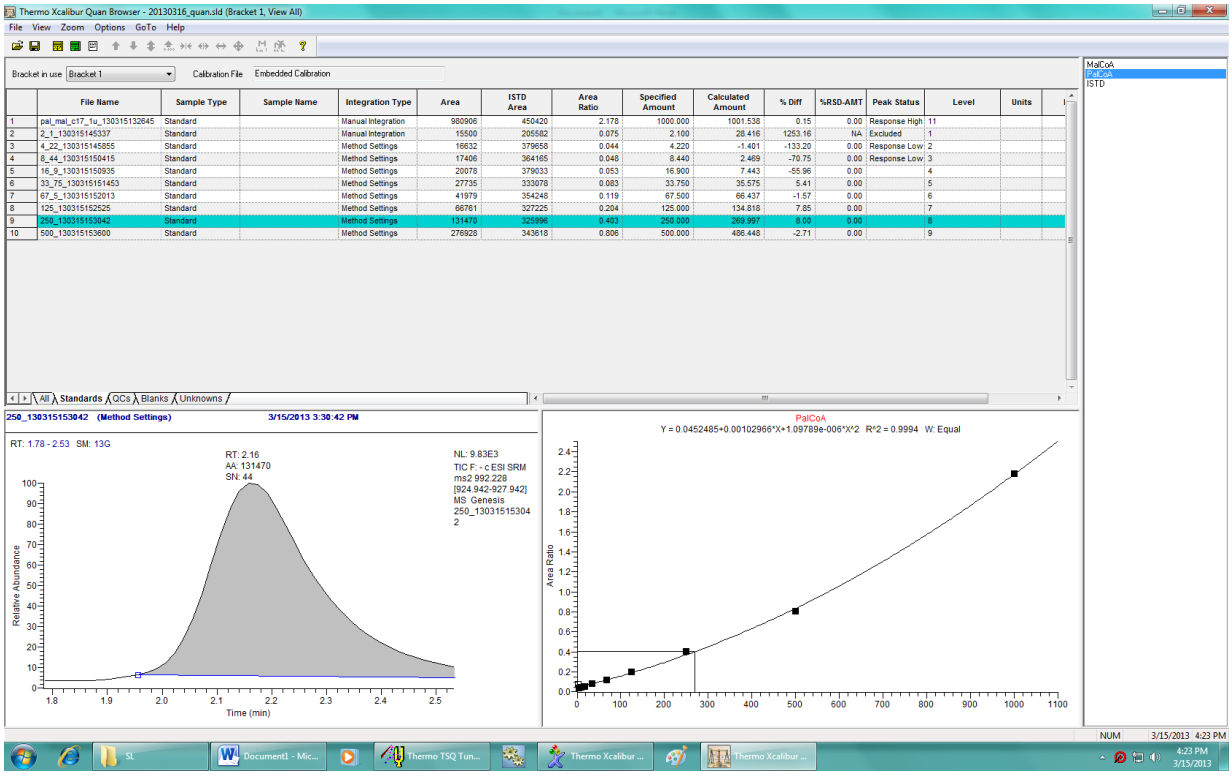

Supplemental data Figure I: Representative Palmitoyl-CoA dilution series

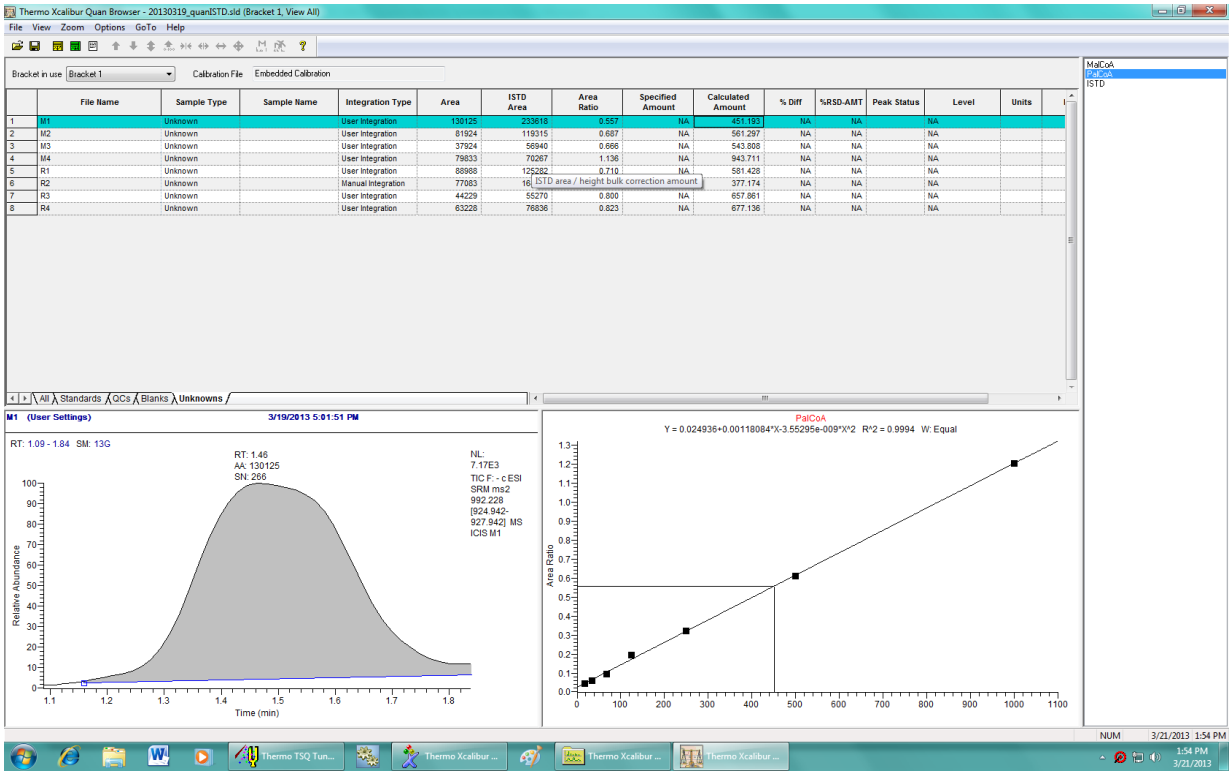

Supplemental data Figure II: Representative palmitoyl-CoA measurement in mouse livers

Supplemental data Table

Nr.	diagnosis
1	cirrhosis, hepatitis
2	cirrhosis, hepatitis
3	liver cirrhosis, primary biliary cirrhosis
4	cirrhosis
5	cirrhosis, hepatitis
6	cirrhosis, hepatitis
7	liver cirrhosis, hepatitis C virus
8	liver cirrhosis, hepatitis C virus
9	liver cirrhosis, hepatitis B virus
10	liver cirrhosis, alcoholic liver
11	liver cirrhosis, hepatitis B virus
12	cirrhosis, viral hepatitis
13	liver cirrhosis, alcoholic hepatitis
14	liver cirrhosis, hepatitis C virus
15	liver cirrhosis, Budd-chiary-S.
16	liver cirrhosis, hepatitis C virus
17	liver fibrosis, liver cirrhosis
18	liver cirrhosis, liver cirrhosis alcoholic
19	liver cirrhosis
20	liver cirrhosis, viral hepatitis
21	liver cirrhosis, hepatitis C virus
22	liver cirrhosis
23	liver cirrhosis, hepatitis B virus
24	liver cirrhosis
25	cirrhosis, hepatitis C virus
26	liver cirrhosis, hepatitis B virus
27	liver cirrhosis, cryptogen., viral hepatitis
28	liver cirrhosis, viral hepatitis
29	liver cirrhosis, viral hepatitis
30	liver cirrhosis
31	liver cirrhosis, alcoholic liver cirrhosis
32	liver cirrhosis
33	liver cirrhosis, hepatitis B virus, hepatitis C virus
34	liver cirrhosis, hemachromatome
35	liver cirrhosis, alpha-1 antitrypsin deficiency

Supplemental data Table I: Patients / Diagnosis

2.3 *IGF2* mRNA binding protein p62/IMP2-2 in hepatocellular carcinoma: antiapoptotic action is independent of IGF2/PI3K signaling

III

p62 has been shown to promote NAFLD (Laggai et al., 2014; Simon et al., 2014a), and to modify pathways involved in cancerogenesis (Tybl et al., 2011). In this study, the p62-mediated overexpression of the growth factor *IGF2* should also be validated for the human system. Therefore, we investigated the abundance and implications of p62 and *IGF2* in human HCC and in human cell lines. Furthermore, the effect of p62 and IGF2 on antiapoptotic pathways and especially the activation of the protein kinase B (PKB)/AKT/PI3K pathway should be validated.

IGF2 mRNA binding protein p62/IMP2-2 in hepatocellular carcinoma: antiapoptotic action is independent of IGF2/PI3K signaling.

Sonja M. Kessler, Juliane Pokorny, Vincent Zimmer, **Stephan Laggai**, Frank Lammert, Rainer M. Bohle, and Alexandra K. Kiemer.

This research was originally published in American Journal of Physiology - Gastrointestinal and Liver Physiology. Kessler, S.M., Pokorny, J., Zimmer, V., **Laggai, S**., Lammert, F., Bohle, R.M., and Kiemer, A.K. *IGF2* mRNA binding protein p62/IMP2-2 in hepatocellular carcinoma: antiapoptotic action is independent of IGF2/PI3K signaling. *AJP-Gastrointest Liver Physiol.* 2013; 304: G328–G336. doi:10.1152/ajpgi.00005.2012. Copyright © 2013, the American Physiological Society.

The full text article can also be found at:
http://ajpgi.physiology.org/content/304/4/G328

2.3.1 Author Contribution

Am J Physiol Gastrointest Liver Physiol. 2013 Feb 15;304(4):G328-36. doi: 10.1152/ajpgi.00005.2012. Epub 2012 Dec 20.

***IGF2* mRNA binding protein p62/IMP2-2 in hepatocellular carcinoma: antiapoptotic action is independent of IGF2/PI3K signaling.**

Kessler SM, Pokorny J, Zimmer V, **Laggai S**, Lammert F, Bohle RM, Kiemer AK.

Kessler SM:
Performed cell culture studies.
Performed capase-3-like activity assays.
Performed immunohistochemistry.
Performed real-time RT-PCR analysis.
Performed Western blot analysis.
Designed experiments, performed data acquisition and statistical analysis.
Wrote and revised the manuscript.

Pokorny J and Bohle RM:
Performed and directed the analysis of human HCC tissues.

Zimmer V and Lammert F:
Performed and directed the acquisition of clinical data.

Laggai S:
Performed p62 knockdown and overexpression studies in HepG2 cells.
Performed *p62* and *IGF2* real-time RT-PCR analysis of HepG2 cells.
Performed ERK Western blot analysis of Hepg2 cells.
Performed data acquisition and statistical analysis.
Participated in manuscript revision.

Kiemer AK:
Initiated and directed the study.
Designed experiments.
Wrote and revised the manuscript.

2.3.2 Title page

BASIC LIVER/PANCREAS/BILIARY - HEPATOCARCINOGENESIS THE *IGF2* mRNA BINDING PROTEIN p62 IN HEPATOCELLULAR CARCINOMA: ANTIAPOPTOTIC ACTION IS INDEPENDENT OF IGF2/PI3-K SIGNALING

Sonja M. Kessler[1], Juliane Pokorny[2], Vincent Zimmer[3], **Stephan Laggai[1]**, Frank Lammert[3], Rainer M. Bohle[2], Alexandra K. Kiemer*[1]

[1]Saarland University, Department of Pharmacy, Pharmaceutical Biology, Saarland University, Saarbrücken, Germany

[2]Department of Pathology, Saarland University, Homburg/Saar, Germany

[3]Department of Internal Medicine II, Saarland University, Homburg/Saar, Germany

Running head: ANTIAPOPTOTIC ACTION OF p62 INDEPENDENT OF IGF2/PI3-K

*To whom correspondence should be addressed

Alexandra K. Kiemer, Ph.D.

Saarland University

P.O. box 15 11 50

66041 Saarbrücken, Germany

phone: +49-681-302 57301

fax: +49-681-302 57302

e-mail: pharm.bio.kiemer@mx.uni-saarland.de

Electronic word count: 5430; abstract: 250

2.3.3 Abstract

Background and aims: The insulin-like growth factor II (*IGF2*) mRNA binding protein (IMP) p62/IMP2-2, originally isolated from an HCC patient, induces a steatotic phenotype when overexpressed in mouse livers. Still, *p62* transgenic livers do not show liver cell damage but exhibit a pronounced induction of *Igf2* and activation of the downstream survival kinase Akt. Aim of this study was to investigate the relation between p62 and IGF2 expression in the human system and to study potential antiapoptotic actions of p62.

Methods: *p62* and *IGF2* mRNA levels in human paraffin-embedded tissue were assessed by real-time RT-PCR. For knockdown and overexpression experiments human hepatoma HepG2 and PLC/PRF/5 cells were transfected with siRNA or plasmid DNA. Phosphorylated AKT and ERK1/2 were analysed by Western blot.

Results: Investigations of 32 human HCC tissues showed a strong correlation between *p62* and *IGF2* expression. Of note, p62 expression was increased markedly in patients with poor outcome. In hepatoma cells overexpression of p62 lowered levels of doxorubicin-induced caspase-3-like activity. *Vice versa*, knockdown of p62 resulted in increased doxorubicin-induced apoptosis. However, neither PI3-K inhibitors nor a neutralizing IGF2 antibody showed any effects. Western blot analysis revealed increased levels of phosphorylated ERK1/2 in hepatoma cells overexpressing p62 and decreased levels in p62 knockdown experiments. When p62 overexpressing cells were treated with ERK1/2 inhibitors, the apoptosis-protecting effect of p62 was completely abrogated.

Conclusions: Our data demonstrate that p62 exerts IGF2-independent antiapoptotic action, which is facilitated *via* phosphorylation of ERK1/2. Furthermore, p62 might serve as a new prognostic marker in HCC.

Keywords: IMP, hepatocellular carcinoma, apoptosis, ERK, chemoresistance

2.3.4 Introduction

The incidence of hepatocellular carcinoma (HCC) is rising in most industrialized countries not least due to metabolic risk factors such as obesity and diabetes mellitus and the increasing prevalence of non-alcoholic fatty liver disease (NAFLD (12, 48). p62/IMP2-2 is a member of the family of insulin-like growth factor II (*IGF2*)-mRNA binding proteins and represents a splice variant of IMP2, where exon 10 of the IMP2 gene is skipped (11). p62 was originally identified as an autoantigen in a patient with HCC (57) and was shown to be expressed in 1/3 to 2/3 of HCC (33, 56). Interestingly, p62 is also expressed in α-fetoprotein negative HCC (33). The family member IMP3 has been shown to be implicated in growth promotion, carcinogenesis, angiogenesis, and tumor progression in different tumor types (6, 20, 22, 25). A pathophysiologic role for p62 in malignant diseases, however, is as yet widely unknown. *p62* transgenic mice expressing the transgene exclusively in the liver develop a fatty liver phenotype (51) suggesting a critical role for p62 in liver metabolism. Still, *p62* transgenic livers do not show liver cell damage but exhibit a pronounced induction of the growth factor *Igf2* and activation of the downstream survival kinase phosphoinositide 3 (PI3)-kinase/Akt pathway. IGF2 plays a key role in mammalian growth through metabolic and growth-promoting effects and exerts antiapoptotic action (36, 37). The interaction of p62 and IGF2 might be of special interest with regard to the tumor promoting nature of IGF2. In fact, overexpression of IGF2 and pronounced activation of AKT has been described in HCC (5, 8, 34, 49). Quite in contrast, reduced IGF2 expression was shown to enhance survival from HCC (54).

Since a potential interaction of p62 and IGF2 is unknown in human HCC, we investigated their relationship and functional aspects regarding cell survival and proliferation. We observed that p62 expression correlates with both IGF2 expression and poor outcome in human hepatocellular carcinoma. p62 exerted antiapoptotic action in human hepatoma cells independent of PI3-K signaling, but rather facilitated *via* extracellular regulated kinases (ERK) 1/2.

2.3.5 Materials and Methods

Animals

All animal procedures and protocols were approved by an independent review committee (AZ: 391 2.2.2) Mice were kept under controlled conditions in terms of temperature, humidity, 12 h day/night rhythm and food delivery. *p62* transgenic mice were established as

previously described (51). In short, mice carrying a liver enriched activator protein promoter under the control of a tetracycline transactivator were crossed with p62 transgenic mice, in which the human p62 is under the control of the transrepressive responsive element cytomegaly virus (TRE-CMVmin). The double positive offspring expresses p62 exclusively in the liver.

Real-time quantitative polymerase chain reaction

Experiments and quantification were performed as described in detail previously (2). RNA from human HCC samples was isolated using the QiaAmp RNA-FFPE-Kit according to manufacturers' instructions. Sequences and conditions are given in table 1.

Isolation of primary murine hepatocytes

Hepatocytes were isolated according to a modified version of the two-step collagenase perfusion method of Seglen (13, 44) with a viability exceeding 80%. Cells were cultured on collagen-coated plates for one day before treatment.

MTT Assay

Cells were cultured on 96-well tissue culture plates and every 24 h an MTT assay was performed for up to 4 days. Cells were then incubated with MTT (0.5 mg/ml) solution for 2 h, MTT solution was aspirated, cells were lysed and measured at 550 nm and at 690 nm as control wavelength.

Caspase-3-like activity assay

In primary murine hepatocytes apoptosis was induced by addition of 0.4 µg/ml actinomycin D (Act D) for 15 min and 100 ng/ml TNF-α for 20 h. HepG2 cells were treated with 12.5 µg/ml, PLC/PRF/5 with 50.0 µg/ml doxorubicin for 20 h. Cells were then washed twice, lysed and centrifuged. The substrate solution containing benzyloxycarbonyl-Asp-Glu-Val-Asp-aminofluoromethylcoumarin was added to the supernatant, and generation of free fluorescent 7-amino-4-trifluoromethyl coumarin was determined according to Kulhanek-Heinze et al. (28).

Western blot analysis

Western blots were performed as previously described (51). Antibodies used were specific to phospho-AKT (Ser473), phospho-ERK1/2, total ERK1/2, phospho-Insulin Receptor, total

Insulin Receptor (New England Biolabs, Frankfurt a. M., Germany), and α-tubulin (Sigma, Thermo Fisher Scientific, Karlsruhe, Germany).

Cell transfection

For overexpression assays, pcDNA3.1/CT-GFP-TOPO® p62 sense or the antisense construct was introduced into HepG2 or PLC/PRF/5 cells using jetPEI™-Hepatocyte transfection reagent (Polyplus-transfection, New York, USA). Knockdown was performed with sip62/IMP2 and control siRNA using INTERFERin™ (Polyplus-transfection, New York, USA) transfection reagent as recommended under reverse transfection in the manufacturer's guidelines. Inhibition of the IGF2/PI3-K pathway was done using the PI3-K-inhibitors LY294002 (10 µM) and wortmannin (800 mM) as well as an IGF2 antibody (ab9574, Abcam, United Kingdom). PD98059 and U126 (both 10 µM) served as ERK1/2-inhibitors (17). Inhibition was achieved by pretreatment for 1 h with inhibitors and for 2 h with the IGF2 antibody. Neutralizing effect of IGF2 antibody was verified by Western Blot analysis after treatment with recombinant human IGF2 (R&D Sytems, Wiesbaden, Germany).

Immunohistochemistry

Staining of the paraffin-embedded sections was performed with the CSA II Kit (Dako, Hamburg, Germany). Primary antibodies used were specific to phosphoERK1/2 (New England Biolabs, Frankfurt a. M., Germany) and p62 (33, 51).

Human HCC tissues

Paraffin-embedded liver samples from randomly selected pseudonymised HCC patients who underwent liver resection at the Saarland University Medical Center between 2005 and 2010 were obtained. The study protocol was approved by the local Ethics Committee (Kenn-Nr. 47/07). Table 2 summarizes the clinical data. TNM staging was performed according to the NCCN Hepatobiliary Cancers Clinical Practice Guidelines in Oncology (NCCN Guidelines™ for Hepatobiliary Cancers V2.2012 © 2011 National Comprehensive Cancer Network, Inc. cited with permission from the NCCN). T classification was ascertained on the resected specimen, whereas N and M classifications were determined by clinical radiological staging for most of the patients.

Statistical analysis

Data analysis and statistics were performed using Origin software (OriginPro 8.1G; OriginLabs). All data are displayed as mean values ± SEM. Statistical differences were estimated by independent two-sample t-test. Human FFPE HCC samples were tested by Wilcoxon rank-sum test. Kaplan-Meier-Survival analysis was tested by log rank test. All are two-sided and differences were considered statistically significant when p values were less than 0.05.

2.3.6 Results

p62 and IGF2 expression in human HCC samples

The analysis of 32 human HCC tissues showed increased levels of *p62* and *IGF2* in tumor tissue as compared to matched normal tissue (Fig. 1A). Furthermore, a significant correlation between *p62* and *IGF2* expression was observed (Fig. 1B). Kaplan-Meier survival analysis of patients with high p62 expression (upper quartile) *versus* low p62 expression (lower quartile) was not significant, but revealed a trend to shorter survival in patients with high p62 expression in liver tissue (Fig. 1C). Therefore, p62 expression was tested for different parameters of poor outcome of the corresponding patient. p62 expression was significantly higher in tumors with increased tumor size and in grade 2 and 3 tumors *versus* grade 1 tumors (Fig. 1D). p62 expression correlated with tumor stage using both BCLC and TNM staging system (Fig. 1E, F). Altogether, the subgroup with high p62 expression showed poorer outcome characterized by intermediate to advanced Barcelona staging (stages B or C), TNM staging III or IV, multinodularity, and increased tumor diameter (Fig. 1G).

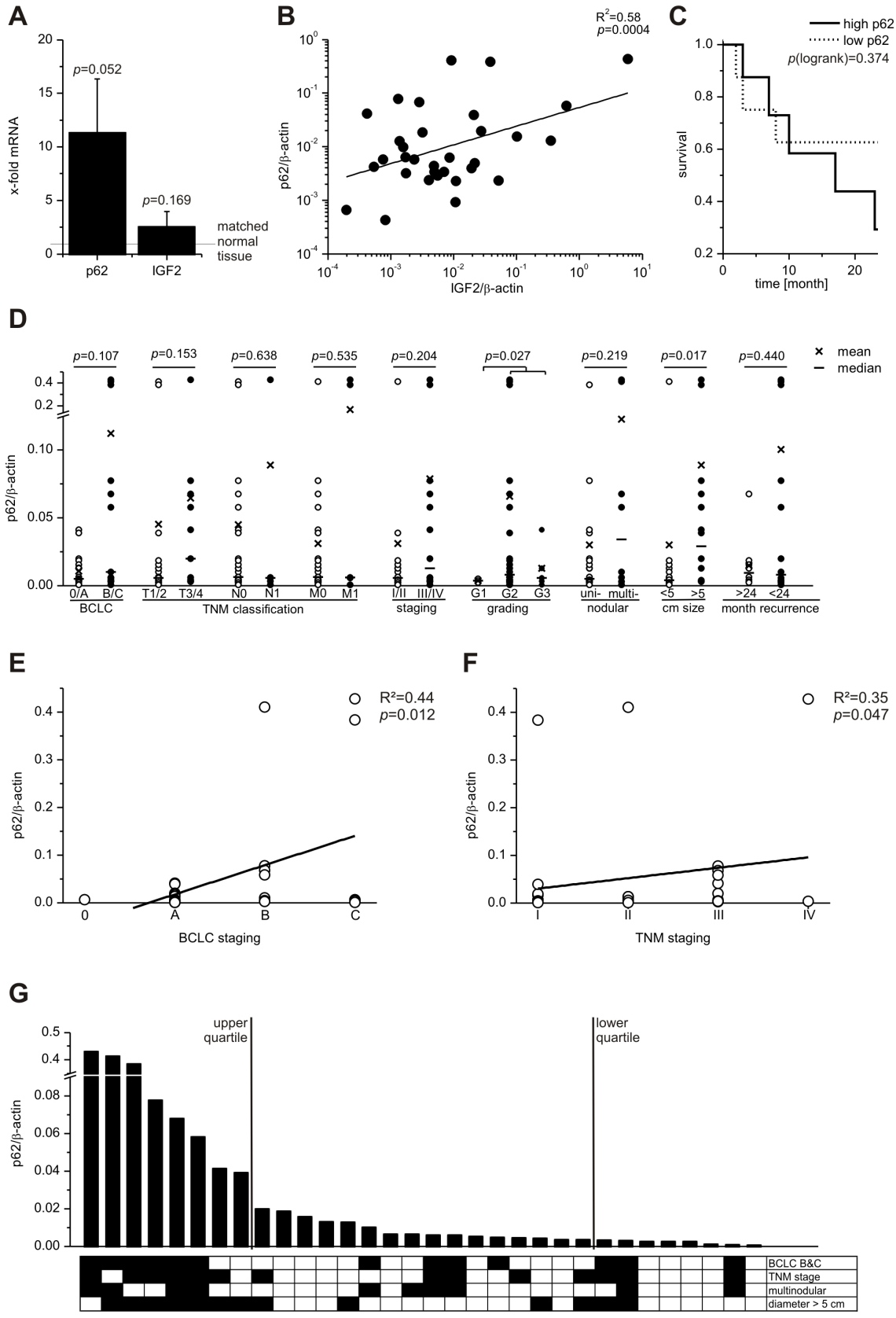

Fig. 1. *p62* and *IGF2* expression in human HCC samples (A) *p62* and *IGF2* mRNA expression in human HCC samples (n=32) compared to matched normal tissue. **(B)** Correlation of *p62* mRNA and *IGF2* mRNA in human HCC samples. **(C)** Kaplan-Meier survival analysis of the upper quartile (high p62) *vs.* the lower quartile (low p62) of p62 mRNA expression in HCC samples. **(D)** *p62* mRNA expression in HCC samples ordered by

different clinicopathological parameters of poor prognosis of the corresponding patient: Barcelona Clinic Liver Cancer (BCLC), TNM classification and staging, grading, uni- or multinodularity, tumor size and recurrence. **(E, F)** Correlation data of *p62* expression to tumor stage for BCLC **(E)** and TNM **(F)** staging system. **(G)** Comparison of *p62* mRNA expression with prognostic clinical data from HCC patients, such as BCLC, TNM staging, multinodularity, and tumor size.

Relationship between p62 and IGF2 expression in human hepatoma cells

In order to determine whether the presence of p62 induces IGF2 expression in the human system as previously observed in *p62* transgenic mice (51), p62 was knocked down by siRNA in HepG2 cells. Knockdown of p62 decreased *IGF2* expression (Fig. 2A). *Vice versa*, overexpression of p62 resulted in increased *IGF2* mRNA levels (Fig. 2B). Because of the proliferating and antiapoptotic features of IGF2 we investigated the effect of p62 on proliferation and apoptosis. After knockdown of p62, however, no effect on cell proliferation was observed (Fig. 2C).

Basal levels of apoptosis were not altered in livers of transgenic animals (data not shown). TNF-α/Act D-induced caspase-3-like activity in primary murine hepatocytes from p62 overexpressing mice, however, was attenuated compared to control cells (Fig. 2D). In the human system overexpression of p62 in HepG2 cells decreased doxorubicin-induced apoptosis (Fig. 2E). *Vice versa*, knockdown of p62 in HepG2 cells resulted in increased doxorubicin-induced caspase-3-like activity (Fig. 2F).

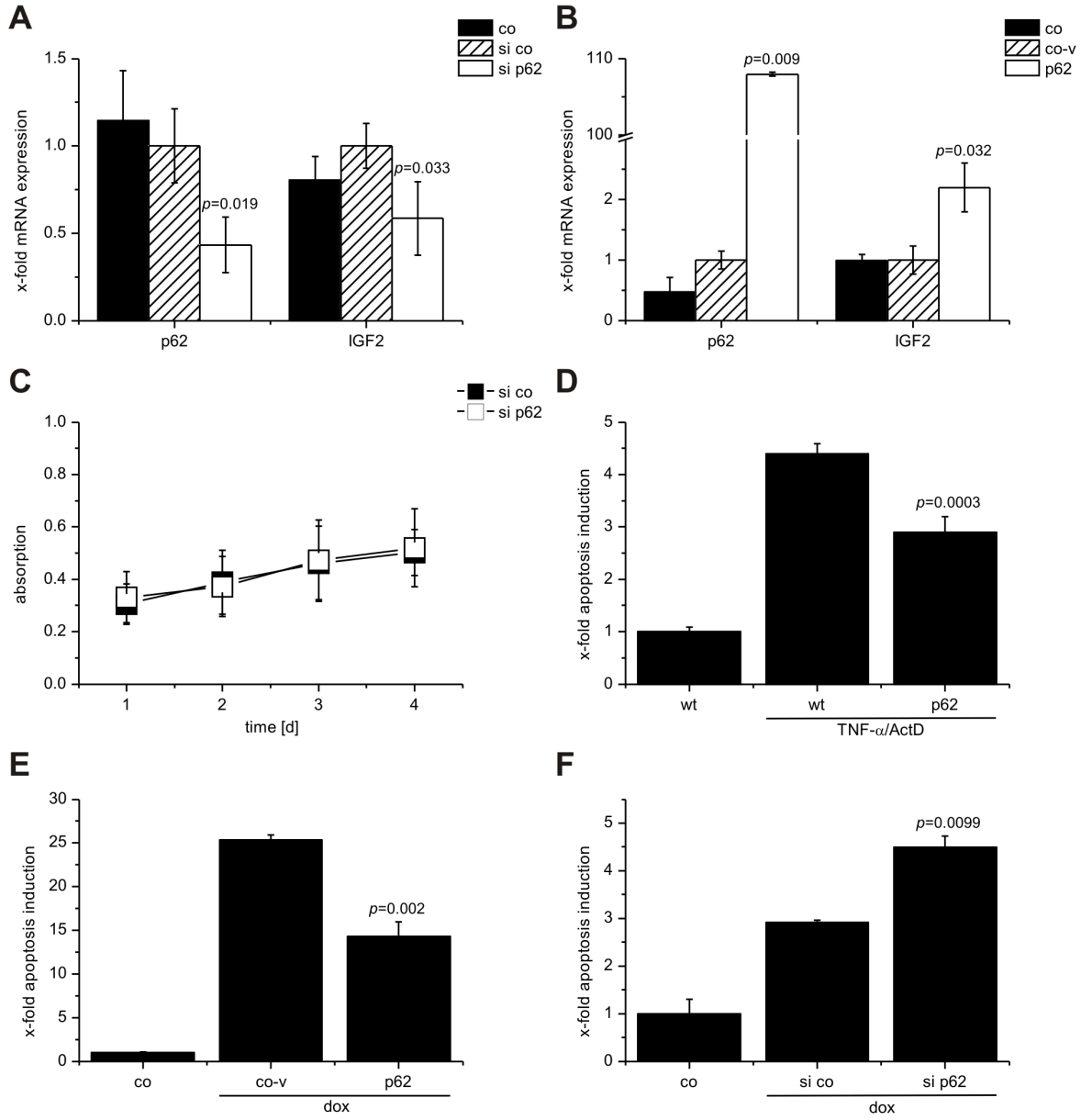

Fig. 2. Proliferation and apoptosis (A) *p62* and *IGF2* mRNA expression 48 h after siRNA knockdown of p62 (si p62) in HepG2 cells compared to random siRNA control (si co). **(B)** *p62* and *IGF2* mRNA expression 48 h after p62 overexpression (p62) in HepG2 normalized to control vector carrying the antisense plasmid (co-v). **(C)** Proliferation of HepG2 cells after knockdown of p62 (si p62) compared to random siRNA (si co). **(D)** Caspase-3-like activity levels of primary murine hepatocytes of *p62* transgenic animals (p62) and wild-type animals (wt) induced by TNF-α/Act D treatment. Data is expressed as fold induction of apoptosis compared to untreated control. **(E, F)** Doxorubicin-induced caspase-3-like activity in HepG2 after transfection either with random siRNA (si co) or p62 siRNA (si p62) **(E)** or with p62 antisense construct (co-v) or p62 sense construct (p62) **(F)**.

Antiapoptotic effect of p62 is independent of PI3-K signaling

Since *p62* transgenic animals showed increased levels of phophorylated Akt (51), we speculated that the IGF2/PI3-K pathway is involved in the antiapoptotic effect of p62. In

order to determine the involvement of IGF2 in the antiapoptotic effect, p62 was overexpressed in HepG2 cells followed by inhibition of the IGF2/PI3-K pathway. Neither the PI3K-inhibitors LY294002 and wortmannin nor a neutralizing IGF2 antibody lowered the antiapoptotic effect of p62 (Fig. 3A). The neutralizing capacity of the IGF2 antibody was confirmed by Western blot analysis of phosphorylated insulin receptor (Fig. 3B). The independence of p62 expression and PI3K/AKT signaling in the human system was confirmed by p62 knockdown or overexpression, and neither approach affected phosphorylation of AKT significantly (Fig. 3C, D).

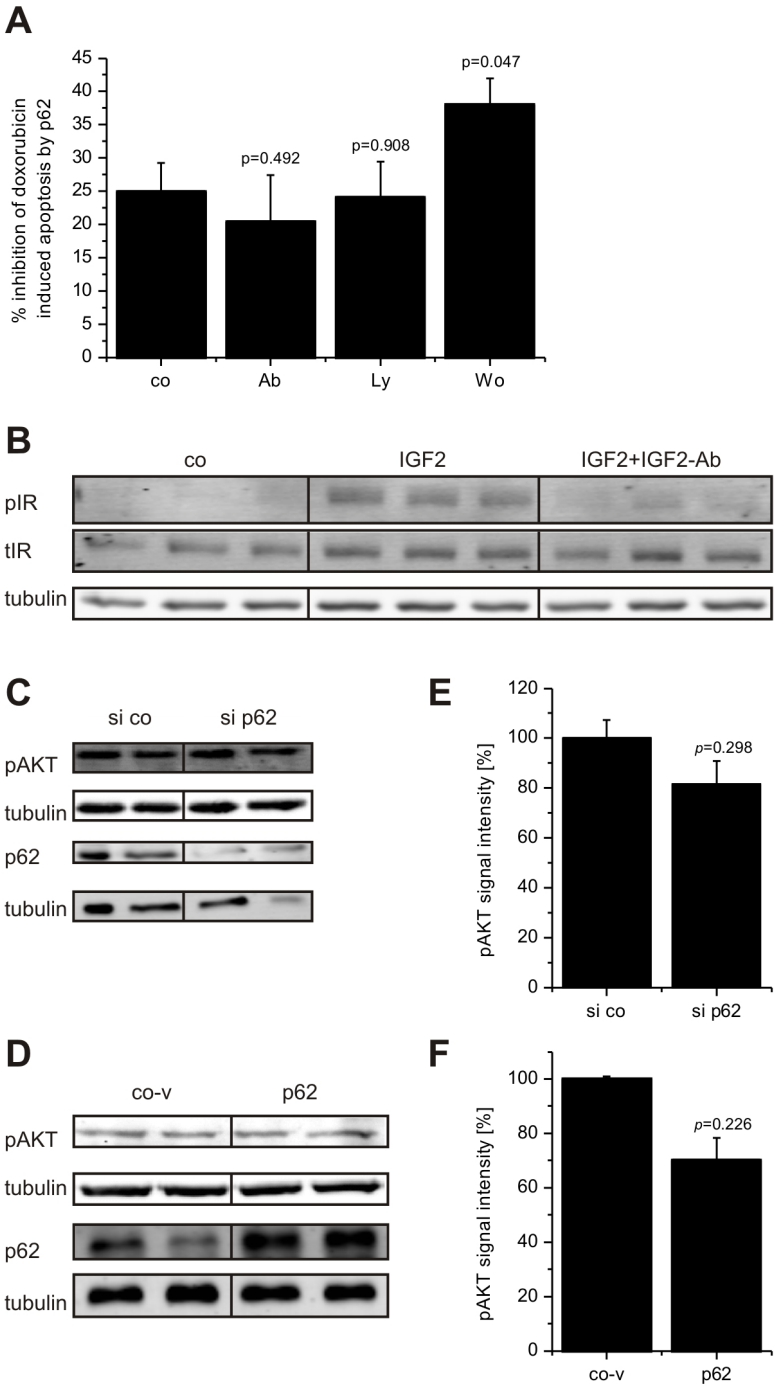

Fig. 3. PI3-K signaling (A) Inhibition of doxorubicin-induced apoptosis by p62 determined by caspase-3-like activity. Inhibition was achieved by using either a neutralizing IGF2 antibody (Ab) or the PI3-K inhibitors Ly294002 (Ly) and wortmannin (Wo). Data are expressed as percent inhibition of doxorubicin-induced apoptosis in p62 transfected cells (co). **(B)** Neutralizing effect of IGF2 antibody verified by Western Blot analysis of phosphorylated (pIR) and total (tIR) insulin receptor levels in HepG2 after treatment with 75 ng/ml recombinant human IGF2 with and without treatment with IGF2 antibody **(C, D)**. Phosphorylated AKT levels after knockdown (si co: random siRNA, si p62: p62 siRNA) **(C)** and overexpression of p62 (co-v: antisense construct, p62: sense construct) **(D)**. **(E, F)**: densitrometric analysis of Western Blots from C and D.

p62 protects from apoptosis via phosphorylation of ERK1/2

Another survival pathway that is often altered in cancer is the mitogen activated protein kinase (MAPK) pathway (29). When p62 overexpressing HepG2 cells were treated with ERK 1/2 inhibitors, the apoptosis-protecting effect of p62 was completely abrogated (Fig. 4A). Knockdown of p62 in HepG2 cells resulted in significantly decreased phophorylation of ERK1/2 (Fig. 4B, D). *Vice versa*, overexpression of p62 activated ERK1/2 markedly (Fig. 4C, D). In order to check the relevance of these findings in another hepatoma cell line, we investigated PLC/PRF/5 cells. p62 regulated *IGF2* expression also in this cell line: p62 knockdown downregulated *IGF2* mRNA by 40.88% (p=0.023) and p62 overexpression induced *IGF2* mRNA 2.01-fold (p=0.016). Still, the IGF2 antibody did not affect chemosensitivity, whereas both ERK inhibitors significantly abrogated apoptosis induction (Fig. 4D). As seen in HepG2 cells, p62 induced ERK activation, as proven by knockdown and overexpression strategies also in PLC/PRF/5 (Fig. 4E-H). Finally, in tissue samples from HCC patients activation of ERK was observed in hepatocytes, which showed high p62 expression (Fig. 4I).

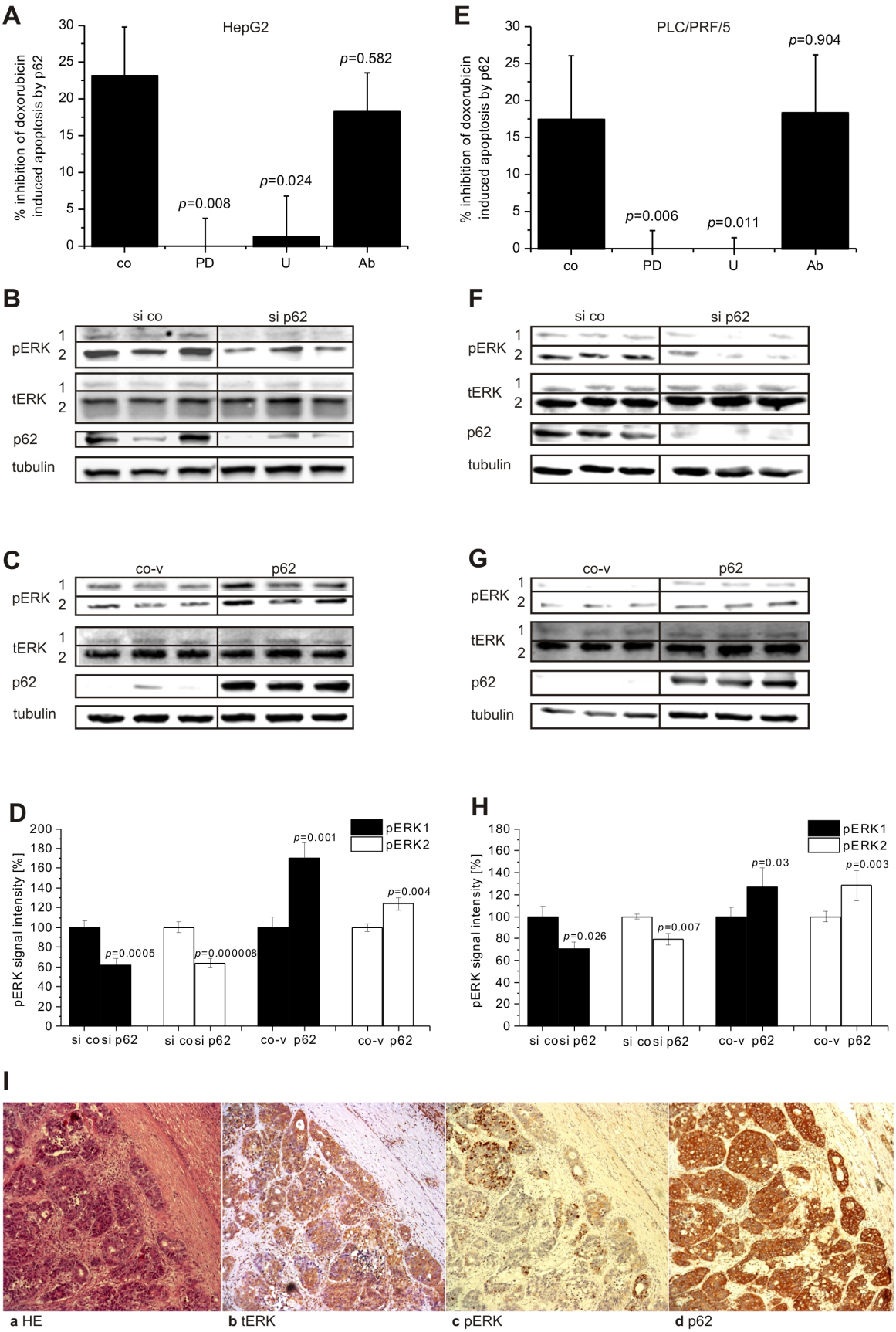

Fig. 4. ERK signaling (A, E) Inhibition of doxorubicin-induced apoptosis by p62 determined by caspase-3-like activity in HepG2 **(A)** and PLC/PRF/5 **(E)** cells. Inhibition was achieved by

using either a neutralizing IGF2 antibody (Ab) or the ERK inhibitors PD98059 (PD) and U126 (U). Data are expressed as percent inhibition of doxorubicin-induced apoptosis in p62 transfected cells (co). **(B-D)** and **(F-H)**: phosphorylated ERK levels after knockdown of p62 in HepG2 **(B)** and PLC/PRF/5 **(F)** cells (si co: random siRNA, si p62: p62 siRNA) and overexpression of p62 in HepG2 **(C)** and PLC/PRF/5 **(G)** cells (co-v: antisense construct, p62: sense construct). Densitrometric analysis of Western blots from HepG2 **(D)** or PLC/PRF/5 **(H)** cells upon knockdown or overexpression of p62. Data are expressed as ratio of phosphorylated ERK to total ERK signal intensities with values for respective controls (si co or co-v) set as 100%. **(I)** Microphotography displaying a representative hepatocellular carcinoma case (a: HE staining, b: total ERK1/2 immunostaining) with positive specific pERK1/2 immunostaining (c) and corresponding positive p62 immunostaining (d) in tumor tissue. Original magnification: 100x.

2.3.7 Discussion

The *IGF2* mRNA binding protein p62 was originally identified as a tumor-associated autoantigen with autoantibodies against p62 detected in 21% of HCC patients (55) and in several other types of cancer (40, 58). p62 protein was reported to be expressed in HCC tissue, but not in healthy surrounding tissue in 30% (33, 56) and up to 61.5% of HCCs (47). Concordantly, our data show significantly increased levels of *p62* mRNA in HCC tissue.

The IMP family member IMP3 was suggested as a prognostic marker for tumor malignancy and prognosis in different cancers, such as pancreatic ductal adenocarcinoma, neuroblastoma, prostate cancer, and colon cancer (7, 22, 24, 47). Similarly, IMP1 was observed to correlate with metastasis and shorter survival in colon cancer (14) and ovarian carcinoma (27). In line with these findings we observed a correlation between p62 expression and poor prognostic markers. Higher p62 expression was observed in tissues from intermediate or advanced tumors showing multinodularity, increased tumor size, poorer differentiation, and early recurrence of tumors, all of which indicate a more severe status of disease. Since *p62* mRNA levels were increased in G2/G3 *vs.* G1 patients one might speculate that p62 expression might serve as a valuable tumor marker in the future. However, higher numbers of patients need to be analyzed.

Our HCC cases comprised different etiologies, hence the limited sample number did not allow to correlate etiologies with the extent of p62 expression. Neither an association between viral infection (21) nor a potential correlation with steatohepatitis caused by NAFLD could be found for p62, although p62 overexpression in mouse livers induced a prominent steatotic phenotype (51).

The *p62* transgenic mouse model showed a pronounced expression of the metabolic and antiapoptotic growth factor *Igf2* (51). We now demonstrate that p62 expression correlates

with IGF2 expression also in human HCC. In fact, a causal effect of p62 on IGF2 expression is proven by both knockdown and overexpression of p62 in two different hepatoma cell lines. IGF2 is a well described antiapoptotic factor overexpressed in HCC (5, 32, 41, 42, 50) and other tumor tissues (3, 9, 45). The balance between apoptosis and survival is often disrupted due to antiapoptotic signals occurring in cancer (16). Accordingly, hepatocarcinogenesis and promotion of HCC is characterized by defective apoptosis and increased cell proliferation (18, 38). Proliferation did not seem to be influenced by p62 expression, which has also been shown for IMP3 in a hepatoma cell line (25). Interestingly, however, both knockdown and overexpression of p62 in hepatoma cells verified an antiapoptotic effect of p62. The IMP famlily members IMP1 and IMP3 have recently been demonstrated to promote cell survival and cancer cell proliferation (26, 31), whereby IGF2 seems to mediate apoptosis protection (31).

HCC is characterized by alterations in several important cellular signaling networks including the PI3-K and the ERK pathways (52). Constitutive activation of the PI3-K/AKT pathway has been firmly established as a major determinant of tumor cell growth and survival in several tumors (8). In HepG2 cells IGF1 has been demonstrated to have the ability to reverse apoptotic signaling by activation of the PI3-K/AKT signaling (1). IGF1 binds to the IGF1 receptor whose autophosphorylation is followed by phosphorylation of intracellular targets and finally leads to activation of the PI3-K and the ERK pathways (39). IGF2 was also demonstrated to act *via* the PI3-K/AKT pathway (30). Unexpectedly, the altered *IGF2* expression after knockdown or overexpression of p62 did not result in changes in AKT activation in HepG2 cells. Another recent study also showed independence of high *IGF2* mRNA expression and phophorylation of AKT in human HCC tissues (50). Interestingly, *p62* transgenic animals only exhibited increased Akt phophorylation in five-week-old animals, although *Igf2* was strongly induced also in animals of other age (51). Together with the lack of effect of a neutralizing anti-IGF2 antibody these findings strongly suggest no direct signaling axis p62-IGF2-PI3-K/Akt. The different results between wortmannin *vs.* LY294002 regarding the extent of apoptosis protection in p62-overexpressing cells is probably due the partial inhibition of proapoptotic p38 kinase by wortmannin (60).

Our data clearly indicate that the antiapoptotic effect of p62 is rather facilitated *via* ERK phosphorylation. In fact, in a rodent model tumor growth and apoptosis resistance of intraperitoneally applied hepatoma cells was enhanced by overexpression of the ERK upstream kinase MEK1 (23), and overactivation of the MAPK pathway in liver tumor cells was reported to play a role in the initiation and development of HCC through resistance to

apoptosis (4). Silencing ERK1/2 expression using RNA interference also led to suppression of cell proliferation in other tumors, such as ovarian cancer (46). In addition to these findings in experimental systems, two clinical reports displayed aberrant ERK phosphorylation, ranging from 23 up to 69% of HCCs (23, 43). Interestingly, Schmitz et al. demonstrated ERK1/2 phosphorylation to correlate with poor prognosis (43). Among the human HCC samples we also observed phosphorylation of ERK in cases with high p62 expression and poor outcome. There were also samples that were negative for phospho-ERK in tumor vessels, serving as staining control. We suggest that the detection of phospho-ERK might have failed, because the stabilization of phosphorylated proteins in formalin-fixed paraffin-embedded tissues is not always successful due to slow tissue penetration (35), and phosphorylation of ERK seems to be less stable as compared to other phospho-proteins (23). Therefore, an even higher frequency of HCC samples with ERK activation might be assumed.

ERK phosphorylation is not only altered in malignant tissues, but also in patients with severe chronic hepatitis B virus (HBV) infection (19), suggesting a transition step towards HCC. In fact, in the context of both HBV and hepatitis C virus (HCV) infection, activation of the ERK pathway was demonstrated to enhance cell cycle progression, cell proliferation, and survival (15, 59). Concordantly, ERK phosphorylation was strongly correlated to HCV infection (43). We demonstrate for the first time that ERK phosphorylation in hepatoma cells, which leads to resistance against apoptosis, is due to expression of the IMP p62. In line with these findings, ERK also seems to be involved in modulating drug resistance of HCC cells (53). Clinical relevance is underlined by the suggestion of a combined doxorubicin and ERK targeted therapy with enhanced anti-cancer effects in HCC (10).

Taken these findings together, p62 seems to play a dominant role in HCC progression and is accompanied by increased expression of the oncogene IGF2. Furthermore, p62-induced ERK activation seems to display a critical step in hepatocarcinogenesis.

2.3.8 Acknowledgements

Acknowledgement

We thank Elisabeth Tybl for the experiments with primary murine hepatocytes. We thank Nikolaus Gladel, Gertrud Walter, Nadja Chomyn, and Julia Michaely for excellent technical assistance and Dr. Britta Diesel for providing advice in cloning the p62 overexpression vector. We thank Dr. Eng M. Tan for critical reading of the article.

Grants

The project was funded by the Deutsche Krebshilfe (#107751). This work was supported in part by Deutsche Forschungsgemeinschaft (SFB/TRR 57 TP01 to F. Lammert), the HOMFOR program of Saarland University (to V. Zimmer) and the research committee of Saarland University (61-cl/Anschub2012/bew-ansch_bew_kessler to S.M. Kessler).

Author Contribution

S.M.K., J.P., V.Z., F.L., R.M.B., and A.K.K. conception and design of research; S.M.K., J.P., and S.L. performed experiments; S.M.K., J.P., V.Z., S.L., and A.K.K. analyzed data; S.M.K., J.P., V.Z., S.L., F.L., R.M.B., and A.K.K. interpreted results of experiments; S.M.K. prepared figures; S.M.K., S.L., and A.K.K. drafted manuscript; S.M.K., J.P., V.Z., S.L., F.L., R.M.B., and A.K.K. edited and revised manuscript; S.M.K., J.P., V.Z., S.L., F.L., R.M.B., and A.K.K. approved final version of manuscript.

2.3.9 References

1. **Alexia C, Fourmatgeat P, Delautier D, and Groyer A.** Insulin-like growth factor-I stimulates H4II rat hepatoma cell proliferation: Dominant role of PI-3'K/Akt signaling. *Experimental Cell Research* 312: 1142, 2006.
2. **Bouayed J, Desor F, Rammal H, Kiemer AK, Tybl E, Schroeder H, Rychen G, and Soulimani R.** Effects of lactational exposure to benzo[alpha]pyrene (B[alpha]P) on postnatal neurodevelopment, neuronal receptor gene expression and behaviour in mice. *Toxicology* 259: 97, 2009.
3. **Bussey KJ and Demeure MJ.** Genomic and expression profiling of adrenocortical carcinoma: Application to diagnosis, prognosis and treatment. *Future Oncology* 5: 641, 2009.
4. **Caja L, Sancho P, Bertran E, Iglesias-Serret D, Gil J, and Fabregat I.** Overactivation of the MEK/ERK pathway in liver tumor cells confers resistance to TGF-beta-induced cell death through impairing up-regulation of the NADPH oxidase NOX4. *Cancer Research* 69: 7595, 2009.

5. **Cariani E, Lasserre C, Seurin D, Hamelin B, Kemeny F, Franco D, Czech MP, Ullrich A, and Brechot C.** Differential Expression of Insulin-like Growth Factor II mRNA in Human Primary Liver Cancers, Benign Liver Tumors, and Liver Cirrhosis. *Cancer Res* 48: 6844-6849, 1988.
6. **Chen P, Wang S-j, Wang H-b, Ren P, Wang X-q, Liu W-g, Gu W-l, Li D-q, Zhang T-g, and Zhou C-j.** The distribution of IGF2 and IMP3 in osteosarcoma and its relationship with angiogenesis. *Journal of Molecular Histology*: 1, 2011.
7. **Chen S-T, Jeng Y-M, Chang C-C, Chang H-H, Huang M-C, Juan H-F, Hsu C-H, Lee H, Liao Y-F, Lee Y-L, Hsu W-M, and Lai H-S.** Insulin-like growth factor II mRNA-binding protein 3 expression predicts unfavorable prognosis in patients with neuroblastoma. *Cancer Science*: 2191, 2011.
8. **Chen YL, Law PY, and Loh HH.** Inhibition of PI3K/Akt signaling: An emerging paradigm for targeted cancer therapy. *Current Medicinal Chemistry - Anti-Cancer Agents* 5: 575, 2005.
9. **Cheng YW, Idrees K, Shattock R, Khan SA, Zeng Z, Brennan CW, Paty P, and Barany F.** Loss of imprinting and marked gene elevation are 2 forms of aberrant IGF2 expression in colorectal cancer. *International Journal of Cancer* 127: 568, 2010.
10. **Choi J, Yip-Schneider M, Albertin F, Wiesenauer C, Wang Y, and Schmidt CM.** The Effect of Doxorubicin on MEK-ERK Signaling Predicts Its Efficacy in HCC. *Journal of Surgical Research* 150: 219, 2008.
11. **Christiansen J, Kolte AM, Hansen TVO, and Nielsen FC.** IGF2 mRNA-binding protein 2: Biological function and putative role in type 2 diabetes. *Journal of Molecular Endocrinology* 43: 187, 2009.
12. **Cohen JC, Horton JD, and Hobbs HH.** Human fatty liver disease: Old questions and new insights. *Science* 332: 1519, 2011.
13. **Diesel B, Kulhanek-Heinze S, Höltje M, Brandt B, Höltje HD, Vollmar AM, and Kiemer AK.** Alpha-lipoic acid as a directly binding activator of the insulin receptor: Protection from hepatocyte apoptosis. *Biochemistry* 46: 2146, 2007.
14. **Dimitriadis E, Trangas T, Milatos S, Foukas PG, Gioulbasanis I, Courtis N, Nielsen FC, Pandis N, Dafni U, Bardi G, and Ioannidis P.** Expression of oncofetal RNA-binding protein CRD-BP/IMP1 predicts clinical outcome in colon cancer. *International Journal of Cancer* 121: 486, 2007.
15. **Ewings KE, Hadfield-Moorhouse K, Wiggins CM, Wickenden JA, Balmanno K, Gilley R, Degenhardt K, White E, and Cook SJ.** ERK1/2-dependent phosphorylation of BimEL promotes its rapid dissociation from Mcl-1 and Bcl-xL. *EMBO Journal* 26: 2856, 2007.
16. **Fabregat I, Roncero C, and Fernández M.** Survival and apoptosis: A dysregulated balance in liver cancer. *Liver International* 27: 155, 2007.
17. **Fürst R, Brueckl C, Kuebler WM, Zahler S, Krötz F, Görlach A, Vollmar AM, and Kiemer AK.** Atrial natriuretic peptide induces mitogen-activated protein kinase phosphatase-1 in human endothelial cells via Rac1 and NAD(P)H oxidase/Nox2-activation. *Circulation Research* 96: 43, 2005.
18. **Guicciardi ME and Gores GJ.** Apoptosis: A mechanism of acute and chronic liver injury. *Gut* 54: 1024, 2005.
19. **Han M, Yan W, Guo W, Xi D, Zhou Y, Li W, Gao S, Liu M, Levy G, Luo X, and Ning Q.** Hepatitis B virus-induced hFGL2 transcription is dependent on c-Ets-2 and MAPK signal pathway. *Journal of Biological Chemistry* 283: 32715, 2008.
20. **Hansen TVO, Hammer NA, Nielsen J, Madsen M, Dalbaeck C, Wewer UM, Christiansen J, and Nielsen FC.** Dwarfism and Impaired Gut Development in Insulin-Like Growth Factor II mRNA-Binding Protein 1-Deficient Mice. *Mol Cell Biol* 24: 4448-4464, 2004.

21. **Haybaeck J, Zeller N, Wolf MJ, Weber A, Wagner U, Kurrer MO, Bremer J, Iezzi G, Graf R, Clavien P-A, Thimme R, Blum H, Nedospasov SA, Zatloukal K, Ramzan M, Ciesek S, Pietschmann T, Marche PN, Karin M, Kopf M, Browning JL, Aguzzi A, and Heikenwalder M.** A Lymphotoxin-Driven Pathway to Hepatocellular Carcinoma. *Cancer Cell* 16: 295, 2009.
22. **Hutchinson L.** Medical oncology: IMP3 is a novel prognostic marker for colon cancer. *Nature Reviews Clinical Oncology* 7: 123, 2010.
23. **Huynh H, Nguyen TTT, Chow K-HP, Tan PH, Soo KC, and Tran E.** Over-expression of the mitogen-activated protein kinase (MAPK) kinase (MEK)-MAPK in hepatocellular carcinoma: Its role in tumor progression and apoptosis. *BMC Gastroenterology* 3: 19, 2003.
24. **Ikenberg K, Fritzsche FR, Zuerrer-Haerdi U, Hofmann I, Hermanns T, Seifert H, Müntener M, Provenzano M, Sulser T, Behnke S, Gerhardt J, Mortezavi A, Wild P, Hofstädter F, Burger M, Moch H, and Kristiansen G.** Insulin-like growth factor II mRNA binding protein 3 (IMP3) is overexpressed in prostate cancer and correlates with higher Gleason scores. *BMC Cancer* 10, 2010.
25. **Jeng YM, Chang CC, Hu FC, Chou HY, Kao HL, Wang TH, and Hsu HC.** RNA-binding protein insulin-like growth factor II mRNA-binding protein 3 expression promotes tumor invasion and predicts early recurrence and poor prognosis in hepatocellular carcinoma. *Hepatology (Baltimore, Md)* 48: 1118, 2008.
26. **Kawakami Y, Kubota N, Ekuni N, Suzuki-Yamamoto T, Kimoto M, Yamashita H, Tsuji H, Yoshimoto T, Jisaka M, Tanaka J, Fujimura HF, Miwa Y, and Takahashi Y.** Tumor-Suppressive Lipoxygenases Inhibit the Expression of c-myc mRNA Coding Region Determinant-Binding Protein/Insulin-Like Growth Factor II mRNA-Binding Protein 1 in Human Prostate Carcinoma PC-3 Cells. *Bioscience, Biotechnology, and Biochemistry* 73: 1811, 2009.
27. **Kobel M, Weidensdorfer D, Reinke C, Lederer M, Schmitt WD, Zeng K, Thomssen C, Hauptmann S, and Huttelmaier S.** Expression of the RNA-binding protein IMP1 correlates with poor prognosis in ovarian carcinoma. *Oncogene* 26: 7584, 2007.
28. **Kulhanek-Heinze S, Gerbes AL, Gerwig T, Vollmar AM, and Kiemer AK.** Protein kinase a dependent signalling mediates anti-apoptotic effects of the atrial natriuretic peptide in ischemic livers. *Journal of Hepatology* 41: 414, 2004.
29. **Leicht DT, Balan V, Kaplun A, Singh-Gupta V, Kaplun L, Dobson M, and Tzivion G.** Raf kinases: Function, regulation and role in human cancer. *Biochimica et Biophysica Acta - Molecular Cell Research* 1773: 1196, 2007.
30. **Liang L, Guo WH, Esquiliano DR, Asai M, Rodriguez S, Giraud J, Kushner JA, White MF, and Lopez MF.** Insulin-like growth factor 2 and the insulin receptor, but not insulin, regulate fetal hepatic glycogen synthesis. *Endocrinology* 151: 741, 2010.
31. **Liao B, Hu Y, and Brewer G.** RNA-binding protein insulin-like growth factor mRNA-binding protein 3 (IMP-3) promotes cell survival via insulin-like growth factor II signaling after ionizing radiation. *Journal of Biological Chemistry* 286: 31145, 2011.
32. **Liu P, Terradillos O, Renard CA, Feldmann G, Buendia MA, and Bernuau D.** Hepatocarcinogenesis in woodchuck hepatitis virus/c-myc mice: Sustained cell proliferation and biphasic activation of insulin-like growth factor II. *Hepatology* 25: 874, 1997.
33. **Lu M, Nakamura RM, Dent ED, Zhang J-Y, Nielsen FC, Christiansen J, Chan EKL, and Tan EM.** Aberrant Expression of Fetal RNA-Binding Protein p62 in Liver Cancer and Liver Cirrhosis. *Am J Pathol* 159: 945-953, 2001.

34. **Lu ZL, Luo DZ, and Wen JM.** Expression and significance of tumor-related genes in HCC. *World Journal of Gastroenterology* 11: 3850, 2005.
35. **Mueller C, Edmiston KH, Carpenter C, Gaffney E, Ryan C, Ward R, White S, Memeo L, Colarossi C, Petricoin EF, III, Liotta LA, and Espina V.** One-Step Preservation of Phosphoproteins and Tissue Morphology at Room Temperature for Diagnostic and Research Specimens. *PLoS ONE* 6: e23780, 2011.
36. **Nielsen FC.** The molecular and cellular biology of insulin-like growth factor II. *Cytokine and Growth Factor Reviews* 4: 257, 1992.
37. **O'Dell SD and Day INM.** Insulin-like growth factor II (IGF-II). *International Journal of Biochemistry and Cell Biology* 30: 767, 1998.
38. **Park YN, Chae KJ, Kim YB, Park C, and Theise N.** Apoptosis and proliferation in hepatocarcinogenesis related to cirrhosis. *Cancer* 92: 2733, 2001.
39. **Pollak MN, Schernhammer ES, and Hankinson SE.** Insulin-like growth factors and neoplasia. *Nature Reviews Cancer* 4: 505, 2004.
40. **Rom WN, Goldberg JD, Addrizzo-Harris D, Watson HN, Khilkin M, Greenberg AK, Naidich DP, Crawford B, Eylers E, Liu D, and Tan EM.** Identification of an autoantibody panel to separate lung cancer from smokers and nonsmokers. *BMC Cancer* 10, 2010.
41. **Scharf JG and Braulke T.** The Role of the IGF Axis in Hepatocarcinogenesis. *Hormone and Metabolic Research* 35: 685, 2003.
42. **Schirmacher P, Held WA, Yang D, Chisari FV, Rustum Y, and Rogler CE.** Reactivation of insulin-like growth factor II during hepatocarcinogenesis in transgenic mice suggests a role in malignant growth. *Cancer Research* 52: 2549, 1992.
43. **Schmitz KJ, Wohlschlaeger J, Lang H, Sotiropoulos GC, Malago M, Steveling K, Reis H, Cicinnati VR, Schmid KW, and Baba HA.** Activation of the ERK and AKT signalling pathway predicts poor prognosis in hepatocellular carcinoma and ERK activation in cancer tissue is associated with hepatitis C virus infection. *Journal of Hepatology* 48: 83, 2008.
44. **Seglen PO.** Preparation of rat liver cells. III. Enzymatic requirements for tissue dispersion. *Experimental Cell Research* 82: 391, 1973.
45. **Somers GR, Michael HO, Pienkowska M, Shlien A, Malkin D, Ackerley C, and Zielenska M.** IGF2 is highly expressed in pediatric undifferentiated sarcomas and reveals two distinct cytoplasmic trafficking patterns. *Pediatric and Developmental Pathology* 13: 169, 2010.
46. **Steinmetz R, Wagoner HA, Zeng P, Hammond JR, Hannon TS, Meyers JL, and Pescovitz OH.** Mechanisms regulating the constitutive activation of the extracellular signal-regulated kinase (ERK) signaling pathway in ovarian cancer and the effect of ribonucleic acid interference for ERK1/2 on cancer cell proliferation. *Molecular Endocrinology* 18: 2570, 2004.
47. **Su Y, Qian H, Zhang J, Wang S, Shi P, and Peng X.** The diversity expression of p62 in digestive system cancers. *Clinical Immunology* 116: 118, 2005.
48. **Takamatsu S, Noguchi N, Kudoh A, Nakamura N, Kawamura T, Teramoto K, Igari T, and Arii S.** Influence of risk factors for metabolic syndrome and non-alcoholic fatty liver disease on the progression and prognosis of hepatocellular carcinoma. *Hepato-Gastroenterology* 55: 609, 2008.
49. **Thorgeirsson SS and Grisham JW.** Molecular pathogenesis of human hepatocellular carcinoma. *Nature Genetics* 31: 339, 2002.
50. **Tovar V, Alsinet C, Villanueva A, Hoshida Y, Chiang DY, Solé M, Thung S, Moyano S, Toffanin S, Mínguez B, Cabellos L, Peix J, Schwartz M, Mazzaferro V, Bruix J, and Llovet JM.** IGF activation in a molecular subclass of hepatocellular

carcinoma and pre-clinical efficacy of IGF-1R blockage. *Journal of Hepatology* 52: 550, 2010.

51. **Tybl E, Shi F-D, Kessler SM, Tierling S, Walter J, Bohle RM, Wieland S, Zhang J, Tan EM, and Kiemer AK.** Overexpression of the IGF2-mRNA binding protein p62 in transgenic mice induces a steatotic phenotype. *Journal of Hepatology* 54: 994, 2011.
52. **Whittaker S, Marais R, and Zhu AX.** The role of signaling pathways in the development and treatment of hepatocellular carcinoma. *Oncogene* 29: 4989, 2010.
53. **Yan F, Wang XM, Pan C, and Ma QM.** Down-regulation of extracellular signal-regulated kinase 1/2 activity in P-glycoprotein-mediated multidrug resistant hepatocellular carcinoma cells. *World Journal of Gastroenterology* 15: 1443, 2009.
54. **Yao X, Hu JF, Daniels M, Shiran H, Zhou X, Yan H, Lu H, Zeng Z, Wang Q, Li T, and Hoffman AR.** A methylated oligonucleotide inhibits IGF2 expression and enhances survival in a model of hepatocellular carcinoma. *Journal of Clinical Investigation* 111: 265, 2003.
55. **Zhang J-Y, Chan EKL, Peng X-X, and Tan EM.** A Novel Cytoplasmic Protein with RNA-binding Motifs Is an Autoantigen in Human Hepatocellular Carcinoma. *J Exp Med* 189: 1101-1110, 1999.
56. **Zhang J and Chan EKL.** Autoantibodies to IGF-II mRNA binding protein p62 and overexpression of p62 in human hepatocellular carcinoma. *Autoimmunity Reviews* 1: 146, 2002.
57. **Zhang JY, Chan EK, Peng XX, and Tan EM.** A novel cytoplasmic protein with RNA-binding motifs is an autoantigen in human hepatocellular carcinoma. *JExpMed* 189: 1101-1110, 1999.
58. **Zhang JY, Chan EKL, Peng XX, Lu M, Wang X, Mueller F, and Tan EM.** Autoimmune responses to mRNA binding proteins p62 and Koc in diverse malignancies. *Clinical Immunology* 100: 149, 2001.
59. **Zhao LJ, Wang L, Ren H, Cao J, Li L, Ke JS, and Qi ZT.** Hepatitis C virus E2 protein promotes human hepatoma cell proliferation through the MAPK/ERK signaling pathway via cellular receptors. *Experimental Cell Research* 305: 23, 2005.
60. **Davies SP, Reddy, Caivano M, and Cohen P.** Specificity and mechanism of action of some commonly used protein kinase inhibitors. *Biochem J* 351: 95-105, 2000.

2.4 Lipid Metabolism Signatures in NASH-Associated HCC - Letter

IV

A publication reporting that ELOVL6 was upregulated in a murine NASH model and in murine NASH-associated HCC (Muir et al., 2013) drew our attention, since ELOVL6 has been reported to promote NASH in mice and humans (Matsuzaka et al., 2012) and is also overexpressed in the p62-induced steatosis, which is accompanied by mild signs of inflammation (Laggai et al., 2014). However, the authors proposed ELOVL6 as a pharmacological target for the treatment of human HCC, without showing ELOVL6 expression data or showing elevated fatty acid elongation in the human system (Muir et al., 2013). Our own data obtained from the analysis of human HCC data from a Gene Expression Omnibus dataset and a murine HCC model suggested decreased expression of ELOVL6 in HCC.

Lipid Metabolism Signatures in NASH-Associated HCC - Letter.

Sonja M. Kessler, **Stephan Laggai**, Ahmad Barghash, Volkhard Helms, and Alexandra K. Kiemer.

This research was originally published in Cancer Research. Kessler, S.M., Laggai, S., Barghash, A., Helms, V., and Kiemer A.K. Lipid Metabolism Signatures in NASH-Associated HCC—Letter. *Cancer Res.* 2014; **74**, 2903-2904. doi: 10.1158/0008-5472.CAN-13-2852. Copyright © 2014, American Association for Cancer Research.

The full text article can also be found at:
http://cancerres.aacrjournals.org/content/74/10/2903.full.pdf+html

2.4.1 Author Contribution

Published Online First April 28, 2014; doi: 10.1158/0008-5472.CAN-13-2852. *Cancer Res* May 15, 2014 74; 2903

Lipid Metabolism Signatures in NASH-Associated HCC - Letter.

Kessler SM, **Laggai S**, Barghash A, Helms V, Kiemer AK.

Kessler SM:
Performed animal procedures.
Coordinated the analysis of the Gene Expression Omnibus dataset samples.
Designed the DEN animal model study and experiments.
Wrote and revised the manuscript.

Laggai S:
Performed real-time RT-PCR analysis.
Performed data acquisition and statistical analysis.
Wrote and revised the manuscript.

Barghash A and Helms V:
Performed and directed the bioinformatical analysis of the Gene Expression Omnibus dataset.
Wrote and revised the manuscript.

Kiemer AK:
Initiated and directed the study.
Designed experiments.
Wrote and revised the manuscript.

2.4.2 Title page

Lipid Metabolism Signatures in NASH-Associated HCC - Letter

Sonja M. Kessler[1], **Stephan Laggai[1]**, Ahmad Barghash[2], Volkhard Helms[2], Alexandra K. Kiemer[1*]

[1] Department of Pharmacy, Pharmaceutical Biology, Saarland University, Saarbrücken, Germany

[2] Center for Bioinformatics, Saarland University, Saarbrücken, Germany

*To whom correspondence should be addressed

Alexandra K. Kiemer, Ph.D.

Saarland University, Pharmaceutical Biology

P.O. box 15 11 50

66041 Saarbrücken, Germany

phone: +49-681-302 57301

fax: +49-681-302 57302

e-mail: pharm.bio.kiemer@mx.uni-saarland.de

Word count: 399

Number of figures: 2

2.4.3 Letter

An article published recently in *Cancer Research* elegantly performed lipidomic and gene expression analyses in a murine model of NASH-associated hepatocellular carcinoma (HCC) and compared the findings to serum samples from fibrosis and HCC patients (1).

The study reports that the expression of the C18 fatty acid producing elongase 6 (*ELOVL6*) is elevated in a mouse non-alcoholic steatohepatitis model. The animals also exhibited elevated oleic acid (18:1n9) and vaccenic acid (18:1n7) abundance in livers and serum. Thereby, the study supports findings about increased hepatic *ELOVL6* expression in other models of NASH, such as a fructose feeding model (2) and low-density lipoprotein receptor (LDLR) knockout animals fed a western type diet (3). In line with these findings, a causal role for ELOVL6 in the development of NASH was published recently in a comprehensive work employing overexpression and knockdown strategies (4).

HCC represents a rare but important complication of non-alcoholic steatohepatitis (NASH) (5). The study by Muir et al. reports an increased expression of ELOVL6 not only in murine NASH but also in murine NASH-associated HCC. Because lipidomic analyses of sera of 15 patients with HCC showed a higher prevalence of the C18 vaccenic acid (18:1n7) than serum of cirrhosis patients, the authors suggested elevated ELOVL6 expression in human HCC. Although they observed lower levels of the more abundant linoleic acid (18:2n6) and they do not show any data on ELOVL6 expression in patients with HCC, they propose ELOVL6 as a pharmacological target for patients predisposed to HCC.

We investigated differential *ELOVL6* gene expression between HCC (n=247) and non-tumor (n=239) samples of a Gene Expression Omnibus dataset (GSE14520, Fig. 1).

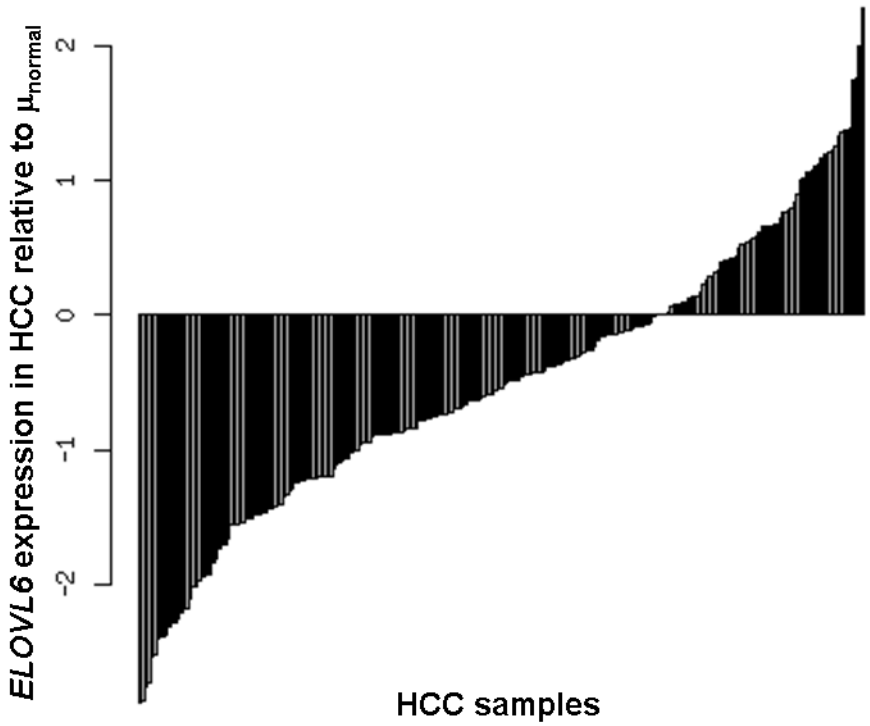

Figure 1: mRNA levels of *ELOVL6* in 247 human HCC samples relative to the mean of 239 non-tumor liver tissue (μ_{normal}). Samples of dataset GSE14520 [$\log_2$ (expression) values from GEO after Robust Multi-array Average normalization] were mapped to hgu133a.db using bioconductor. Significance values: *p*=3.8E-11, Kolmogorov-Smirnov test; *p*= 6.7E-11 t-test; 5.1E-11, Mann-Whitney U test.

Interestingly, in contrast to Muir and colleagues, our results from this large data set revealed significantly decreased levels of *ELOVL6* gene expression in the majority of human liver tumors compared to non-tumorous tissue. We also observed a decreased expression of *Elovl6* in the widely accepted murine diethylnitrosamine (DEN) HCC model (Fig. 2).

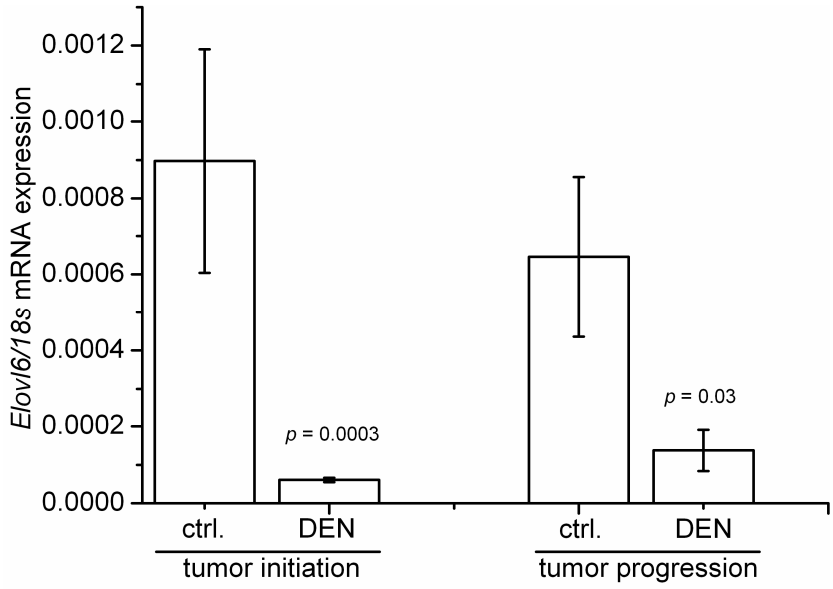

Figure 2: Wild-type mice were treated with the carcinogen diethylnitrosamine (DEN) at the age of 2 weeks. Livers were analyzed after 24 weeks to assess the tumor initiation state. Analyses in the tumor progression stadium were done after 36 weeks. *Elovl6* mRNA expression as determined by real-time RT-PCR with n=8-18 per group. Data were normalized to 18s. Statistical differences compared to untreated animals of the same age (ctrl.) were calculated by Mann-Whitney U-test.

Taken together, different recent reports from the literature suggest a pathophysiological role for ELOVL6 in steatohepatitis. Still, a role for ELOVL6 in HCC is as yet elusive and our data show ELOVL6 expression to be reduced in a common murine non-NASH-associated HCC model as well as in a large proportion of patients with HCC. In our opinion the data available on ELOVL6 in HCC do not justify proposing ELOVL6 as a therapeutic target in either prevention or treatment of HCC.

2.4.4 References

1. Muir K, Hazim A, He Y, Peyressatre M, Kim DY, Song X, et al. Proteomic and lipidomic signatures of lipid metabolism in NASH-associated hepatocellular carcinoma. Cancer Res 2013;73:4722-4731.
2. Mori T, Kondo H, Hase T, Murase T. Dietary phospholipids ameliorate fructose-induced hepatic lipid and metabolic abnormalities in rats. J Nutr 2011;141:2003-2009.
3. Hoekstra M, van der Sluis RJ, Kuiper J, Van Berkel TJC. Nonalcoholic fatty liver disease is associated with an altered hepatocyte microRNA profile in LDL receptor knockout mice. J Nutr 2012;23:622-628.
4. Matsuzaka T, Atsumi A, Matsumori R, Nie T, Shinozaki H, Suzuki-Kemuriyama N, et al. Elovl6 promotes nonalcoholic steatohepatitis in mice and humans. Hepatology 2012;56:2199-2208.
5. Li Y, Tang ZY, Hou JX. Hepatocellular carcinoma: Insight from animal models. Nat Rev Gastroenterol and Hepatol 2012;9:32-43.

3 Unpublished data

The following part contains new data, which will be submitted for publication after submission of my PhD thesis.

3.1 Abstract

p62 has been found to upregulate *Igf2* and *H19* mRNA expression in murine livers and our unpublished data suggest that p62 strongly amplifies tumor incidence. *Igf2* and *H19* genes are regulated by epigenetic mechanisms and are encoding for microRNAs.

The aim of our study was to evaluate the impact of p62 on microRNA regulation and to link them to p62-mediated hepatocarcinogenesis.

We performed microRNA array analysis of *p62* transgenic livers and compared them to wild-type controls. The microRNA array revealed an interesting effect of p62 on up to 25 microRNAs located in the imprinted *Dlk1* and *Gtl2* (human homologue *MEG3*) domain, whereby the maternally expressed *Gtl2* represents a non-coding microRNA precursor RNA.

We could identify that p62 also induces miR-483 and -675, which are encoded by *Igf2* and *H19*.

The paternally expressed Dlk1 encodes for a protein, which has been suggested to be involved in hepatocarcinogenesis, we looked at *Dlk1* and *Gtl2* expression. In line with the finding that p62 induces the miRNAs located in the *Dlk1-Gtl2* cluster, we were able to demonstrate that p62 also induces *Dlk1* and *Gtl2* mRNA and DLK1 protein in untreated animals. Besides, we found elevated levels of *Dlk1* and the Rho GTPase *Rac1* mRNAs in *p62* transgenics challenged with the potent carcinogen DEN. *RAC1* mRNA was regulated dependent on p62 as found in human HepG2 cells challenged by p62 knockdown or overexpression. An additional finding revealed that DLK1 induces *RAC1*.

DLK1 and RAC1 might be responsible for ERK activation as found in *p62* transgenic animals treated with or without DEN.

Taken together, we could decipher parts of the pathway how p62 might exert its carcinogenic and antiapoptotic effects, which seems mainly mediated by affecting imprinting, regulation of microRNAs, and the activation of the ERK pathway *via* DLK1/RAC1.

3.2 Introduction

Previous data showed that p62 acts as a regulator of gene expression with distinct effects on imprinted genes (Tybl et al., 2011) as well as metabolic and inflammatory regulators (Laggai et al., 2014; Simon et al., 2014a; Simon et al., 2014b). We hypothesized that p62 might exert its actions in liver pathophysiology also by affecting the expression of microRNAs (miRs). MicroRNAs are small non-protein-coding RNAs, which can negatively control their respective gene targets (Esquela-Kerscher and Slack, 2006). MicroRNAs are transcribed by RNA polymerase II, resulting in a large RNA precursor called primary microRNA, processed by the RNase III enzyme Drosha and the double-stranded-RNA-binding protein Pasha into the respective precursor microRNA (~70 nucleotides)(Lee et al., 2002). The precursor microRNA is cleaved by another RNase III enzyme called Dicer and the mature double-stranded microRNA (~22 nucleotides) is incorporated into the microRNA induced silencing complex (Meister, 2013), which finally can bind to and regulate its target RNAs. In addition to their action within their cell of origin, microRNAs can also be secreted into the circulating blood included in lipid or lipoprotein complexes, such as exosomes, and act by modulating the gene expression within their recipient cells (Hu et al., 2012). Circulating microRNAs were suggested as new biomarkers for liver diseases (Kosaka et al., 2010).

MicroRNAs play a pivotal role also in the normal liver development. In this context, members of the miR-181 family are highly expressed in embryonic liver and involved in liver differentiation (Ji et al., 2009). Aberrant expression of microRNAs correlates with all stages of NAFLD (Wang et al., 2012) and in various human cancer types. MicroRNAs can act as tumor suppressors as well as oncogenes (Esquela-Kerscher and Slack, 2006).

Literature regarding microRNA profiles and mechanisms in NAFLD is rather underrepresented compared to liver cancer. However, some microRNAs are regarded as potential biomarkers for NAFLD progression:

miR-15b was elevated in two different NAFLD rat models (Zhang et al., 2013), and circulating levels of miR-122, -34a, -16 (Cermelli et al., 2011), and -15b were significantly higher in sera of NAFLD patients (Zhang et al., 2013). miR-29 was shown to be implicated in the regulation of human and murine liver fibrosis (Roderburg et al., 2011), and miR-106b and -181b were suggested as potential biomarkers for liver cirrhosis (Chen et al., 2013).

MicroRNA profiling in liver cancer is currently the most studied topic regarding microRNAs in liver disease. There are several studies, which identified let-7, miR-122, -26, and -101 to be downregulated, and miR-221, -181, and -17-92 , -21 to be upregulated in serum and tissue of

HCC patients (Karakatsanis et al., 2013; Wang et al., 2014; Wang et al., 2012; Xu et al., 2011; Xu et al., 2014). Reduced expression of miR-122 often correlates with poor prognosis (Coulouarn et al., 2009). Furthermore, miR-21 was highly upregulated in human HCC tissue and modulated the expression of the tumor suppressor phosphatase and tensin homolog, which was responsible for increased cell growth, migration, and invasion in human hepatocytes and liver cancer cell lines (Meng et al., 2007).

The aim of our study was to decipher the influence of p62 on microRNA expression and to link them to p62-mediated pathophysiologic actions in the liver.

3.3 Materials and Methods

3.3.1 Animals

All animal procedures were performed in accordance with the local animal welfare committee (permission 48/2009). *p62* transgenic mice were established as previously described (Tybl et al., 2011).

Mice were treated with diethylnitrosamine (DEN) at the age of two weeks by an intraperitonneal injection with 5 mg/kg body weight. Mice were sacrificed at the indicated time. All animal procedures were performed by Dr. Sonja M. Kessler (Pharmaceutical Biology, Saarland University, Saarbruecken, Germany).

3.3.2 Cell culture experiments

HepG2 cells were cultured in RPMI-1640 (Sigma Aldrich, Taufkirchen, Germany) with supplementation of 10% [v/v] FCS (Sigma Aldrich), 1% [v/v] glutamine (Sigma Aldrich), and 1% [v/v] penicillin/streptomycin (Sigma Aldrich) at 37°C and 5% CO_2.

Knockdown and overexpression experiments were performed as previously described (Laggai et al., 2014).

HepG2 cells were treated with 1 µg/ml human recombinant DLK1 in complete RPMI-1640 media for 48 h (1144-PR-025, R&D Systems, Minneapolis, USA).

3.3.3 microRNA array

The microRNA array was performed in cooperation with the group of Prof. Meese (Dr. Petra Leidinger, Humangenetik, Universitaetsklinikum Saarland, Homburg, Germany). RNA from

tissues were isolated using the miRNeasy mini kit (217004, Qiagen, Hilden, Germany), and the microRNA array was performed with a mouse miRNA microarray, Release 17.0, 8x60K (G4872A-035430, Agilent Technologies, Waldbronn, Germany) as recommended by the manufacturer.

3.3.4 Real-time RT-PCR

Real-time RT-PCR was performed as previously described (Laggai et al., 2014; Tybl et al., 2011). Primer sequences and conditions can be found in the supplementary part (page 117-119)

3.3.5 Extracellular-signal regulated kinase (ERK) Western Blot

ERK Western blot and analysis was performed by Dr. Sonja M. Kessler as previously described (Kessler et al., 2013).

3.3.6 ELISA

DLK1 ELISA was performed with a Mouse Protein delta homolog 1 (DLK1) ELISA kit (CSB-EL006945MO, Cusabio, Wuhan, China) as recommended by the manufacturer.

3.3.7 Statistical analysis

Statistical differences were estimated using the Mann-Whitney-U test or Fisher exact test (tumor incidence, 6 months, DEN mice). Calculations were performed using the software package Origin (Origin pro 8.6G, OriginLab Corporation, Northampton, USA). Pearson's correlation was used to determine the relationship between *Dlk1* and *Rac1* in 8 months old transgenic animals treated with DEN. Values of $p<0.05$ were considered statistically significant.

3.4 Results

microRNA array analysis of most distinctly altered microRNAs in *p62* transgenic mice revealed that microRNAs from the delta-like 1 homologue (*Drosophila*) (*DLK1*) / maternally expressed gene 3 (*MEG3*)(human), gene-trap locus 2 (*Gtl2*)(mouse) (*MEG3*/*Gtl2*) cluster were altered and showed a total regulation of 25 microRNAs (fold change > 1.4)(Fig. 3.1).

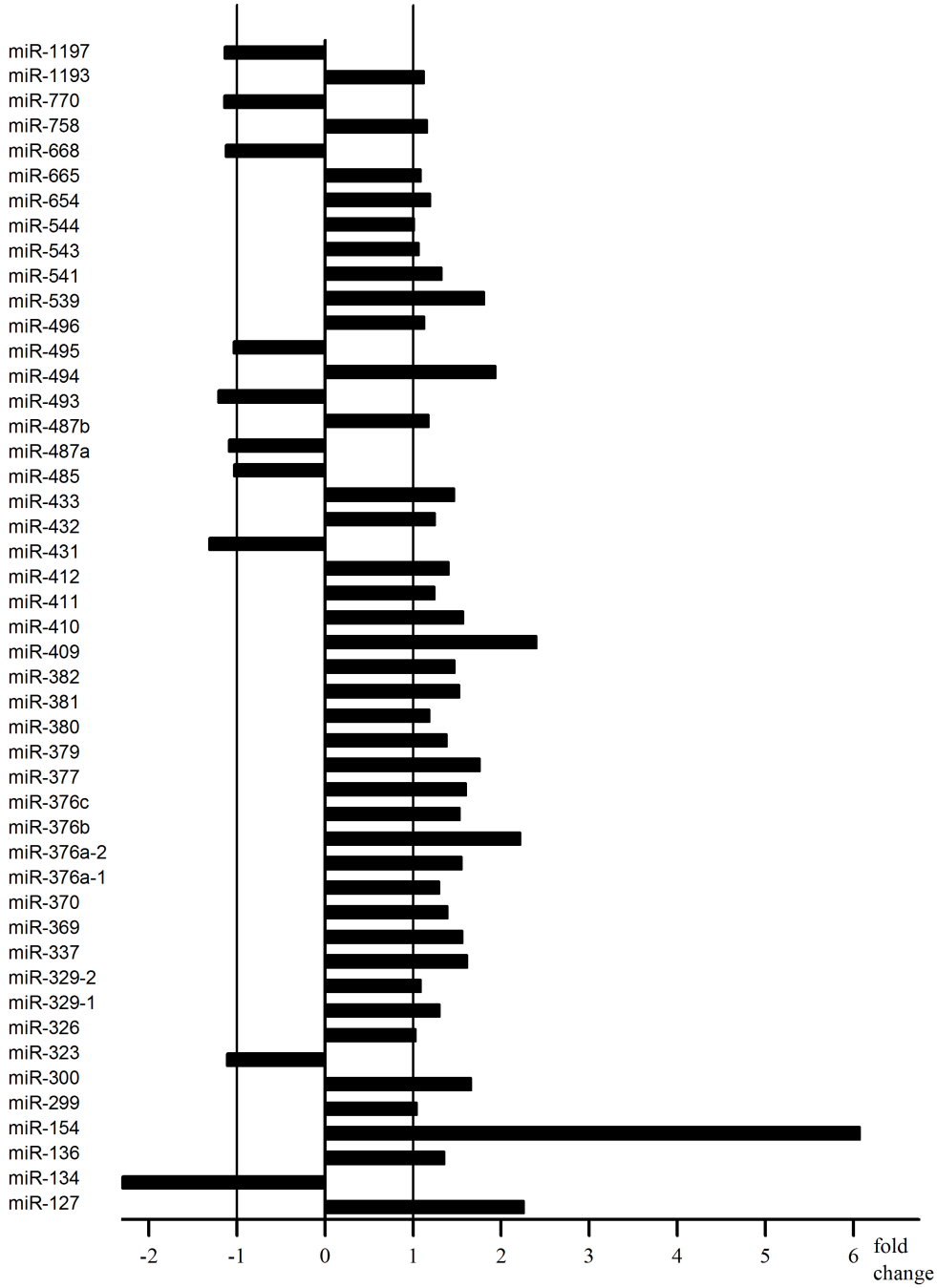

Fig. 3.1: p62-dependent changes in microRNA expression from the *Dlk1-Gtl2* cluster. Total RNA from wild-type and *p62* transgenic animals (5 weeks, n = 2, each) were analyzed by microRNA array. Results are presented as fold change compared to wild-type animals.

Furthermore, data from the microRNA array revealed that *p62* transgenic mice exhibited increased levels of miR-675-3p (1.7 fold, 5 weeks), which is encoded by *H19 (Keniry et al., 2012)*, and miR-483-3p (1.5 fold, 2.5 weeks), as an intronic transcript from the *Igf2* gene (Liu et al., 2013). The paternally expressed *IGF2* and the maternally expressed non-coding gene *H19* are imprinted genes, which are co-expressed and respond in a reciprocal manner to loss of DNA methylation (Schmidt et al., 2000).

Also the *Dlk1-Gtl2* cluster represents an imprinted genomic region. *Gtl2* is a maternally expressed non-coding gene (Schmidt et al., 2000), which encodes for 54 microRNAs (Benetatos et al., 2013). With 25 of these microRNAs being regulated in *p62* transgenic animals we hypothesized that p62 upregulates *Gtl2* expression. We in fact found elevated levels of *Gtl2* mRNA (Fig. 3.2A). Interestingly, *DLK1*/pre-adipocyte factor-1 (*Pref-1*) as a paternally expressed protein coding gene (Schmidt et al., 2000) was also elevated in our *p62* transgenics (Fig. 3.2B). Since only the secreted form of DLK1 is active (Wang et al., 2006), we validated the expression of the active form of DLK1 by ELISA in mouse serum (Fig. 3.2C).

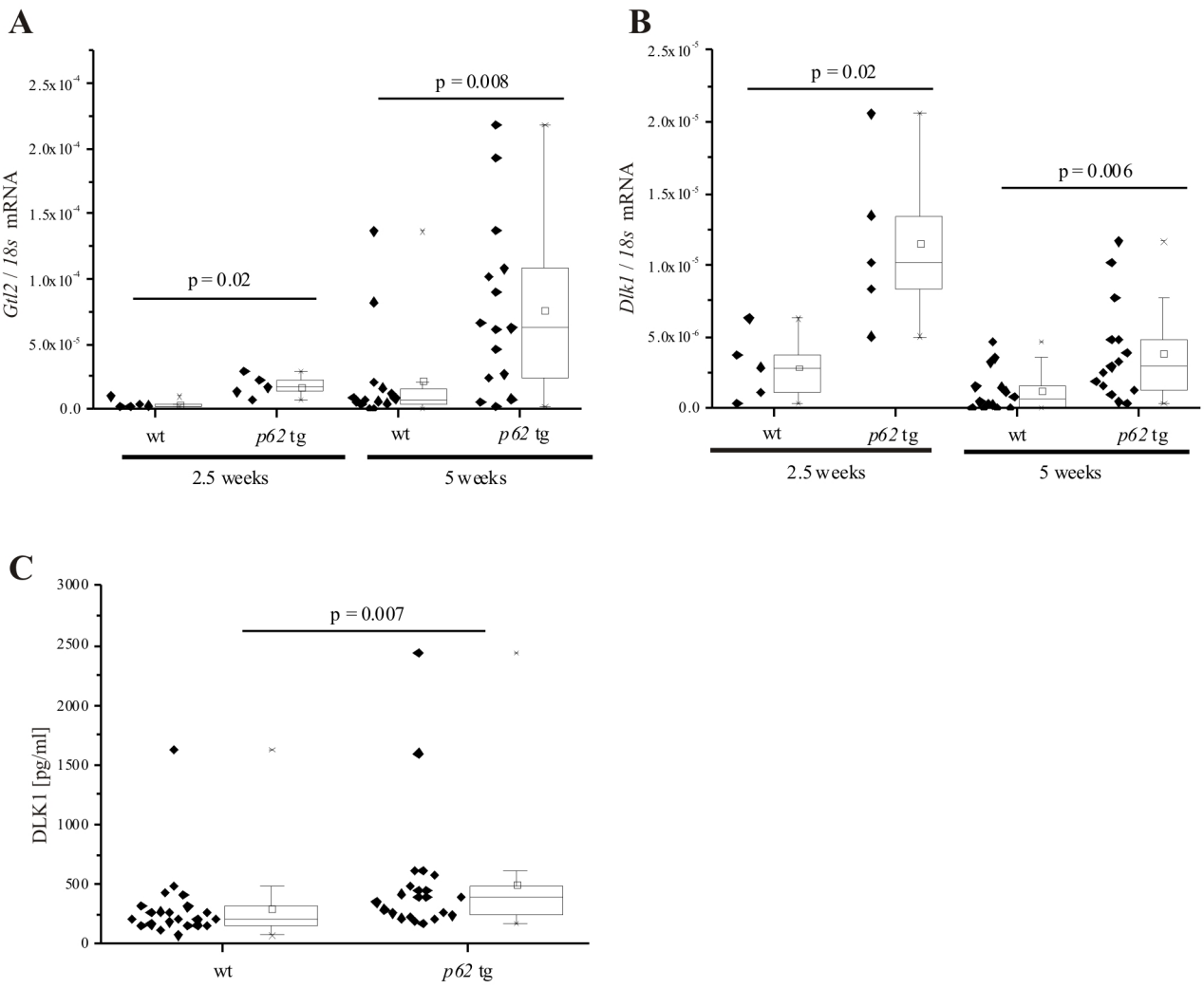

Fig. 3.2: A) Real-time RT-PCR for *Gtl2* mRNA expression from wild-type (wt) and *p62* transgenic mice (*p62* tg) at the age of 2.5 (wt: n = 5, *p62* tg n = 5) and 5 weeks (wt: n = 14; *p62* tg: n = 15). **B)** Real-time RT-PCR for *Dlk1* mRNA expression from wt and *p62* tg at the age of 2.5 (wt: n = 5, *p62* tg n = 5) and 5 weeks (wt: n = 14; *p62* tg: n = 15). **C)** DLK1 ELISA of sera from 5 week old wt and *p62* tg animals (wt, *p62* tg: n=22, each).

With DLK1 being an oncofetal marker (Falix et al., 2012) we hypothesized that elevated levels might support tumorigenic actions. We therefore challenged *p62* transgenic and wild-type mice with the carcinogen DEN in order to simulate states of tumor initiation and progression. We in fact observed a higher tumor incidence in *p62* transgenic animals (Fig. 3.3).

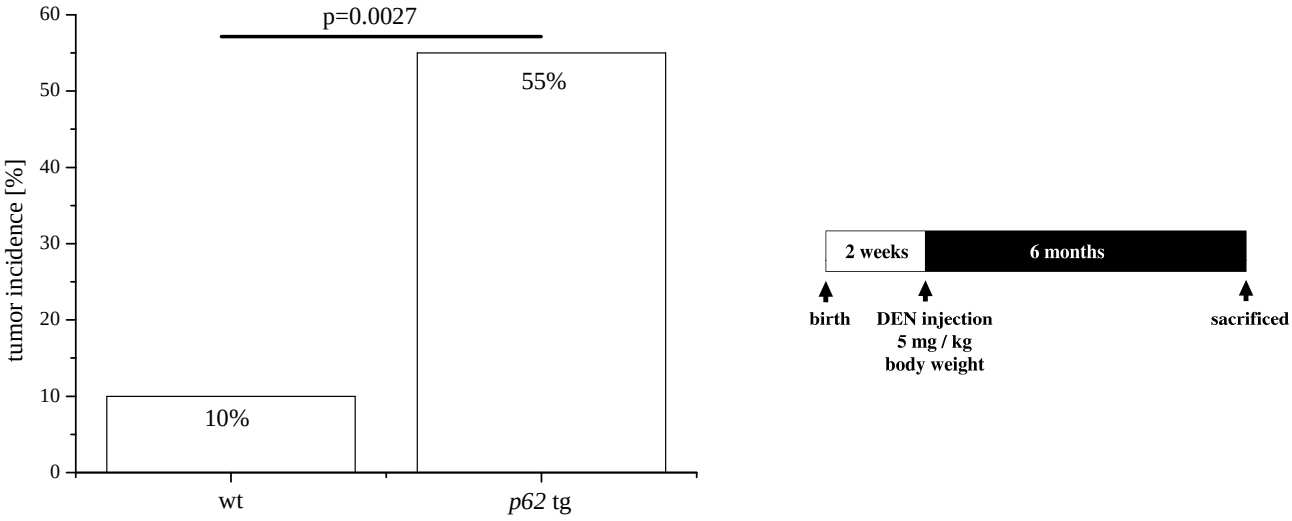

Fig. 3.3: Tumor incidence of wild-type (wt, n = 20) and *p62* transgenic animals (*p62* tg, n = 20) 6 months after treatement with DEN (data provided by Dr. Sonja M. Kessler).

DLK1 has been shown to activate extracellular-signal regulated kinase (ERK) by inducing ras-related C3 botulinum toxin substrate 1 (RAC1) in adipocytes (Wang et al., 2010). Since p62 induces ERK activation as an important tumor promoting protein kinase, we hypothesized that a similar signalling is induced by p62 during hepatocarcinogenesis. We in fact found increased levels of *Dlk1*, *Gtl2*, and *Rac1* mRNA (Fig. 3.4A, B, C), DLK1 protein (Fig. 3.4E), and increased amounts of activated ERK in *p62* transgenics (Fig. 3.4F). Interestingly, *Dlk1* was significantly upregulated in tumor tissue compared to non-tumor tissue (Fig. 3.4A). Since *Dlk1* showed only borderline significance in normal tissues of *p62* transgenic mice, we determined the interconnection between *Dlk1* and *Rac1* mRNA from these tissues by Pearson's correlation and indeed found a strong correlation (Fig. 3.4D).

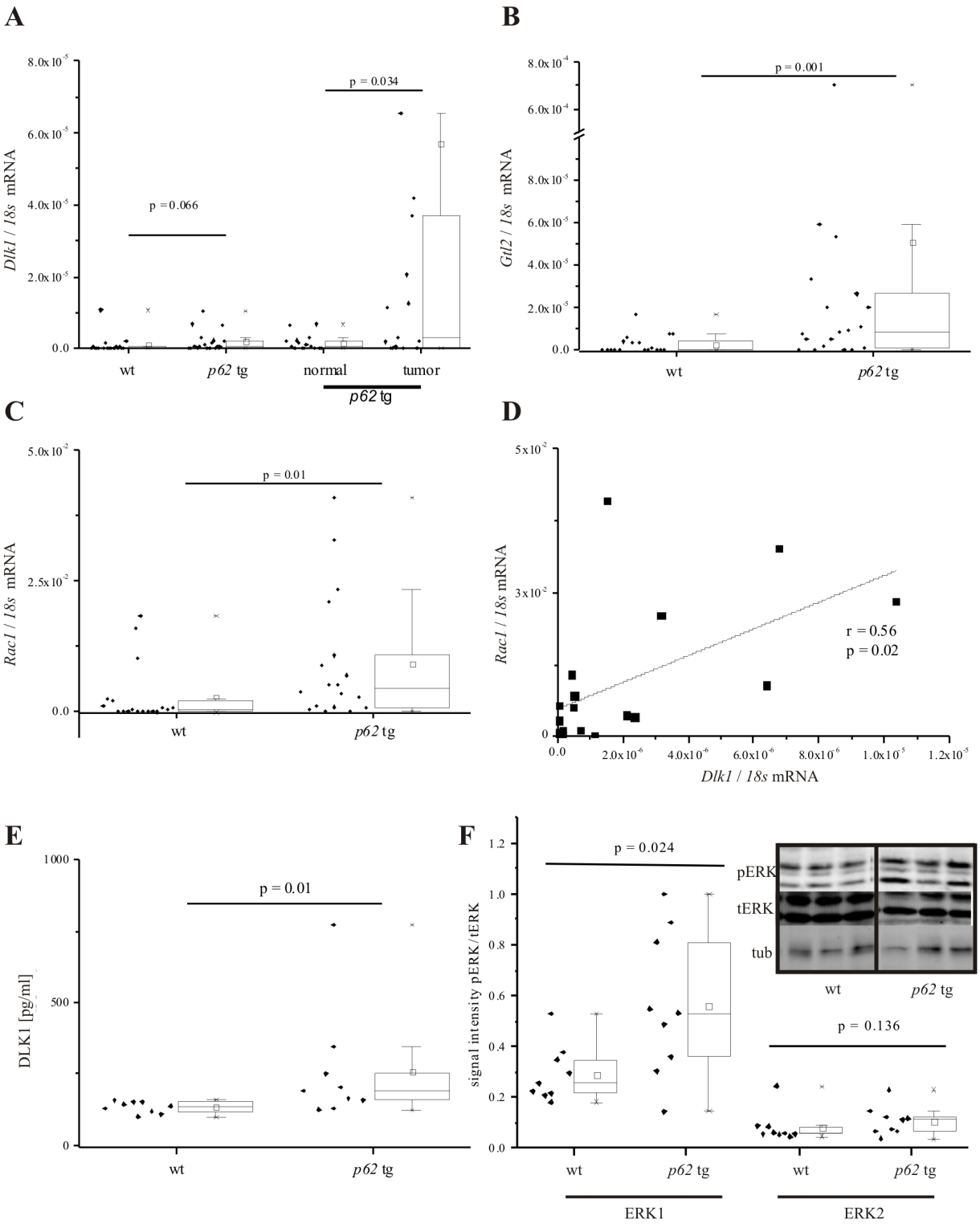

Fig. 3.4: A) Real-time RT-PCR for *Dlk1* mRNA expression from wild-type (wt) and *p62* transgenic mice (*p62* tg) at the age of 8 months treated with DEN, *p62* tg: n = 18, each) and the corresponding normal and tumor tissue from *p62* tg (wt, *p62* tg: n = 15, each). **B)** Real-time RT-PCR for *Gtl2* mRNA expression from wt and *p62* tg at the age of 8 months treated with DEN (wt, *p62* tg: n = 18, each). **C)** Real-time RT-PCR for *Rac1* mRNA expression from wt and *p62* tg at the age of 8 months treated with DEN (wt, *p62* tg: n = 18, each). **D)** Real-time RT-PCR for *Dlk1* and *Rac1* of *p62* tg at the age of 8 months treated with DEN (n = 18) normalized on *18s* mRNA levels. **E)** DLK1 ELISA of sera from 6 months old wt and *p62* tg animals treated with DEN (wt, *p62* tg: n = 9, each). **F)** Phospho-ERK (pERK) Western blot

and quantification of livers from 6 months old wt and *p62* tg animals normalized on total ERK (tERK)(wt, *p62* tg: n = 9, each) (data provided by Sonja M. Kessler).

We performed p62 knockdown and overexpression in human HepG2 cells and in line with the findings from *p62* transgenic animals, we saw that *RAC1* expression was dependent on p62 expression: *RAC1* was increased by overexpressing p62 (Fig. 3.5A) and decreased after p62 knockdown (Fig. 3.5B).

Since also HepG2 were susceptible to p62-mediated *RAC1* induction, we used this HepG2 model to validate that increased levels of *Rac1* were dependent on increased DLK1 levels in our *p62* transgenics. Therefore, we treated HepG2 cells with recombinant DLK1 and observed increased levels of *RAC1* mRNA (Fig. 3.5C).

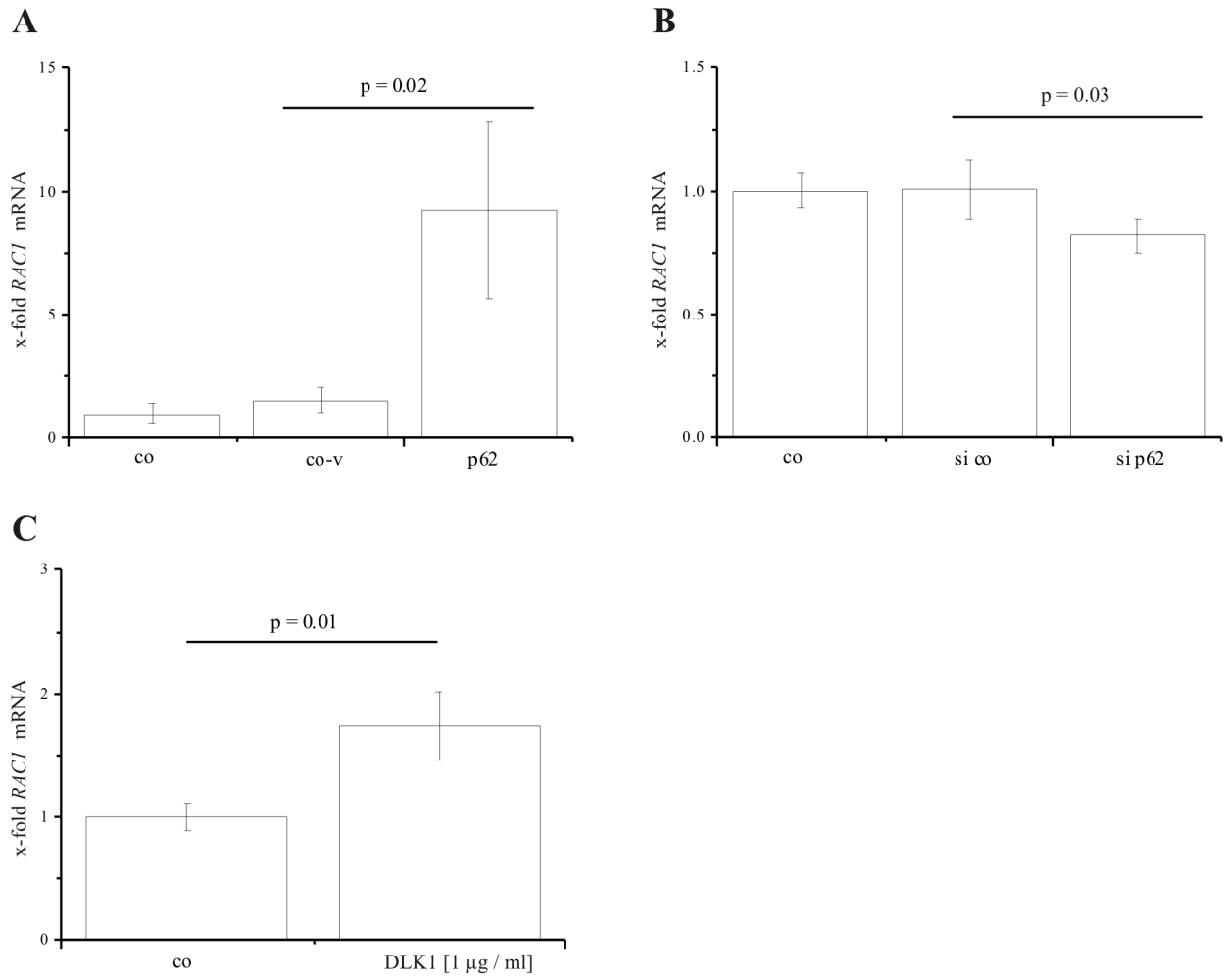

Fig. 3.5: A) Real-time RT-PCR of HepG2 transfected with p62 overexpression vector (p62) or control vector (co-v) for *RAC1* mRNA expression (n = 3, triplicate). **B)** Real-time RT-PCR of HepG2 transfected with p62 siRNA (si p62) or control siRNA (si co) for *RAC1* mRNA expression (n = 3, quadruplicate). **C)** Real-time RT-PCR of HepG2 treated with soluble DLK1 at a concentration of 1 µg / ml or untreated control cells (co) for *RAC1* mRNA expression (n = 3, duplicate).

3.5 Discussion

Aberrant expression of microRNAs of the *DLK1-MEG3* cluster, as also found in our *p62* transgenic animals, are common features in several cancer types, as recently reviewed in detail by Benetatos and colleagues (Benetatos et al., 2013). Interestingly, although the *DLK1-MEG3* cluster is encoding for at least 54 microRNAs (Benetatos et al., 2013) functional implications are rather uncharacterized. One publication suggests that the *DLK1-MEG3* locus is frequently deregulated in human HCC (Anwar et al., 2012). Lim et al. recently found this cluster upregulated in a subtype of human HCC and in three transgenic mouse models and suggested miR-494 as a therapeutic target for the treatment of HCC (Lim et al., 2014). Interestingly, miR-494, among many other microRNAs of this cluster, was also upregulated in the presence of p62.

A crucial role for the imprinted *IGF2-H19* cluster in different cancer types is widely accepted (Kamikihara et al., 2005; Ohlsson et al., 1999; Sakatani et al., 2005). For example, loss of imprinting of the *IGF2-H19* domain leads to the formation of the Beckwith-Wiedemann syndrome and Wilms' tumor (Sakatani et al., 2005). The *IGF2-H19* cluster is encoding for two microRNAs: The long non-coding RNA *H19* encodes for miR-675 (Keniry et al., 2012), and miR-483 is encoded by intronic regions of the *IGF2* gene (Liu et al., 2013). Data from our microRNA array indicated that miR-675 and miR-483 were upregulated and are in line with the finding that both *Igf2* and *H19* were strongly enhanced in *p62* transgenic animals (Tybl et al., 2011). miR-675 suppresses growth and cell proliferation in different cell lines (Keniry et al., 2012) suggesting tumor-suppressive actions. On the other hand, miR-675 is upregulated in human adrenocortical carcinoma and metastases (Schmitz et al., 2011). miR-483 enhances transcription of *Igf2* and tumorigenesis (Liu et al., 2013), and was suggested as a potential biomarker for HCC (Shen et al., 2013). Colon organoid culture revealed miR-483 as a dominant driver oncogene inducing dysplasia *in vitro* and tumorigenicity *in vivo* (Li et al., 2014). Taken together, p62 induces the expression of tumor-associated microRNAs. They might contribute to p62's tumor-promoting actions found in DEN-treated animals. Further comprehensive analysis is required for a detailed mechanistic understanding.

Since p62 induces the coordinated expression of the imprinted *Igf2* and *H19* genes in *p62* transgenic animals (Tybl et al., 2011) and their respective microRNAs, miR-483/miR-675, and p62 is also implicated in the regulation of the imprinted *Dlk1-Gtl2* cluster in these mice leads us to speculate that p62 is a general regulator of imprinted genes.

We observed that DLK1 mRNA and protein was elevated in *p62* transgenics. Interestingly, DLK1 protein has been shown to be expressed in hepatocellular, colon, pancreas, and breast carcinoma at a high frequency (Yanai et al., 2010). *DLK1* is induced specifically in HCC tissue and not in adjacent tissue, and suppression of DLK1 in human cancer cell lines can inhibit cell growth, colony formation, and tumorigenicity (Huang et al., 2007). DLK1 is a transmembrane protein, which is cleaved by tumor necrosis factor converting enzyme, secreted in its soluble form, and can therefore act as an autocrine / paracrine factor (Hudak and Sul, 2013). Recently, DLK1 has also been reported as a serum marker of hepatoblastoma in young infants (Falix et al., 2012) and as a marker for stem cells (Falix et al., 2012; Oertel et al., 2008; Tanimizu et al., 2003).

The finding that the antiapoptotic effect of p62 is dependent on the ERK signalling pathway and independent of IGF2 in *p62* transgenic mice and human (Kessler et al., 2013) raised the question how p62 induces activation of the ERK pathway.

The ERK signalling pathway plays a central role in cell proliferation and survival and increased ERK activity is found in many human cancer types (Montagut and Settleman, 2009; Thompson and Lyons, 2005). Also HCC is associated with overexpression and activation of ERK (Huynh et al., 2003) and activation of ERK correlates with poor prognosis (Schmitz et al., 2008).

DLK1 has been shown to activate ERK (Niba et al., 2013; Wang et al., 2010), which was postulated to be mediated *via* RAC1 (Wang et al., 2010).

RAC1 belongs to the family of small GTPases and controls cytoskeletal rearrengements and cell growth, is overexpressed in aggressive breast cancer (Schnelzer et al., 2000) and gastric cancer (Walch et al., 2008), and correlates with poor prognosis in HCC patients (Yang et al., 2010).

We found that DLK1 was strongly induced in our *p62* transgenic animal model, and led to increased expression of *RAC1* and activated ERK in DEN-challenged *p62* transgenics as well as elevated *RAC1* mRNA in a human cell line treated with DLK1 protein. HepG2 cells, in which p62 was modulated by knockdown or overexpression, revealed activated ERK levels (Kessler et al., 2013) corresponding to the levels of RAC1 found in this study. When p62 was absent, activated ERK and RAC1 levels decreased. *Vice versa*, when p62 was overexpressed activated ERK and RAC1 levels increased. Since DLK1 has been shown to induce the activation of ERK *via* RAC1 (Wang et al., 2010), we conclude that p62 induces DLK1 in our *p62* transgenic animals, which leads to increased RAC1 levels and subsequent activation of

ERK (Fig. 3.6). We suppose that DLK1 might be the missing link for the mechanism how p62 induces ERK activation.

Taken together, our data show that p62 (*I*) promotes tumor development (Fig. 3.6), (*II*) deregulates microRNAs, which are involved in hepatocarcinogenesis (Fig. 3.6), (*III*) regulates imprinting networks linked to hepatocarcinogenesis, as found for the *Igf2*/*H19* and *Dlk1*/*Gtl2* cluster (Fig. 3.6), and (*IV*) leads to the activation of the survival pathway ERK *via* DLK1/RAC1 (Fig. 3.6).

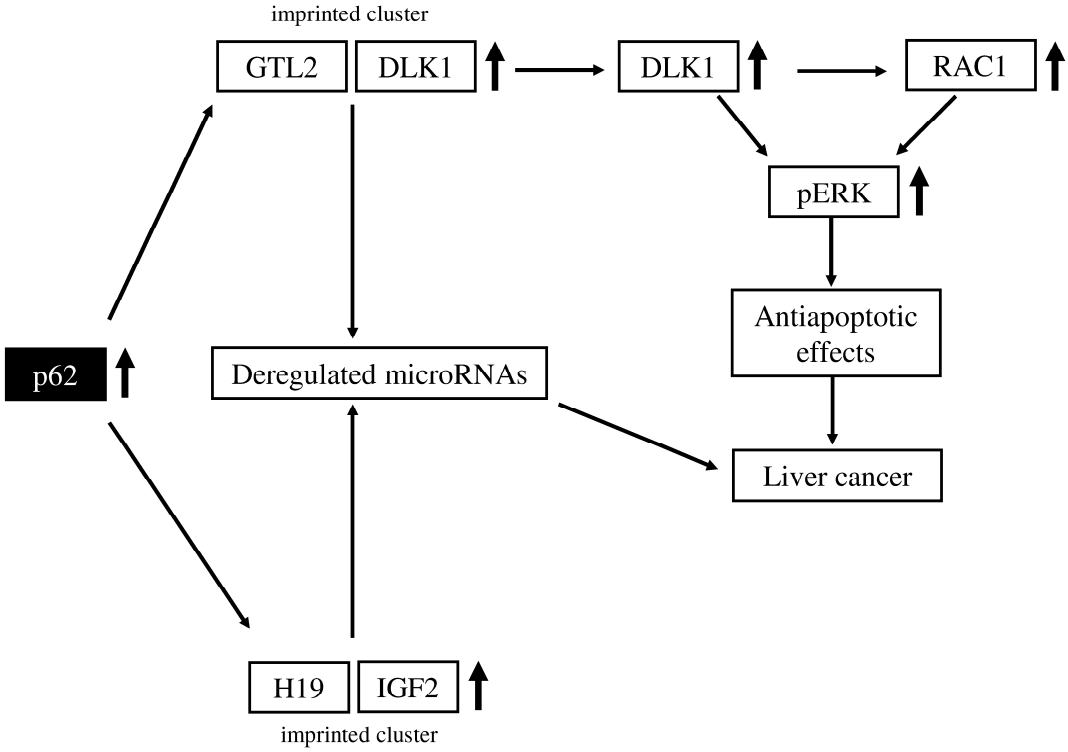

Fig. 3.6: Mechanisms of p62-mediated ERK activation and cancer development.

These findings support p62 as a potential biomarker and target for the treatment of HCC.

4 Extended summary

The insulin-like growth factor 2 (*IGF2*) mRNA binding protein p62/IGF2B2-2/IMP2-2 induces hepatic steatosis in mice, is overexpressed in patients with hepatocellular carcinoma (HCC), and is associated with the overexpression of the tumorigenic growth factor IGF2.

With hepatic steatosis being a crucial step in HCC development, the mechanisms by which p62 promotes malignant transformations in liver disease progression are poorly characterized.

Therefore, the aim of this study was to elucidate the implications of p62 on lipogenic and tumorigenic pathways.

Since alterations in hepatic lipid and fatty acid composition are linked to liver pathogenesis we analyzed the liver lipids of *p62* transgenic animals. Almost all lipid classes were elevated in the *p62* transgenic livers, with triglycerides showing the strongest increase. The lipid profile indicated that *p62* transgenic animals might develop signs of inflammation within their livers. Concordantly, we found elevated hepatic levels of the inflammatory marker F4/80 and leukocyte infiltrates (Fig. 4.1).

The fatty acid composition revealed an increased ratio of C18 to C16 fatty acids. In line with this finding, the enzyme ELOVL fatty acid elongase 6 (ELOVL6), responsible for the elongation of C16 to C18 fatty acids and implicated in the development of steatohepatits, was upregulated by p62 and the subsequent induction of IGF2 (Fig. 4.1). Concordantly, we found that *p62* and *IGF2* mRNA strongly correlated with *ELOVL6* mRNA also in human liver disease. IGF2 mediated its effect by inducing the maturation of sterol regulatory element binding transcription factor 1 (SREBF1) (Fig. 4.1), one of the pivotal transcriptional regulators of ELOVL6.

p62-induced steatosis was not mediated by increased *de novo* lipogenesis, decreased peroxisomal lipid degradation, decreased lipid export, or increased lipid uptake in the liver. In fact, decreased levels of C16 fatty acids, elongated to C18 fatty acids by ELOVL6, were responsible for carnitine palmitoyltransferase 1A (CPT1A) inhibition and a subsequently decreased mitochondrial fatty acid degradation, which finally led to hepatic lipid accumulation and steatosis (Fig. 4.1).

These results demonstrate an important role of p62 and p62-induced ELOVL6 levels in the development of steatosis and steatohepatitis.

We found that p62 correlates with poor prognosis in patients with HCC, induces *IGF2* in human hepatoma cell lines and exerts its antiapoptotic effect dependent on the extracellular-signal regulated kinase (ERK) pathway (Fig. 4.1).

In HCC, however, the role of ELOVL6 is still elusive. We could demonstrate that ELOVL6 was downregulated in a large proportion of HCC patients and in a murine HCC model.

p62 amplifies HCC development, which might be partly attributed to delta-like 1 homolog (DLK1) mediated upregulation of ras-related C3 botulinum toxin substrate 1 (RAC1) and the subsequent activation of the antiapoptotic ERK pathway, as found in our *p62* transgenic mice and cell culture experiments (Fig. 4.1).

Taken together, our data underline the crucial role of p62 in liver diseases and provide further evidence that p62 might serve as prognostic marker and target for treatment options in liver diseases.

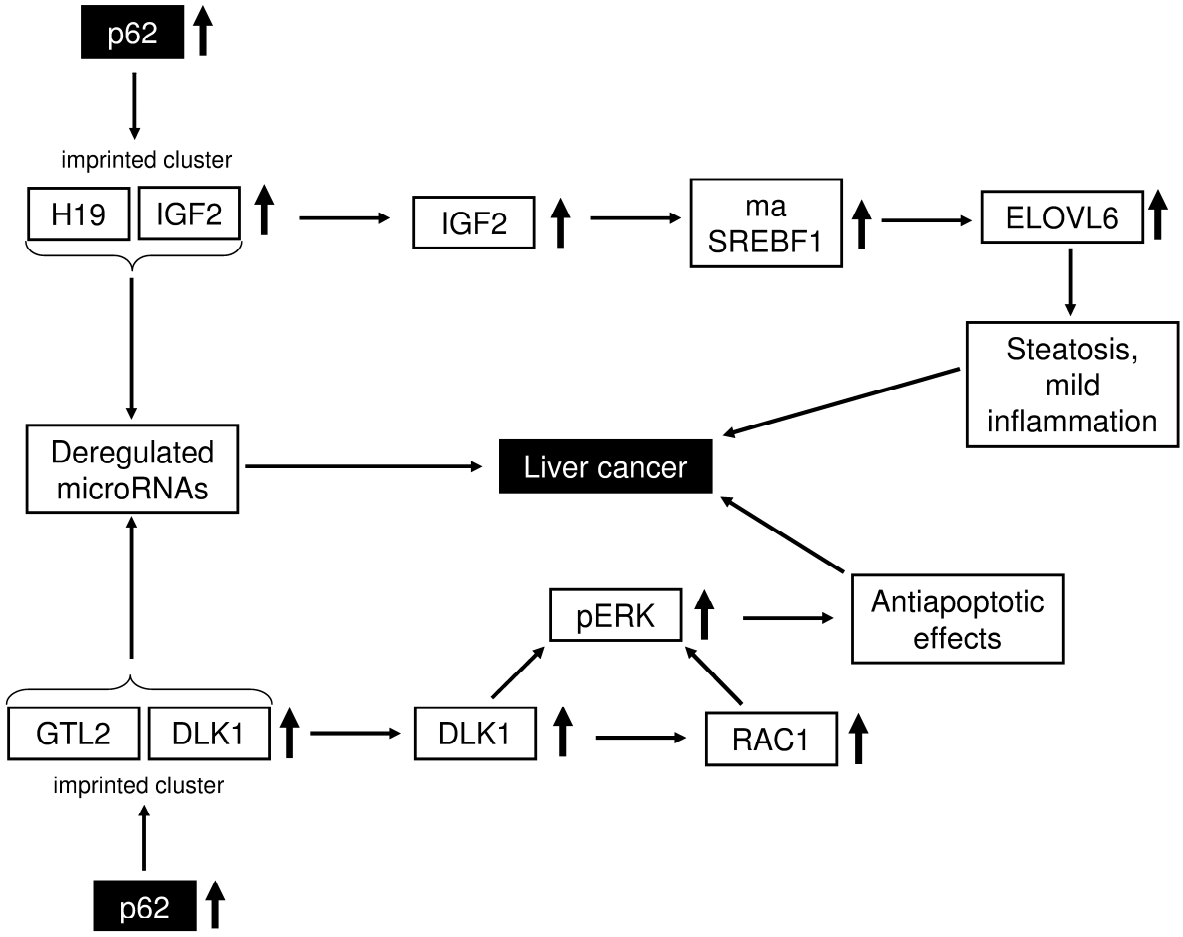

Fig. 4.1: Summary: Pathophysiological effects of p62.

5 Supplemental part

5.1 Supplemental materials and methods

5.1.1 Preparation of nuclear extracts

Nuclear extracts from HepG2 cells and murine liver tissue were prepared as described by Azzout-Marniche et al. (Azzout-Marniche et al., 2000). 500,000 cells in 2 ml media were grown over night in 6 well plates prior to the respective treatment. After the treatment, cells were washed twice with ice cold PBS and lysed in 100 µl buffer A and homogenized with a syringe and transferred to a clean vial. Liver tissue (approximately 100 mg) was homogenized in 200 µl buffer A with a pestle homogenizer (*749540-0000*, Kontes *Glass Company*, Vineland, USA) and a syringe. The cell or tissue lysates were centrifuged at 500 *x g* for 10 min at 4 °C. The supernatant was transferred to a clean vial and stored at -80 °C until SDS-PAGE as cytosolic fraction. The pellet was washed twice with buffer A. The washed pellet was resuspended in 20 µl (cells) or 50 µl (tissue) buffer B and incubated for 30 min on ice. Afterwards, the nuclear fraction was centrifuged at 12,000 x *g* for 30 min at 4 °C. The supernatant was stored at -80 °C and subjected to SDS-PAGE as nuclear fraction. Anti-lamin A/C antibody (#2032, Cell Signaling Technology, Danvers, USA) for nuclear fraction and anti-α–tubulin for cytosolic fraction were used as loading controls.

Buffer A:

	1l	concentration
Tris-HCl	1.6 g	10 mM
NaCl	0.584 g	10 mM
$MgCl_2x6H_2O$	0.61 g	3 mM

Freshly add to 5 ml Buffer A

Nonidet P40	0.25 ml	0.5%
Complete 7	0.83 ml	1x

Buffer B:

	1l	concentration
HEPES	2.4 g	10 mM
NaCl	58.44 g	0.42 M
$MgCl_2x6H_2O$	0.3 g	1.5 mM
Glycerol	25 ml	2.5%
EDTA	0.37 g	1 mM
EGTA	0.38 g	1 mM

Freshly add to 5 ml Buffer B

DTT	50 µl	1 mM
Complete 7	0.83 ml	1x

5.1.2 Immunocytochemistry

HepG2 cells were grown on coverslips. After 48 h they were washed with phosphate buffered saline (PBS, pH 7.4) and fixed with 4% paraformaldehyde in PBS for 10 min at RT. The samples were washed with ice cold PBS and incubated with 1% [m/v] BSA/10% [v/v] FCS/0.3 M glycin in PBS + 0.1% [v/v] Tween® 20. After washing with PBS, the primary antibodies against ELOVL6 (PRS4571, Sigma Aldrich, Taufkirchen, Germany), SREBF1 (ab3259, Abcam, Cambridge, United Kingdom), and PDI (610946, BD Biosciences, Franklin Lakes, USA) were incubated at 1 µg/ml in PBS + 0.1% [v/v] Tween® 20 and 1% BSA [m/v] overnight at 4°C. The samples were washed with PBS and the secondary antibodies Alexa Fluor® 594 $F(ab')_2$ fragment of goat anti-rabbit IgG (H+L) and Alexa Fluor® 498 $F(ab')_2$ fragment of goat anti-mouse IgG (H+L) (A-11037, A-11017, Life technologies, Darmstadt, Germany) was added in a dilution of 1:1,000 in PBS + 0.1% [v/v] Tween® 20 and 1% BSA [m/v] for 1 h at RT under exclusion of light. After washing with PBS, the samples were treated with 0.2 µg/ml diaminophenylindol HCl (DAPI) (D9542, Sigma Aldrich, Taufkirchen, Germany) for 1 min. The cells were washed with PBS, mounted in FluoroSafe™ mounting medium (#345789, Merck, Darmstadt, Germany), and visualised with an inverse fluorescence microscope (Axio Observer, Zeiss, Feldbach, Swiss).

5.1.3 Primer and conditions

gene	forward primer sequence 5´-3´	reverse primer sequence 5´-3´	amplicon size [bp]	gene bank accession number	primer amount [µl/reaction [10 µM]] / annealing temp [°C]
huACTB	TGCGTGACATTAAGGAGAAG	GTCAGGCAGCTCGTAGCTCT	107	NM_001101	0.4 60
huACACA	TCCGACCAGTAATCACTTTGC	GGGAACGTTATCCCCAAACC	139	NM_198834.1	0.5 60
huELOVL6	CACTGTGAGCTGGAAAAGGGAG	GTGTGAAGTCAAACAGGGAGGG	104	NM_024090.2	0.4 60
huFASN	ACTTCCCCAACGGTTCAGGTTC	GCGTCTTCCACACTATGCTCAG	150	NM_004104.4	0.4 62
huGCK	CCTTACGCTCCAAGGCTACA	TCTCTCCGAGGGGCTAAGAG	93	NM_033508.1	0.4 60
huIGF2	GGACTTGAGTCCCTGAACCA	TGAAAATTCCCGTGAGAAGG	100	NM_000612	0.5 56
huMLXIPL	CCCAAGTGGAAGAATTTCAAAG	CTCTTCCTCCGCTTCACATACT	110	NM_032952.2	0.4 59
huNR1H3	TCATCAACCCCATCTTCGAG	GCAATGAGCAAGGCAAACTC	79	NM_005693	0.2 60
hup62	GTTCCCGCATCATCACTCTTAT	GAATCTCGCCAGCTGTTTGA	117	AF057352	0.4 62
huPKLR	CCCACACTGAAAGCATGTCG	CTCCTGGAGCCCCAATCAG	114	NM_000298.5	0.4 60
huPPARA	TGCGTAGAAGAGCCCAGAAA	GTTGACTGGACGGAGCTGAG	137	NM_001001928.2	0.2 60
huRAC1	AAGAGAAAATGCCTGCTGTTGTAA	GCGTACAAAGGTTCCAAGGG	72	NM_006908.4	0.4 60
huSCD	GCCAATTTCCTCTCCACTGCTG	AAGTTCGCTCTTAGAAGCTGCC	80	NM_005063.4	0.4 60
huSREBF1	CCATGGATTGCACTTTCGAA	GGCCAGGGAAGTCACTGTCTT	66	NM_001005291.2	0.4 60

Suppl. table 1: Real-time RT-PCR primer and conditions for human genes and 5 x HOT FIREPol® EvaGreen® qPCR Mix.

gene	forward primer sequence 5´-3´	reverse primer sequence 5´-3´	amplicon size [bp]	gene bank accession number	primer amount [µl/reaction [10 µM]] / annealing temp. [°C]
mu18s	GTAACCCGTTGAACCCCATT	CCATCCAATCGGTAGTAGCG	151	NR_003278.1	0.4 58
mu91H	CCGTGTGCTTGAGGCCTCGCCT	CAACCTCCCCCCATGAGTCG	194	NR_001592.1 NC_000073.6	0.4 61
muAire	CGGAGCTACCTGCAGAGAC	GTGACAGCAGCATCAGAGC	106	NM_009646	0.3 55
muDlk1	ACTTGCGTGGACCTGGAGAA	CTGTTGGTTGCGGCTACGAT	221	NM_010052.5	0.3 58
muF4/80 / EMR1	CTTTGGCTATGGGCTTCCAGTC	GCAAGGAGGACAGAGTTTATCGTG	165	NM_010130	0.3 60
muElovl6	ACAATGGACCTGTCAGCAAA	GTACCAGTGCAGGAAGATCAGT	119	NM_130450.2	0.2 60
muGtl2	AAGCACCATGAGCCACTAGG	TTGCACATTTCCTGTGGGAC	288	NR_104450.1	0.4 62
muH19spec	GGAGACTAGGCCAGGTCTC	GCCCATGGTGTTCAAGAAGGC	159	NR_001592.1 reverse primer	0.5 60
muIl1β	GAGAGCCTGTGTTTTCCTCC	GAGTGCTGCCTAATGTCCC	115	NM_008361.3	0.5 60
muMlxipl	CTGGGGACCTAAACAGGAGC	GAAGCCACCCTATAGCTCCC	166	NM_021455.4	0.5 60
mup62	TTGGATGGGCTGTTGGCTGA	GTGACGTTGACAACGGCAGTT	86	NM_183029.2	0.4 60
muPpara	CCTTCCCTGTGAACTGACG	CCACAGAGCGCTAAGCTGT	77	NM_001113418.1	0.5 60
muRac1	GCGAAAGAGATCGGTGCTGT	GACAGAGAACCGCTCGGATAG	100	NM_009007.2	0.4 62
muPten	GTGAGGATGGTAGGGGAAT	CACCACGCTTCAAAGAGAAA	88	NM_008960.2	0.4 60
muWnt10b	ATCGCCGTTCACGAGTGTC	GGAAACCGCGCTTGAGGAT	111	NM_011718.2	0.4 61

Suppl. table 2: Real-time RT-PCR primer and conditions for murine genes and 5 x HOT FIREPol® EvaGreen® qPCR Mix.

gene	forward primer sequence 5´-3´	reverse primer sequence 5´-3´	Probe, 5'-3'	amplicon size [bp]	gene bank accession number	dNTPs / Probe [pmol]	$MgCl_2$ / Temp [°C]
cyclophillin	GGCCGATGACGAGCCC	TGTCTTTGGAACTTTGTCTGC	TGGGCCGCGTCTCCTTCGA	64	NM_008907.1	125 µM 1.5	3 mM 60
H19	CAGAGGTGGATGTGCCTGCC	CGGACCATGTCATGTCTTTCTGTC	TCACTGAAGGCGAGGATGACAGGT GTGG	80	NR_001592.1	125 µM 2.5	3 mM 58
Igf2	GGAAGTCGATGTTGGTGCTTCTC	CGAACAGACAAACTGAAGCGTGT	CCTTCGCCTTGTGCTGCATCGCTGCT	121	NM_010514.3	125 µM 1.5	4 mM 60

Suppl. table 3: Real-time RT-PCR primer and conditions for murine genes and taq man probes (6-FAM-BHQ1).

5.1.4 Antibodies and conditions

primary antibodies (anti-human/mouse)	dilution buffer	temp.	Time	manufacturer / order number
anti-p62, rabbit IgG	1:1,000 in PBST + 5% BSA	RT	2 h	selfmade; Zhang et al. 1999
anti-alpha-tubulin, mouse IgG	1:1,000 in PBST + 5% dry milk	RT	2 h	Sigma Aldrich T9026
anti-SREBF1, mouse IgG	1:200 in RBB	RT	2 h	Abcam ab3259 [2A4]
anti-PPARA; rabbit IgG	1:1,000 in PBST + 5% dry milk	4°C	overnight	Abcam ab8934
anti-ELOVL6, rabbit IgG	1:1,000 in PBST + 5% BSA	4°C	overnight	Sigma Aldrich PRS4571
anti-FASN, rabbit IgG	1:1,000 in RBB	RT	2 h	Cell Signaling Technology #3180 [C20G5]
anti-lamin A/C, rabbit IgG	1:1,000 in RBB	4°C	overnight	Cell Signaling Technology #2032

Suppl. table 4: Antibodies and conditions for Western blot analysis.

5.2 Supplemental figures

The following figures show results obtained within the PhD thesis from gene expression analysis by Real-time RT-PCR done on tissue from DEN-treated animals. They either revealed non-statistically significant effects for p62 or are related to other projects. This is why they will not be discussed in detail.

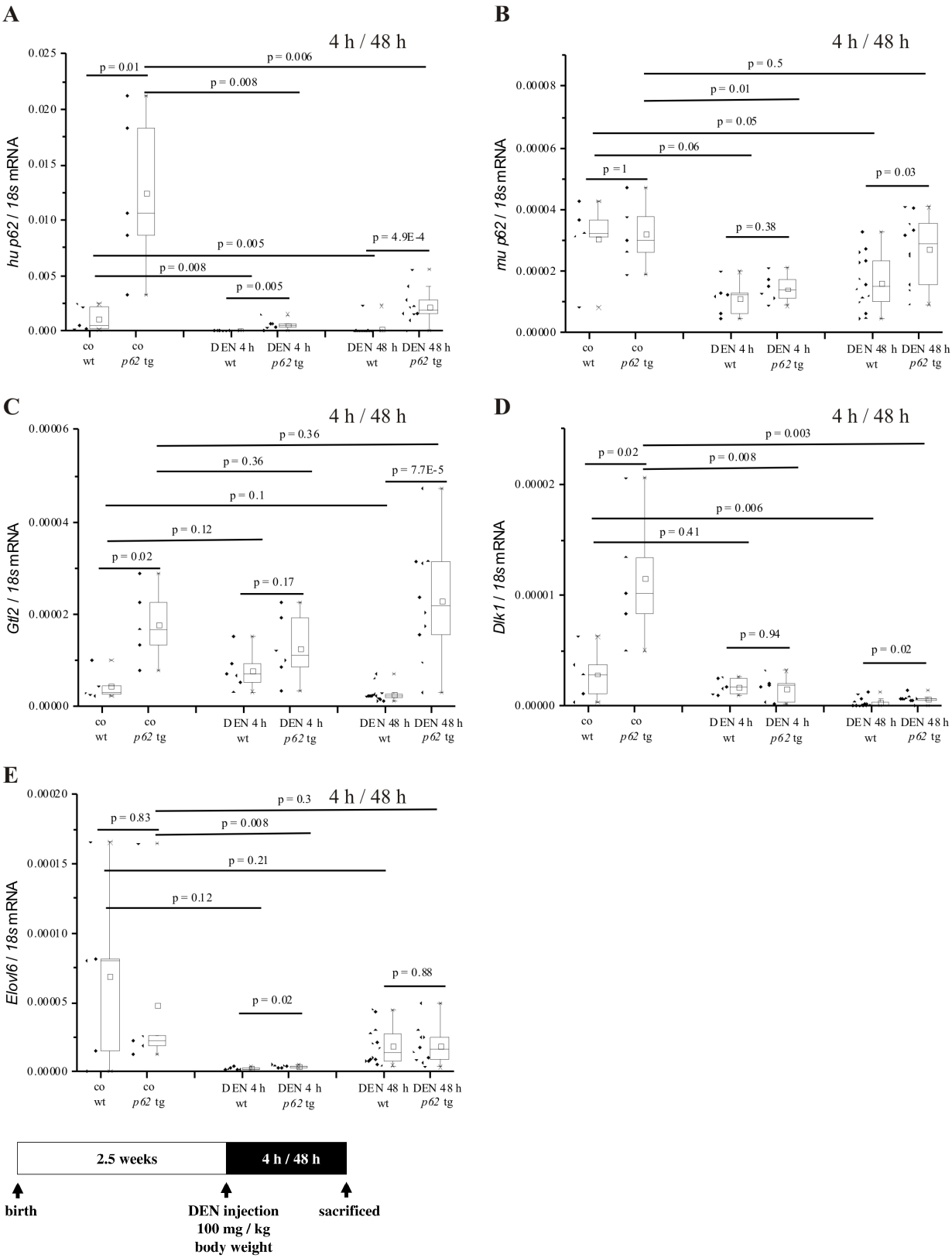

Suppl. Fig. 1: mRNA expression in livers from wild-type (co wt) and *p62* transgenic mice (co *p62* tg) (co wt, co *p62* tg, n = 5, each) and mice treated with DEN for 4 h (DEN 4 h wt, *p62* tg: n = 6, each) or 48 h (DEN 48 h wt, n = 14, *p62* tg, n = 10) (permission 13/2009) for **A)** transgenic human p62 (*hu p62*), **B)** endogenous murine p62 (*mu p62*), **C)** *Gtl2*, **D)** *Dlk1*, and **E)** *Elovl6*.

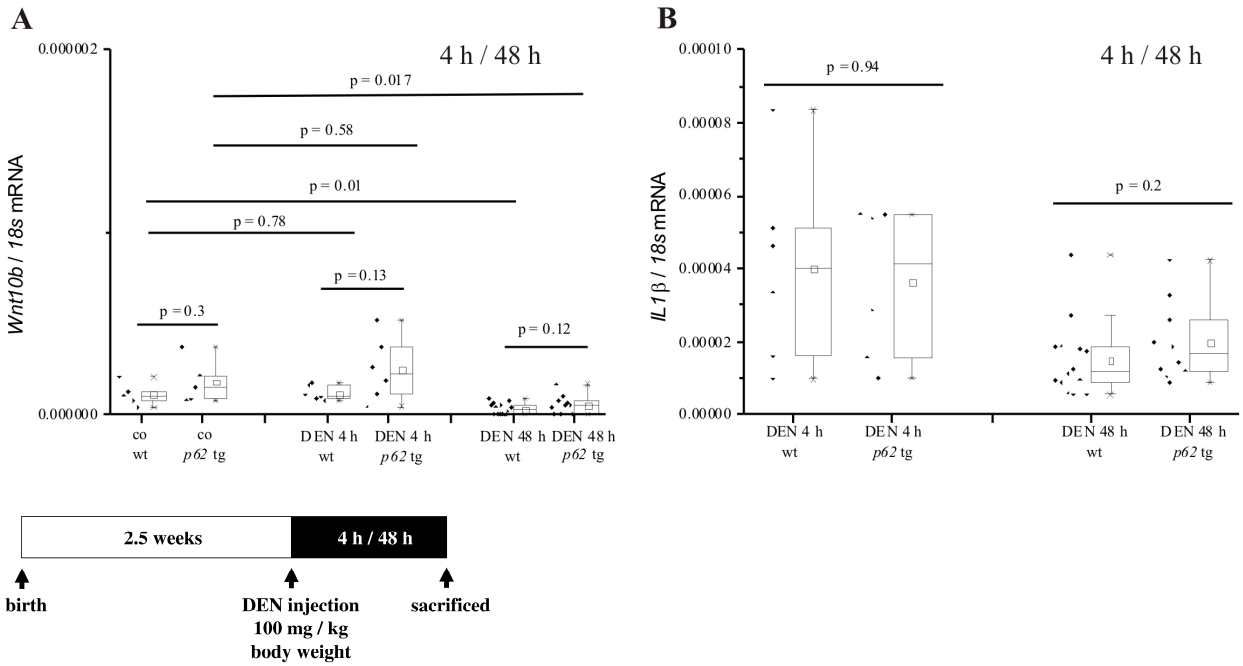

Suppl. Fig. 2: mRNA expression in livers from wild-type (co wt) and *p62* transgenic mice (co *p62* tg) (co wt, co *p62* tg: n = 5, each) and mice treated with DEN for 4 h (DEN 4 h wt, *p62* tg: n = 6, each) or 48 h (DEN 48 h wt, n = 14, *p62* tg, n = 10) (permission 13/2009) for **A)** *Wnt10b*, and **B)** *Il1β*.

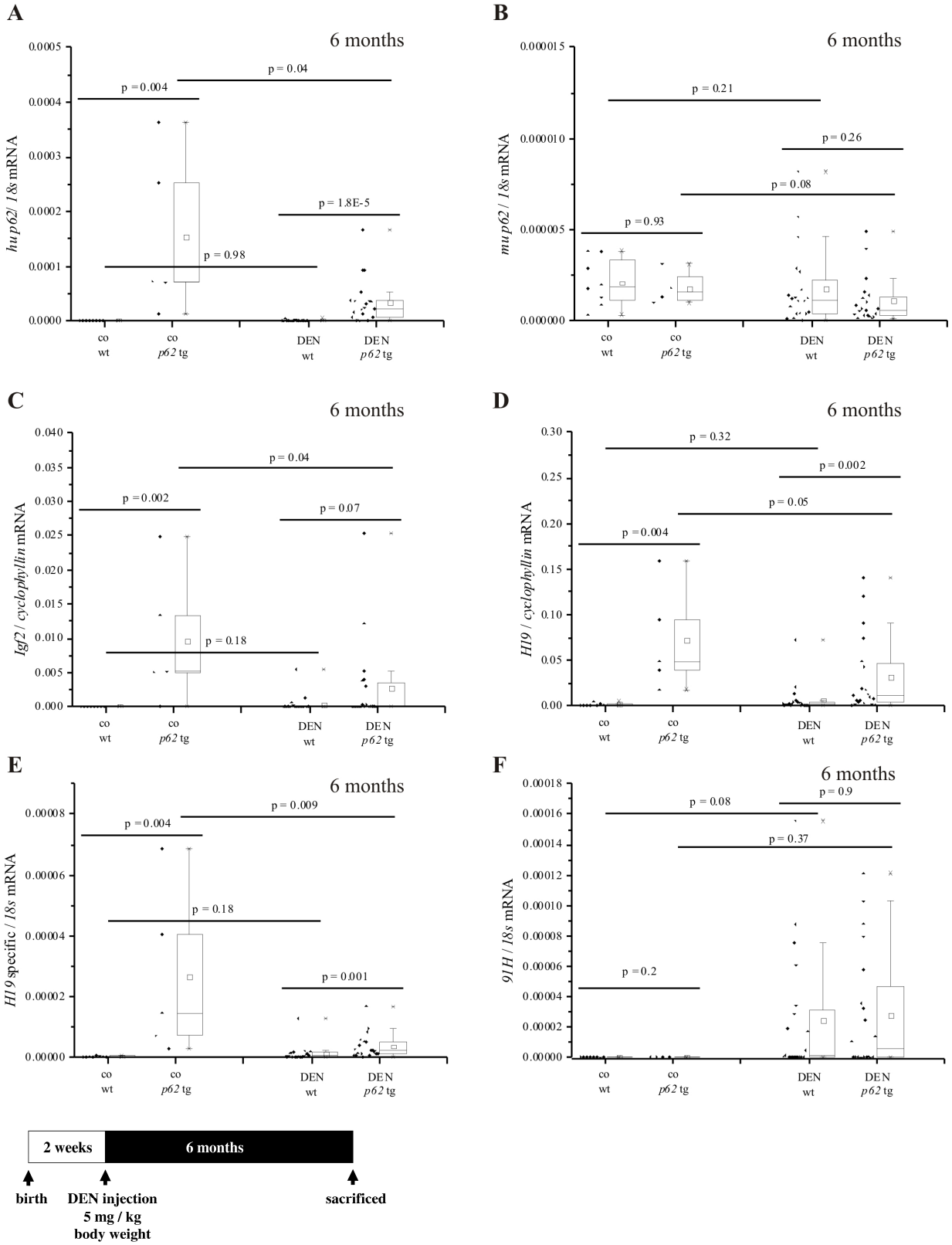

Suppl. Fig. 3: mRNA expression in livers from wild-type (co wt, n = 8) and *p62* transgenic mice (co *p62* tg, n = 5) and mice treated with DEN (DEN wt, *p62* tg: n = 20, each) (permission 48/2009) for
A) transgenic human p62 (*hu p62*), **B)** endogenous murine p62 (*mu p62*), **C)** *Igf2*, **D)** *H19* using primer, which recognize both *H19* and antisense *91H*, **E)** *H19* using primer specific for *H19*, and **F)** *91H*.

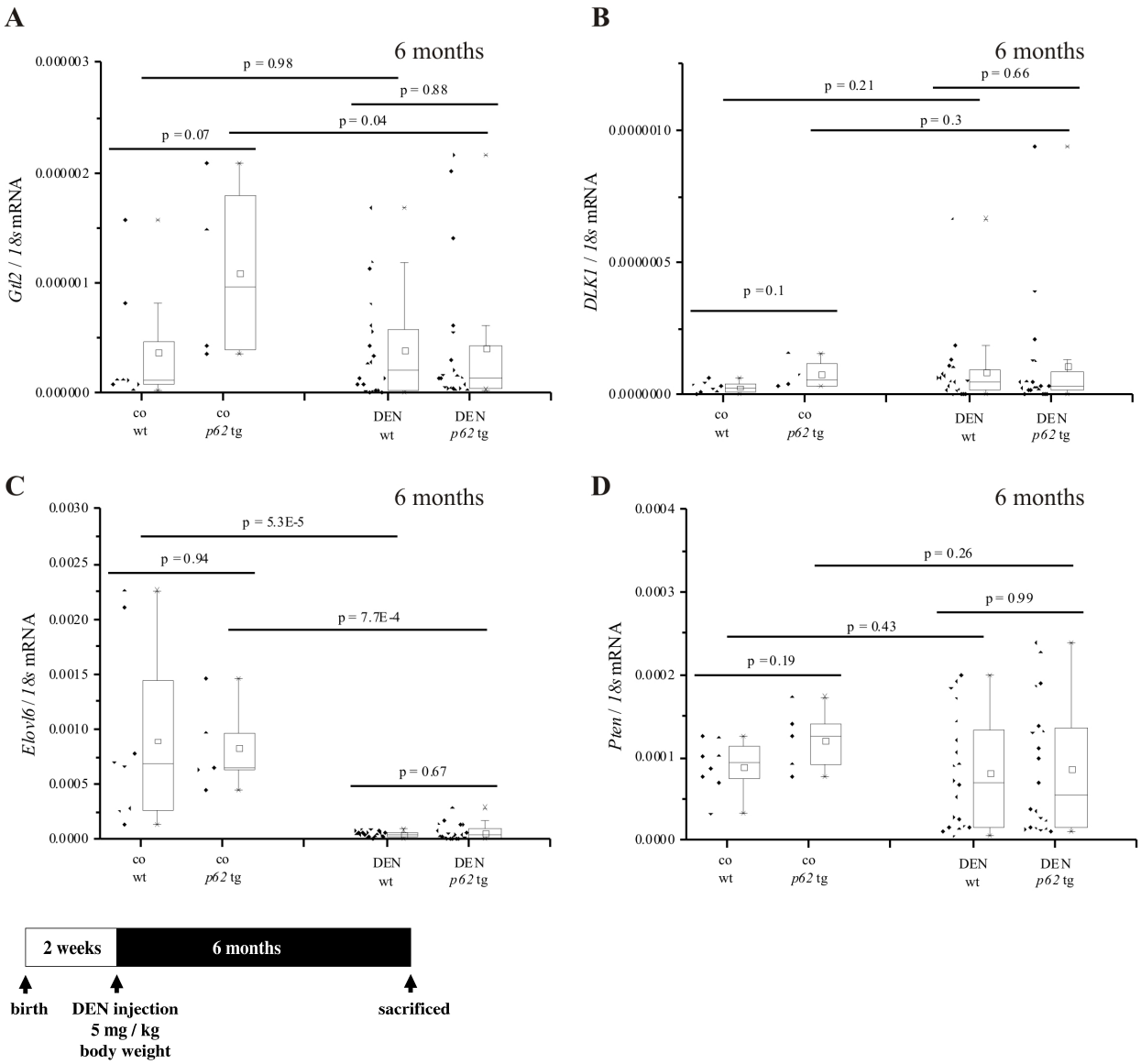

Suppl. Fig. 4: mRNA expression in livers from wild-type (co wt, n = 8) and *p62* transgenic mice (co *p62* tg, n = 5) and mice treated with DEN (DEN wt, *p62* tg: n = 20, each) (permission 48/2009) for
A) *Gtl2*, **B)** *Dlk1*, **C)** *Elovl6*, and **D)** *Pten*.

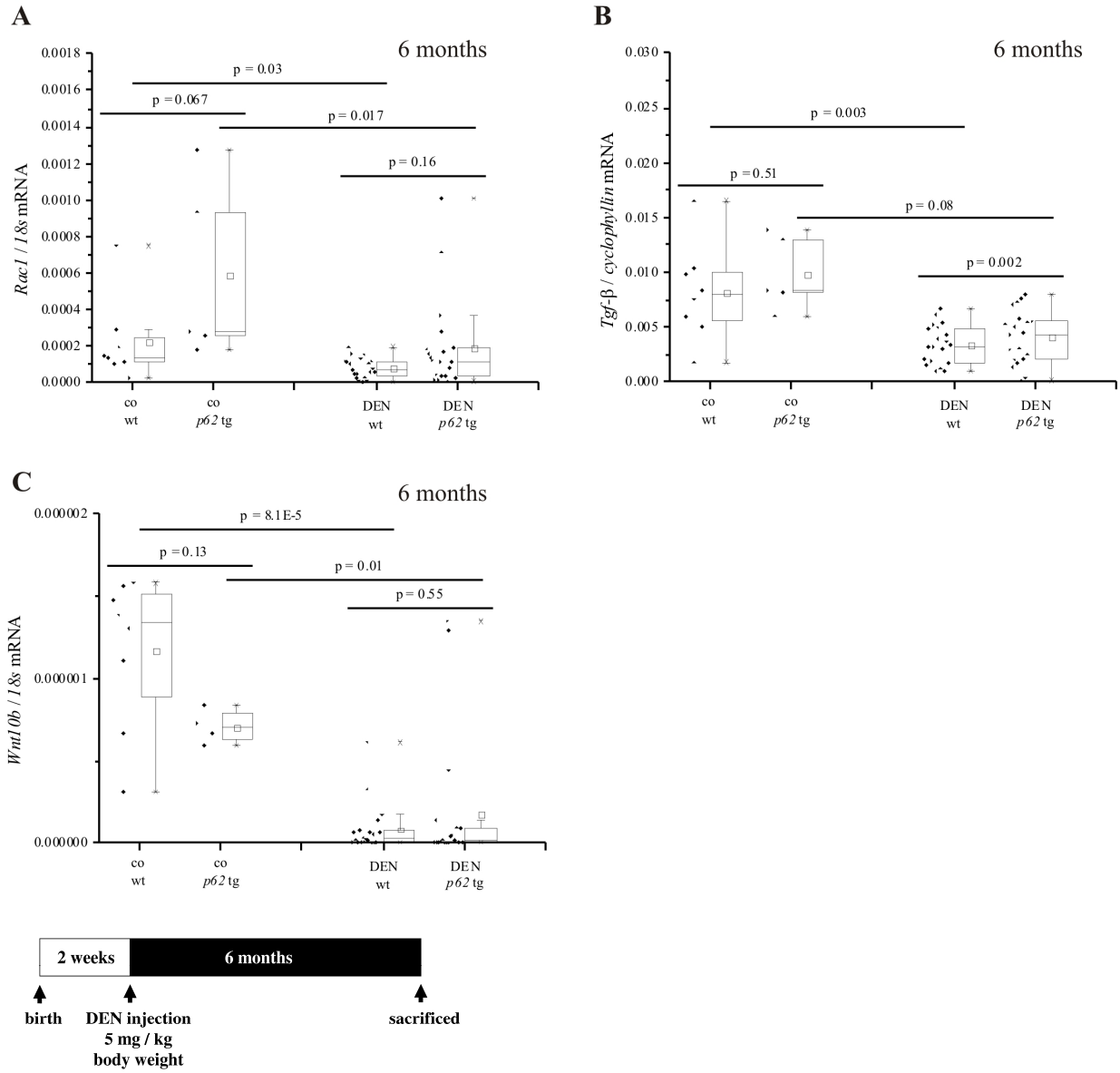

Suppl. Fig. 5: mRNA expression in livers from wild-type (co wt, n = 8) and *p62* transgenic mice (co *p62* tg, n = 5) and mice treated with DEN (DEN wt, *p62* tg: n = 20, each) (permission 48/2009) for

A) *Rac1*, **B)** *Tgf-β*, and **C)** *Wnt10b*.

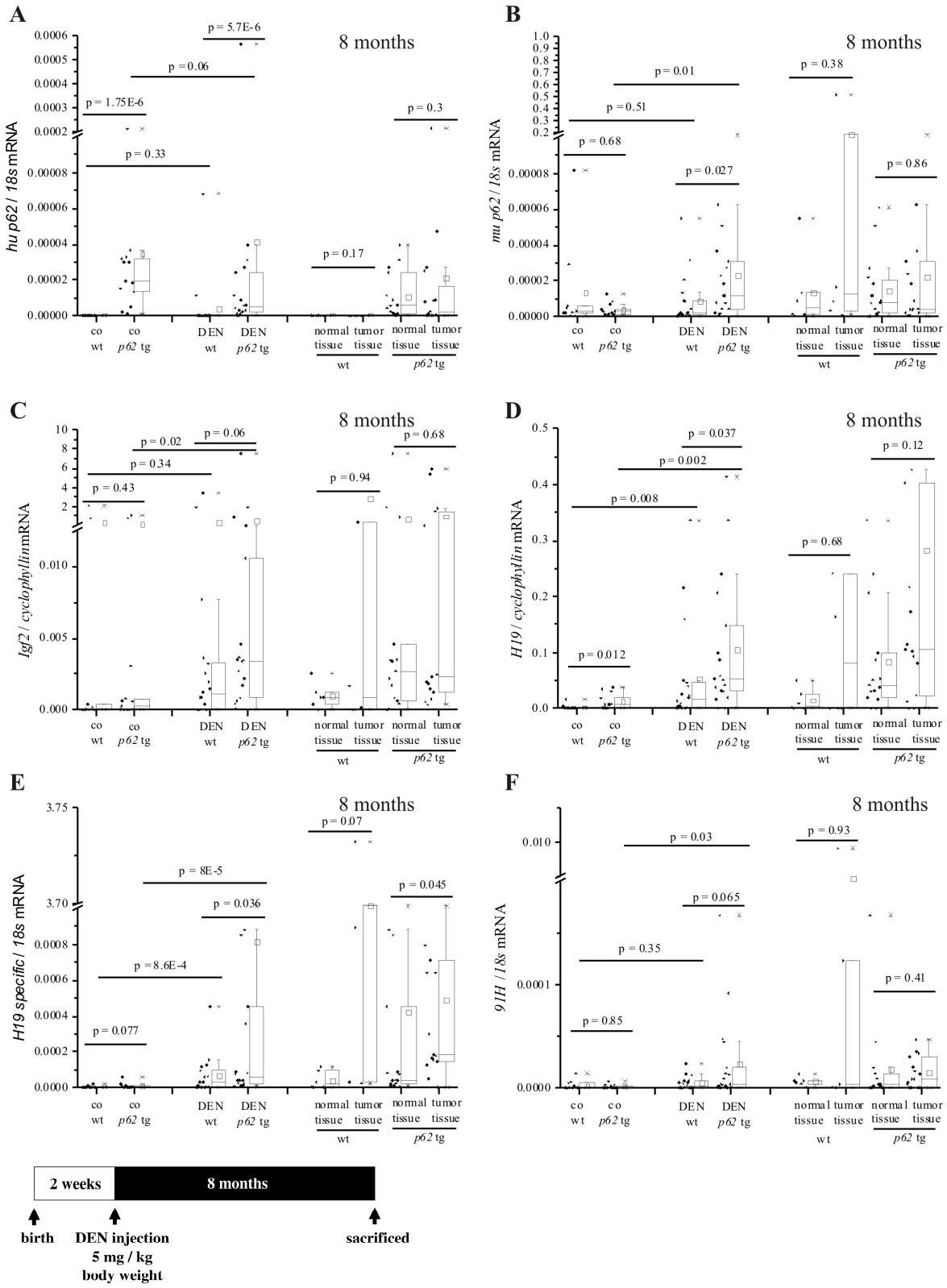

Suppl. Fig. 6: mRNA expression in livers from wild-type (co wt, n = 10) and *p62* transgenic mice (co *p62* tg, n = 13) and mice treated with DEN (DEN wt, *p62* tg: n = 18, each) and the respective normal and tumor tissue from DEN-treated wt (n = 6, each, male) and *p62* tg (n = 15, each, n = 8 male, n = 7 female) (permission 48/2009) for
A) transgenic human p62 (*hu p62*), **B)** endogenous murine p62 (*mu p62*), **C)** *Igf2*, **D)** *H19* using primer, which recognize both *H19* and antisense *91H*, **E)** *H19* using primer specific for *H19*, and **F)** *91H*.

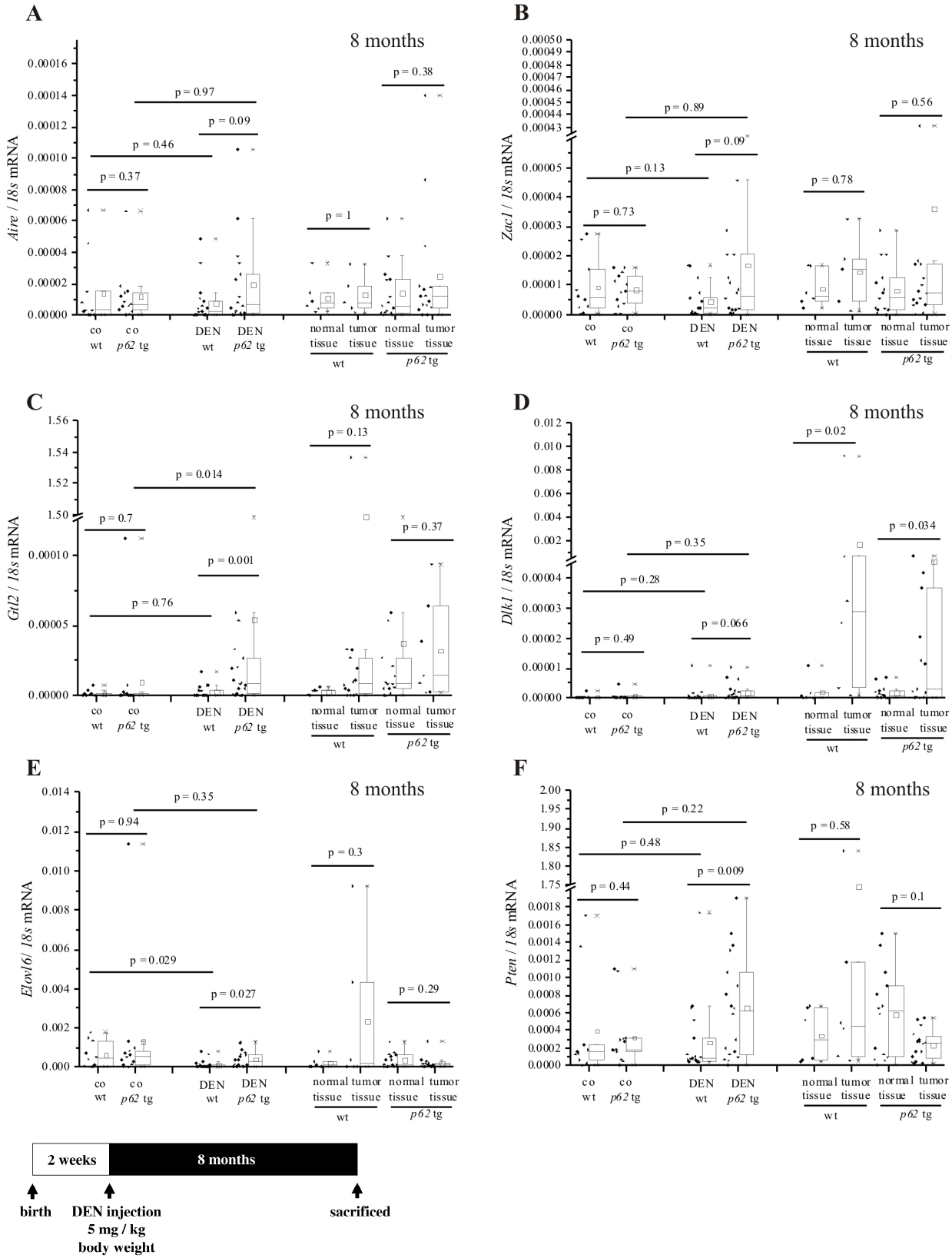

Suppl. Fig. 7: mRNA expression in livers from wild-type (co wt, n = 10) and *p62* transgenic mice (co *p62* tg, n = 13) and mice treated with DEN (DEN wt, *p62* tg: n = 18, each) and the respective normal and tumor tissue from DEN-treated wt (n = 6, each, male) and *p62* tg (n = 15, each, n = 8 male, n = 7 female) (permission 48/2009) for
A) *Aire*, **B)** *Zac1*, **C)** *Gtl2*, **D)** *Dlk1*, **E)** *Elovl6*, and **F)** *Pten*.

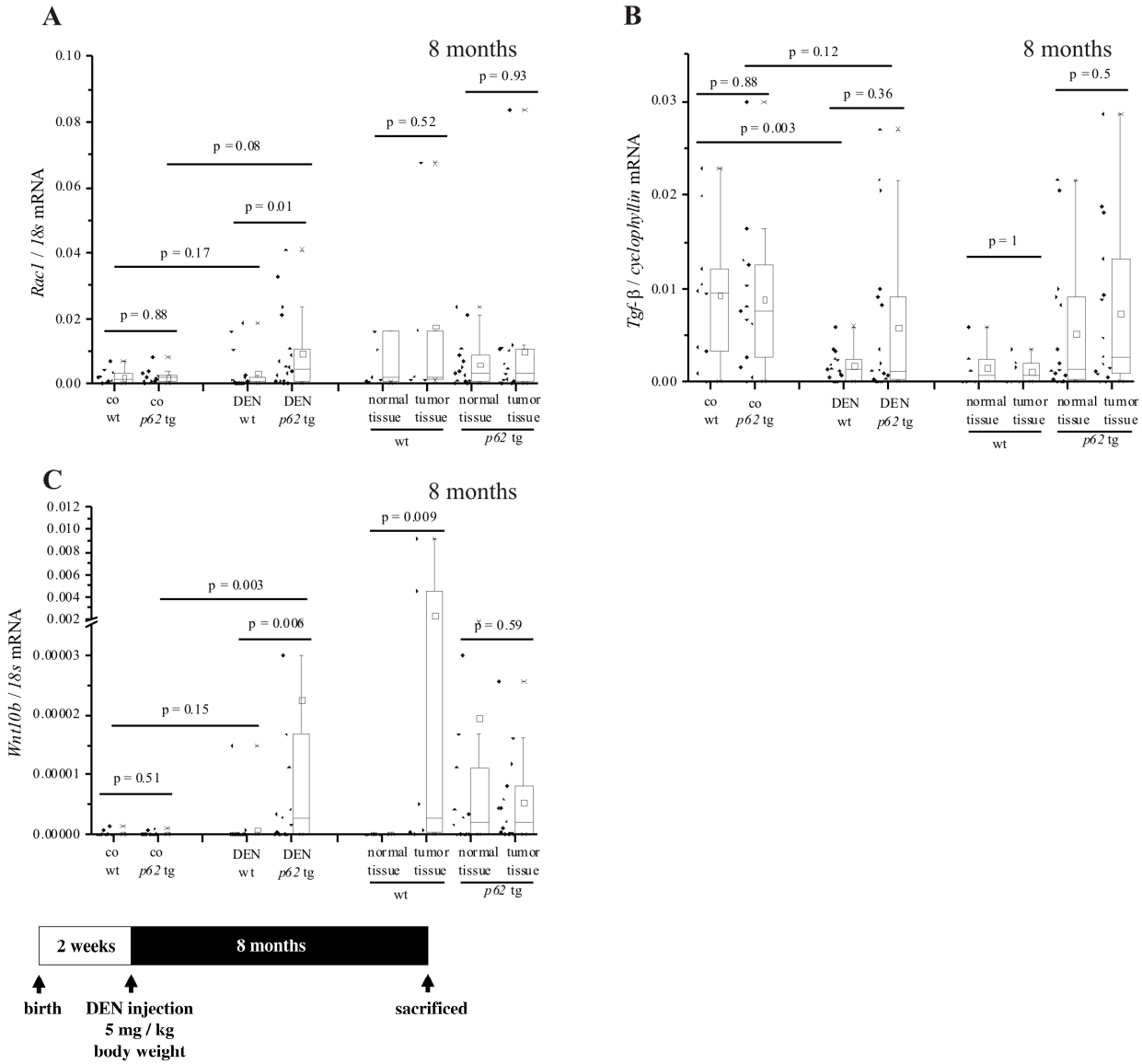

Suppl. Fig. 8: mRNA expression in livers from wild-type (co wt, n = 10) and *p62* transgenic mice (co *p62* tg, n = 13) and mice treated with DEN (DEN wt, *p62* tg: n = 18, each) and the respective normal and tumor tissue from DEN-treated wt (n = 6, each, male) and *p62* tg (n = 15, each, n = 8 male, n = 7 female) (permission 48/2009) for

A) *Rac1*, **B)** *Tgf-β*, and **C)** *Wnt10b*.

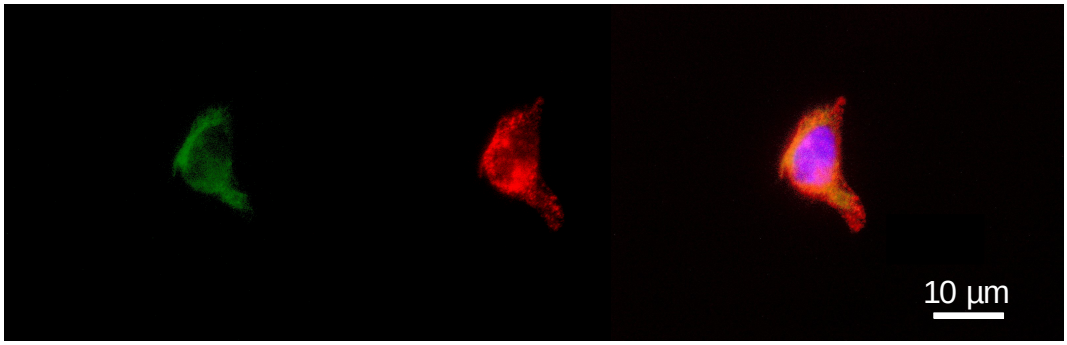

ER ELOVL6 Overlay

Suppl. Fig. 9: ELOVL6 is located in the endoplasmatic reticulum (ER), Immunocytochemistry of HepG2 cells. Left (green) ER (PDI), middle (red) ELOVL6, right merge, (blue) nucleus (DAPI).

6 References

Anderson, E.L., Howe, L.D., Fraser, A., Callaway, M.P., Sattar, N., Day, C., Tilling, K. and Lawlor, D.A. (2014) Weight trajectories through infancy and childhood and risk of non-alcoholic fatty liver disease in adolescence: The ALSPAC study. *J Hepatol*, in press, doi: 10.1016/j.jhep.2014.04.018.

Anderson, N. and Borlak, J. (2008) Molecular mechanisms and therapeutic targets in steatosis and steatohepatitis. *Pharmacol Rev*, **60**, 311-357.

Anwar, S.L., Krech, T., Hasemeier, B., Schipper, E., Schweitzer, N., Vogel, A., Kreipe, H. and Lehmann, U. (2012) Loss of imprinting and allelic switching at the DLK1-MEG3 locus in human hepatocellular carcinoma. *PLoS One*, **7**, e49462.

Armstrong, M.J., Houlihan, D.D., Bentham, L., Shaw, J.C., Cramb, R., Olliff, S., Gill, P.S., Neuberger, J.M., Lilford, R.J. and Newsome, P.N. (2012) Presence and severity of non-alcoholic fatty liver disease in a large prospective primary care cohort. *J Hepatol*, **56**, 234-240.

Azzout-Marniche, D., Becard, D., Guichard, C., Foretz, M., Ferre, P. and Foufelle, F. (2000) Insulin effects on sterol regulatory-element-binding protein-1c (SREBP-1c) transcriptional activity in rat hepatocytes. *Biochem J*, **350 Pt 2**, 389-393.

Benetatos, L., Hatzimichael, E., Londin, E., Vartholomatos, G., Loher, P., Rigoutsos, I. and Briasoulis, E. (2013) The microRNAs within the DLK1-DIO3 genomic region: involvement in disease pathogenesis. *Cell Mol Life Sci*, **70**, 795-814.

Blachier, M., Leleu, H., Peck-Radosavljevic, M., Valla, D.C. and Roudot-Thoraval, F. (2013) The burden of liver disease in Europe: a review of available epidemiological data. *J Hepatol*, **58**, 593-608.

Bohte, A.E., van Werven, J.R., Bipat, S. and Stoker, J. (2011) The diagnostic accuracy of US, CT, MRI and 1H-MRS for the evaluation of hepatic steatosis compared with liver biopsy: a meta-analysis. *Eur Radiol*, **21**, 87-97.

Browning, J.D. and Horton, J.D. (2004) Molecular mediators of hepatic steatosis and liver injury. *J Clin Invest*, **114**, 147-152.

Bruix, J. and Sherman, M. (2011) Management of hepatocellular carcinoma: an update. *Hepatology*, **53**, 1020-1022.

Cermelli, S., Ruggieri, A., Marrero, J.A., Ioannou, G.N. and Beretta, L. (2011) Circulating microRNAs in patients with chronic hepatitis C and non-alcoholic fatty liver disease. *PLoS One*, **6**, e23937.

Chalasani, N., Younossi, Z., Lavine, J.E., Diehl, A.M., Brunt, E.M., Cusi, K., Charlton, M. and Sanyal, A.J. (2012) The diagnosis and management of non-alcoholic fatty liver disease: Practice guideline by the American Association for the Study of Liver Diseases, American College of Gastroenterology, and the American Gastroenterological Association. *Am J Gastroenterol*, **107**, 811-826.

Chen, Y.J., Zhu, J.M., Wu, H., Fan, J., Zhou, J., Hu, J., Yu, Q., Liu, T.T., Yang, L., Wu, C.L., Guo, X.L., Huang, X.W. and Shen, X.Z. (2013) Circulating microRNAs as a Fingerprint for Liver Cirrhosis. *PLoS One*, **8**, e66577.

Christiansen, J., Kolte, A.M., Hansen, T. and Nielsen, F.C. (2009) IGF2 mRNA-binding protein 2: biological function and putative role in type 2 diabetes. *J Mol Endocrinol*, **43**, 187-195.

Cohen, J.C., Horton, J.D. and Hobbs, H.H. (2011) Human fatty liver disease: old questions and new insights. *Science*, **332**, 1519-1523.

Cotler, S.J., Kanji, K., Keshavarzian, A., Jensen, D.M. and Jakate, S. (2004) Prevalence and significance of autoantibodies in patients with non-alcoholic steatohepatitis. *J Clin Gastroenterol*, **38**, 801-804.

Coulouarn, C., Factor, V.M., Andersen, J.B., Durkin, M.E. and Thorgeirsson, S.S. (2009) Loss of miR-122 expression in liver cancer correlates with suppression of the hepatic phenotype and gain of metastatic properties. *Oncogene*, **28**, 3526-3536.

Crabb, D.W. (1999) Pathogenesis of alcoholic liver disease: newer mechanisms of injury. *Keio J Med*, **48**, 184-188.

Dai, L., Ren, P., Liu, M., Imai, H., Tan, E.M. and Zhang, J.Y. (2014) Using immunomic approach to enhance tumor-associated autoantibody detection in diagnosis of hepatocellular carcinoma. *Clin Immunol*, **152**, 127-139.

Day, C.P. and James, O.F. (1998) Steatohepatitis: a tale of two "hits"? *Gastroenterology*, **114**, 842-845.

Day, C.P. and Yeaman, S.J. (1994) The biochemistry of alcohol-induced fatty liver. *Biochim Biophys Acta*, **1215**, 33-48.

de Lope, C.R., Tremosini, S., Forner, A., Reig, M. and Bruix, J. (2012) Management of HCC. *J Hepatol*, **56 Suppl 1**, S75-87.

Dentin, R., Benhamed, F., Hainault, I., Fauveau, V., Foufelle, F., Dyck, J.R., Girard, J. and Postic, C. (2006) Liver-specific inhibition of ChREBP improves hepatic steatosis and insulin resistance in ob/ob mice. *Diabetes*, **55**, 2159-2170.

Esquela-Kerscher, A. and Slack, F.J. (2006) Oncomirs - microRNAs with a role in cancer. *Nat Rev Cancer*, **6**, 259-269.

Falix, F.A., Aronson, D.C., Lamers, W.H., Hiralall, J.K. and Seppen, J. (2012) DLK1, a serum marker for hepatoblastoma in young infants. *Pediatr Blood Cancer*, **59**, 743-745.

Fan, J.G. (2013) Epidemiology of alcoholic and nonalcoholic fatty liver disease in China. *J Gastroenterol Hepatol*, **28 Suppl 1**, 11-17.

Fattovich, G., Stroffolini, T., Zagni, I. and Donato, F. (2004) Hepatocellular carcinoma in cirrhosis: incidence and risk factors. *Gastroenterology*, **127**, S35-50.

Forner, A., Llovet, J.M. and Bruix, J. (2012) Hepatocellular carcinoma. *Lancet*, **379**, 1245-1255.

Foufelle, F. and Ferre, P. (2002) New perspectives in the regulation of hepatic glycolytic and lipogenic genes by insulin and glucose: a role for the transcription factor sterol regulatory element binding protein-1c. *Biochem J*, **366**, 377-391.

Fracanzani, A.L., Valenti, L., Bugianesi, E., Andreoletti, M., Colli, A., Vanni, E., Bertelli, C., Fatta, E., Bignamini, D., Marchesini, G. and Fargion, S. (2008) Risk of severe liver disease in nonalcoholic fatty liver disease with normal aminotransferase levels: a role for insulin resistance and diabetes. *Hepatology*, **48**, 792-798.

Fromenty, B. and Pessayre, D. (1995) Inhibition of mitochondrial beta-oxidation as a mechanism of hepatotoxicity. *Pharmacol Ther*, **67**, 101-154.

Ganapathy-Kanniappan, S., Karthikeyan, S., Geschwind, J.F. and Mezey, E. (2014) Is the pathway of energy metabolism modified in advanced cirrhosis? *J Hepatol*, in press, doi: 10.1016/j.jhep.2014.04.017.

Harano, Y., Yasui, K., Toyama, T., Nakajima, T., Mitsuyoshi, H., Mimani, M., Hirasawa, T., Itoh, Y. and Okanoue, T. (2006) Fenofibrate, a peroxisome proliferator-activated receptor alpha agonist, reduces hepatic steatosis and lipid peroxidation in fatty liver Shionogi mice with hereditary fatty liver. *Liver Int*, **26**, 613-620.

Hoyumpa, A.M., Jr., Greene, H.L., Dunn, G.D. and Schenker, S. (1975) Fatty liver: biochemical and clinical considerations. *Am J Dig Dis*, **20**, 1142-1170.

Hu, G., Drescher, K.M. and Chen, X.M. (2012) Exosomal miRNAs: Biological Properties and Therapeutic Potential. *Front Genet*, **3**, 56.

Huang, J., Zhang, X., Zhang, M., Zhu, J.D., Zhang, Y.L., Lin, Y., Wang, K.S., Qi, X.F., Zhang, Q., Liu, G.Z., Yu, J., Cui, Y., Yang, P.Y., Wang, Z.Q. and Han, Z.G. (2007)

Up-regulation of DLK1 as an imprinted gene could contribute to human hepatocellular carcinoma. *Carcinogenesis*, **28**, 1094-1103.

Hudak, C.S. and Sul, H.S. (2013) Pref-1, a gatekeeper of adipogenesis. *Front Endocrinol (Lausanne)*, **4**, 79.

Huynh, H., Nguyen, T.T., Chow, K.H., Tan, P.H., Soo, K.C. and Tran, E. (2003) Over-expression of the mitogen-activated protein kinase (MAPK) kinase (MEK)-MAPK in hepatocellular carcinoma: its role in tumor progression and apoptosis. *BMC Gastroenterol*, **3**, 19.

Ji, J., Yamashita, T., Budhu, A., Forgues, M., Jia, H.L., Li, C., Deng, C., Wauthier, E., Reid, L.M., Ye, Q.H., Qin, L.X., Yang, W., Wang, H.Y., Tang, Z.Y., Croce, C.M. and Wang, X.W. (2009) Identification of microRNA-181 by genome-wide screening as a critical player in EpCAM-positive hepatic cancer stem cells. *Hepatology*, **50**, 472-480.

Kamikihara, T., Arima, T., Kato, K., Matsuda, T., Kato, H., Douchi, T., Nagata, Y., Nakao, M. and Wake, N. (2005) Epigenetic silencing of the imprinted gene ZAC by DNA methylation is an early event in the progression of human ovarian cancer. *Int J Cancer*, **115**, 690-700.

Karakatsanis, A., Papaconstantinou, I., Gazouli, M., Lyberopoulou, A., Polymeneas, G. and Voros, D. (2013) Expression of microRNAs, miR-21, miR-31, miR-122, miR-145, miR-146a, miR-200c, miR-221, miR-222, and miR-223 in patients with hepatocellular carcinoma or intrahepatic cholangiocarcinoma and its prognostic significance. *Mol Carcinog*, **52**, 297-303.

Keniry, A., Oxley, D., Monnier, P., Kyba, M., Dandolo, L., Smits, G. and Reik, W. (2012) The H19 lincRNA is a developmental reservoir of miR-675 that suppresses growth and Igf1r. *Nat Cell Biol*, **14**, 659-665.

Kessler, S.M., Pokorny, J., Zimmer, V., Laggai, S., Lammert, F., Bohle, R.M. and Kiemer, A.K. (2013) IGF2 mRNA binding protein p62/IMP2-2 in hepatocellular carcinoma: antiapoptotic action is independent of IGF2/PI3K signaling. *Am J Physiol Gastrointest Liver Physiol*, **304**, G328-G336.

Kim, K.H., Shin, H.J., Kim, K., Choi, H.M., Rhee, S.H., Moon, H.B., Kim, H.H., Yang, U.S., Yu, D.Y. and Cheong, J. (2007) Hepatitis B virus X protein induces hepatic steatosis via transcriptional activation of SREBP1 and PPARgamma. *Gastroenterology*, **132**, 1955-1967.

Kopec, K.L. and Burns, D. (2011) Nonalcoholic fatty liver disease: a review of the spectrum of disease, diagnosis, and therapy. *Nutr Clin Pract*, **26**, 565-576.

Kosaka, N., Iguchi, H. and Ochiya, T. (2010) Circulating microRNA in body fluid: a new potential biomarker for cancer diagnosis and prognosis. *Cancer Sci*, **101**, 2087-2092.

Kostapanos, M.S., Kei, A. and Elisaf, M.S. (2013) Current role of fenofibrate in the prevention and management of non-alcoholic fatty liver disease. *World J Hepatol*, **5**, 470-478.

Koteish, A. and Diehl, A.M. (2001) Animal models of steatosis. *Semin Liver Dis*, **21**, 89-104.

Kotronen, A. and Yki-Jarvinen, H. (2008) Fatty liver: a novel component of the metabolic syndrome. *Arterioscler Thromb Vasc Biol*, **28**, 27-38.

Kotronen, A., Yki-Jarvinen, H., Mannisto, S., Saarikoski, L., Korpi-Hyovalti, E., Oksa, H., Saltevo, J., Saaristo, T., Sundvall, J., Tuomilehto, J. and Peltonen, M. (2010) Non-alcoholic and alcoholic fatty liver disease - two diseases of affluence associated with the metabolic syndrome and type 2 diabetes: the FIN-D2D survey. *BMC Public Health*, **10**, 237.

Laggai, S., Kessler, S.M., Boettcher, S., Lebrun, V., Gemperlein, K., Lederer, E., Leclercq, I.A., Mueller, R., Hartmann, R.W., Haybaeck, J. and Kiemer, A.K. (2014) The IGF2 mRNA binding protein p62/IGF2BP2-2 induces fatty acid elongation as a critical feature of steatosis. *J Lipid Res*, **55**, 1087-1097.

Laggai, S., Simon, Y., Ranssweiler, T., Kiemer, A.K. and Kessler, S.M. (2013) Rapid chromatographic method to decipher distinct alterations in lipid classes in NAFLD/NASH. *World J Hepatol*, **5**, 558-567.

Lee, Y., Jeon, K., Lee, J.T., Kim, S. and Kim, V.N. (2002) MicroRNA maturation: stepwise processing and subcellular localization. *EMBO J*, **21**, 4663-4670.

Li, X., Nadauld, L., Ootani, A., Corney, D.C., Pai, R.K., Gevaert, O., Cantrell, M.A., Rack, P.G., Neal, J.T., Chan, C.W., Yeung, T., Gong, X., Yuan, J., Wilhelmy, J., Robine, S., Attardi, L.D., Plevritis, S.K., Hung, K.E., Chen, C.Z., Ji, H.P. and Kuo, C.J. (2014) Oncogenic transformation of diverse gastrointestinal tissues in primary organoid culture. *Nat Med*, in press, doi: 10.1038/nm.3585.

Lim, L., Balakrishnan, A., Huskey, N., Jones, K.D., Jodari, M., Ng, R., Song, G., Riordan, J., Anderton, B., Cheung, S.T., Willenbring, H., Dupuy, A., Chen, X., Brown, D., Chang, A.N. and Goga, A. (2014) MicroRNA-494 within an oncogenic microRNA megacluster regulates G1/S transition in liver tumorigenesis through suppression of mutated in colorectal cancer. *Hepatology*, **59**, 202-215.

Liu, M., Roth, A., Yu, M., Morris, R., Bersani, F., Rivera, M.N., Lu, J., Shioda, T., Vasudevan, S., Ramaswamy, S., Maheswaran, S., Diederichs, S. and Haber, D.A. (2013) The IGF2 intronic miR-483 selectively enhances transcription from IGF2 fetal promoters and enhances tumorigenesis. *Genes Dev*, **27**, 2543-2548.

Liu, X., Ye, H., Li, L., Li, W., Zhang, Y. and Zhang, J.-Y. (2014) Humoral Autoimmune Responses to Insulin-Like Growth Factor II mRNA-Binding Proteins IMP1 and p62/IMP2 in Ovarian Cancer. *Journal of Immunology Research*, **2014**, 7.

Lonardo, A., Adinolfi, L.E., Loria, P., Carulli, N., Ruggiero, G. and Day, C.P. (2004) Steatosis and hepatitis C virus: mechanisms and significance for hepatic and extrahepatic disease. *Gastroenterology*, **126**, 586-597.

Loomba, R. and Sanyal, A.J. (2013) The global NAFLD epidemic. *Nat Rev Gastroenterol Hepatol*, **10**, 686-690.

Lu, M., Nakamura, R.M., Dent, E.D., Zhang, J.Y., Nielsen, F.C., Christiansen, J., Chan, E.K. and Tan, E.M. (2001) Aberrant expression of fetal RNA-binding protein p62 in liver cancer and liver cirrhosis. *Am J Pathol*, **159**, 945-953.

Matsuda, Y., Matsumoto, K., Yamada, A., Ichida, T., Asakura, H., Komoriya, Y., Nishiyama, E. and Nakamura, T. (1997) Preventive and therapeutic effects in rats of hepatocyte growth factor infusion on liver fibrosis/cirrhosis. *Hepatology*, **26**, 81-89.

Matsuzaka, T., Atsumi, A., Matsumori, R., Nie, T., Shinozaki, H., Suzuki-Kemuriyama, N., Kuba, M., Nakagawa, Y., Ishii, K., Shimada, M., Kobayashi, K., Yatoh, S., Takahashi, A., Takekoshi, K., Sone, H., Yahagi, N., Suzuki, H., Murata, S., Nakamuta, M., Yamada, N. and Shimano, H. (2012) Elovl6 promotes nonalcoholic steatohepatitis. *Hepatology*, **56**, 2199-2208.

Meister, G. (2013) Argonaute proteins: functional insights and emerging roles. *Nat Rev Genet*, **14**, 447-459.

Meng, F., Henson, R., Wehbe-Janek, H., Ghoshal, K., Jacob, S.T. and Patel, T. (2007) MicroRNA-21 regulates expression of the PTEN tumor suppressor gene in human hepatocellular cancer. *Gastroenterology*, **133**, 647-658.

Miyoshi, H., Moriya, K., Tsutsumi, T., Shinzawa, S., Fujie, H., Shintani, Y., Fujinaga, H., Goto, K., Todoroki, T., Suzuki, T., Miyamura, T., Matsuura, Y., Yotsuyanagi, H. and Koike, K. (2011) Pathogenesis of lipid metabolism disorder in hepatitis C: polyunsaturated fatty acids counteract lipid alterations induced by the core protein. *J Hepatol*, **54**, 432-438.

Montagut, C. and Settleman, J. (2009) Targeting the RAF-MEK-ERK pathway in cancer therapy. *Cancer Lett*, **283**, 125-134.

Moriya, K., Todoroki, T., Tsutsumi, T., Fujie, H., Shintani, Y., Miyoshi, H., Ishibashi, K., Takayama, T., Makuuchi, M., Watanabe, K., Miyamura, T., Kimura, S. and Koike, K. (2001) Increase in the concentration of carbon 18 monounsaturated fatty acids in the liver with hepatitis C: analysis in transgenic mice and humans. *Biochem Biophys Res Commun*, **281**, 1207-1212.

Muir, K., Hazim, A., He, Y., Peyressatre, M., Kim, D.Y., Song, X. and Beretta, L. (2013) Proteomic and lipidomic signatures of lipid metabolism in NASH-associated hepatocellular carcinoma. *Cancer Res*, **73**, 4722-4731.

Nagrath, D. and Soto-Gutierrez, A. (2014) Reply to: "Is the pathway of energy metabolism modified in advanced cirrhosis?" *J Hepatol*, in press, doi: 10.1016/j.jhep.2014.04.040.

Nascimento, A.C., Maia, D.R., Neto, S.M., Lima, E.M., Twycross, M., Baquette, R.F. and Lobato, C.M. (2012) Nonalcoholic Fatty liver disease in chronic hepatitis B and C patients from Western Amazon. *Int J Hepatol*, **2012**, 695950.

Neuschwander-Tetri, B.A. and Caldwell, S.H. (2003) Nonalcoholic steatohepatitis: summary of an AASLD Single Topic Conference. *Hepatology*, **37**, 1202-1219.

Niba, E.T., Nagaya, H., Kanno, T., Tsuchiya, A., Gotoh, A., Tabata, C., Kuribayashi, K., Nakano, T. and Nishizaki, T. (2013) Crosstalk between PI3 kinase/PDK1/Akt/Rac1 and Ras/Raf/MEK/ERK pathways downstream PDGF receptor. *Cell Physiol Biochem*, **31**, 905-913.

Nielsen, F.C., Nielsen, J. and Christiansen, J. (2001) A family of IGF-II mRNA binding proteins (IMP) involved in RNA trafficking. *Scand J Clin Lab Invest Suppl*, **234**, 93-99.

Nielsen, J., Christiansen, J., Lykke-Andersen, J., Johnsen, A.H., Wewer, U.M. and Nielsen, F.C. (1999) A family of insulin-like growth factor II mRNA-binding proteins represses translation in late development. *Mol Cell Biol*, **19**, 1262-1270.

Nishikawa, T., Bellance, N., Damm, A., Bing, H., Zhu, Z., Handa, K., Yovchev, M.I., Sehgal, V., Moss, T.J., Oertel, M., Ram, P.T., Pipinos, II, Soto-Gutierrez, A., Fox, I.J. and Nagrath, D. (2014) A switch in the source of ATP production and a loss in capacity to perform glycolysis are hallmarks of hepatocyte failure in advance liver disease. *J Hepatol*, in press, doi: 10.1016/j.jhep.2014.02.014.

Oertel, M., Menthena, A., Chen, Y.Q., Teisner, B., Jensen, C.H. and Shafritz, D.A. (2008) Purification of fetal liver stem/progenitor cells containing all the repopulation potential for normal adult rat liver. *Gastroenterology*, **134**, 823-832.

Ohlsson, R., Cui, H., He, L., Pfeifer, S., Malmikumpu, H., Jiang, S., Feinberg, A.P. and Hedborg, F. (1999) Mosaic allelic insulin-like growth factor 2 expression patterns reveal a link between Wilms' tumorigenesis and epigenetic heterogeneity. *Cancer Res*, **59**, 3889-3892.

Postic, C. and Girard, J. (2008) Contribution of de novo fatty acid synthesis to hepatic steatosis and insulin resistance: lessons from genetically engineered mice. *J Clin Invest*, **118**, 829-838.

Puri, P., Baillie, R.A., Wiest, M.M., Mirshahi, F., Choudhury, J., Cheung, O., Sargeant, C., Contos, M.J. and Sanyal, A.J. (2007) A lipidomic analysis of nonalcoholic fatty liver disease. *Hepatology*, **46**, 1081-1090.

Puri, P., Wiest, M.M., Cheung, O., Mirshahi, F., Sargeant, C., Min, H.K., Contos, M.J., Sterling, R.K., Fuchs, M., Zhou, H., Watkins, S.M. and Sanyal, A.J. (2009) The plasma lipidomic signature of nonalcoholic steatohepatitis. *Hepatology*, **50**, 1827-1838.

Qian, H.L., Peng, X.X., Chen, S.H., Ye, H.M. and Qiu, J.H. (2005) p62 Expression in primary carcinomas of the digestive system. *World J Gastroenterol*, **11**, 1788-1792.

Ratziu, V., Bellentani, S., Cortez-Pinto, H., Day, C. and Marchesini, G. (2010) A position statement on NAFLD/NASH based on the EASL 2009 special conference. *J Hepatol*, **53**, 372-384.

Ray, K. (2013) NAFLD-the next global epidemic. *Nat Rev Gastroenterol Hepatol*, **10**, 621.

Reddy, J.K. (2001) Nonalcoholic steatosis and steatohepatitis. III. Peroxisomal beta-oxidation, PPAR alpha, and steatohepatitis. *Am J Physiol Gastrointest Liver Physiol*, **281**, G1333-1339.

Reddy, J.K. and Rao, M.S. (2006) Lipid metabolism and liver inflammation. II. Fatty liver disease and fatty acid oxidation. *Am J Physiol Gastrointest Liver Physiol*, **290**, G852-858.

Roderburg, C., Urban, G.W., Bettermann, K., Vucur, M., Zimmermann, H., Schmidt, S., Janssen, J., Koppe, C., Knolle, P., Castoldi, M., Tacke, F., Trautwein, C. and Luedde, T. (2011) Micro-RNA profiling reveals a role for miR-29 in human and murine liver fibrosis. *Hepatology*, **53**, 209-218.

Sakatani, T., Kaneda, A., Iacobuzio-Donahue, C.A., Carter, M.G., de Boom Witzel, S., Okano, H., Ko, M.S., Ohlsson, R., Longo, D.L. and Feinberg, A.P. (2005) Loss of imprinting of Igf2 alters intestinal maturation and tumorigenesis in mice. *Science*, **307**, 1976-1978.

Schattenberg, J.M. and Schuppan, D. (2011) Nonalcoholic steatohepatitis: the therapeutic challenge of a global epidemic. *Curr Opin Lipidol*, **22**, 479-488.

Schmidt, J.V., Matteson, P.G., Jones, B.K., Guan, X.J. and Tilghman, S.M. (2000) The Dlk1 and Gtl2 genes are linked and reciprocally imprinted. *Genes Dev*, **14**, 1997-2002.

Schmitz, K.J., Helwig, J., Bertram, S., Sheu, S.Y., Suttorp, A.C., Seggewiss, J., Willscher, E., Walz, M.K., Worm, K. and Schmid, K.W. (2011) Differential expression of microRNA-675, microRNA-139-3p and microRNA-335 in benign and malignant adrenocortical tumours. *J Clin Pathol*, **64**, 529-535.

Schmitz, K.J., Wohlschlaeger, J., Lang, H., Sotiropoulos, G.C., Malago, M., Steveling, K., Reis, H., Cicinnati, V.R., Schmid, K.W. and Baba, H.A. (2008) Activation of the ERK and AKT signalling pathway predicts poor prognosis in hepatocellular carcinoma and ERK activation in cancer tissue is associated with hepatitis C virus infection. *J Hepatol*, **48**, 83-90.

Schnelzer, A., Prechtel, D., Knaus, U., Dehne, K., Gerhard, M., Graeff, H., Harbeck, N., Schmitt, M. and Lengyel, E. (2000) Rac1 in human breast cancer: overexpression, mutation analysis, and characterization of a new isoform, Rac1b. *Oncogene*, **19**, 3013-3020.

Shen, J., Wang, A., Wang, Q., Gurvich, I., Siegel, A.B., Remotti, H. and Santella, R.M. (2013) Exploration of genome-wide circulating microRNA in hepatocellular carcinoma: MiR-483-5p as a potential biomarker. *Cancer Epidemiol Biomarkers Prev*, **22**, 2364-2373.

Sherman, M. (2010) Serological surveillance for hepatocellular carcinoma: time to quit. *J Hepatol*, **52**, 614-615.

Shimada, M., Hashimoto, E., Taniai, M., Hasegawa, K., Okuda, H., Hayashi, N., Takasaki, K. and Ludwig, J. (2002) Hepatocellular carcinoma in patients with non-alcoholic steatohepatitis. *J Hepatol*, **37**, 154-160.

Simon, Y., Kessler, S.M., Bohle, R.M., Haybaeck, J. and Kiemer, A.K. (2014a) The insulin-like growth factor 2 (IGF2) mRNA-binding protein p62/IGF2BP2-2 as a promoter of NAFLD and HCC? *Gut*, **63**, 861-863.

Simon, Y., Kessler, S.M., Gemperlein, K., Bohle, R.M., Mueller, R., Haybaeck, J. and Kiemer, A.K. (2014b) Elevated free cholesterol as a hallmark of NASH in p62/IGF2BP2-2 transgenic animals. *World J Gastroenterol*, in press.

Tanimizu, N., Nishikawa, M., Saito, H., Tsujimura, T. and Miyajima, A. (2003) Isolation of hepatoblasts based on the expression of Dlk/Pref-1. *J Cell Sci*, **116**, 1775-1786.

Targher, G., Bertolini, L., Padovani, R., Rodella, S., Tessari, R., Zenari, L., Day, C. and Arcaro, G. (2007) Prevalence of nonalcoholic fatty liver disease and its association with cardiovascular disease among type 2 diabetic patients. *Diabetes Care*, **30**, 1212-1218.

Thompson, N. and Lyons, J. (2005) Recent progress in targeting the Raf/MEK/ERK pathway with inhibitors in cancer drug discovery. *Curr Opin Pharmacol*, **5**, 350-356.

Tybl, E., Shi, F.D., Kessler, S.M., Tierling, S., Walter, J., Bohle, R.M., Wieland, S., Zhang, J., Tan, E.M. and Kiemer, A.K. (2011) Overexpression of the IGF2-mRNA binding protein p62 in transgenic mice induces a steatotic phenotype. *J Hepatol*, **54**, 994-1001.

Underwood Ground, K.E. (1984) Prevalence of fatty liver in healthy male adults accidentally killed. *Aviat Space Environ Med*, **55**, 59-61.

Vuppalanchi, R., Gould, R.J., Wilson, L.A., Unalp-Arida, A., Cummings, O.W., Chalasani, N. and Kowdley, K.V. (2012) Clinical significance of serum autoantibodies in patients with NAFLD: results from the nonalcoholic steatohepatitis clinical research network. *Hepatol Int*, **6**, 1, 379-385.

Walch, A., Seidl, S., Hermannstadter, C., Rauser, S., Deplazes, J., Langer, R., von Weyhern, C.H., Sarbia, M., Busch, R., Feith, M., Gillen, S., Hofler, H. and Luber, B. (2008) Combined analysis of Rac1, IQGAP1, Tiam1 and E-cadherin expression in gastric cancer. *Mod Pathol*, **21**, 544-552.

Wang, H., Hou, L., Li, A., Duan, Y., Gao, H. and Song, X. (2014) Expression of serum exosomal microRNA-21 in human hepatocellular carcinoma. *BioMed Research International*, **2014**, 864894.

Wang, X.W., Heegaard, N.H. and Orum, H. (2012) MicroRNAs in liver disease. *Gastroenterology*, **142**, 1431-1443.

Wang, Y., Kim, K.A., Kim, J.H. and Sul, H.S. (2006) Pref-1, a preadipocyte secreted factor that inhibits adipogenesis. *J Nutr*, **136**, 2953-2956.

Wang, Y., Zhao, L., Smas, C. and Sul, H.S. (2010) Pref-1 interacts with fibronectin to inhibit adipocyte differentiation. *Mol Cell Biol*, **30**, 3480-3492.

Wong, V.W., Wong, G.L., Tsang, S.W., Hui, A.Y., Chan, A.W., Choi, P.C., Chim, A.M., Chu, S., Chan, F.K., Sung, J.J. and Chan, H.L. (2009) Metabolic and histological features of non-alcoholic fatty liver disease patients with different serum alanine aminotransferase levels. *Aliment Pharmacol Ther*, **29**, 387-396.

Xu, J., Wu, C., Che, X., Wang, L., Yu, D., Zhang, T., Huang, L., Li, H., Tan, W., Wang, C. and Lin, D. (2011) Circulating microRNAs, miR-21, miR-122, and miR-223, in patients with hepatocellular carcinoma or chronic hepatitis. *Mol Carcinog*, **50**, 136-142.

Xu, L., Beckebaum, S., Iacob, S., Wu, G., Kaiser, G.M., Radtke, A., Liu, C., Kabar, I., Schmidt, H.H., Zhang, X., Lu, M. and Cicinnati, V.R. (2014) MicroRNA-101 inhibits human hepatocellular carcinoma progression through EZH2 downregulation and increased cytostatic drug sensitivity. *Journal of Hepatology*, **60**, 590.

Yahagi, N., Shimano, H., Hasty, A.H., Matsuzaka, T., Ide, T., Yoshikawa, T., Amemiya-Kudo, M., Tomita, S., Okazaki, H., Tamura, Y., Iizuka, Y., Ohashi, K., Osuga, J., Harada, K., Gotoda, T., Nagai, R., Ishibashi, S. and Yamada, N. (2002) Absence of sterol regulatory element-binding protein-1 (SREBP-1) ameliorates fatty livers but not obesity or insulin resistance in Lep(ob)/Lep(ob) mice. *J Biol Chem*, **277**, 19353-19357.

Yanai, H., Nakamura, K., Hijioka, S., Kamei, A., Ikari, T., Ishikawa, Y., Shinozaki, E., Mizunuma, N., Hatake, K. and Miyajima, A. (2010) Dlk-1, a cell surface antigen on

foetal hepatic stem/progenitor cells, is expressed in hepatocellular, colon, pancreas and breast carcinomas at a high frequency. *J Biochem*, **148**, 85-92.

Yang, W., Lv, S., Liu, X., Liu, H., Yang, W. and Hu, F. (2010) Up-regulation of Tiam1 and Rac1 correlates with poor prognosis in hepatocellular carcinoma. *Jpn J Clin Oncol*, **40**, 1053-1059.

Zhang, J.Y., Chan, E.K., Peng, X.X. and Tan, E.M. (1999) A novel cytoplasmic protein with RNA-binding motifs is an autoantigen in human hepatocellular carcinoma. *J Exp Med*, **189**, 1101-1110.

Zhang, Y., Cheng, X., Lu, Z., Wang, J., Chen, H., Fan, W., Gao, X. and Lu, D. (2013) Upregulation of miR-15b in NAFLD models and in the serum of patients with fatty liver disease. *Diabetes Res Clin Pract*, **99**, 327-334.

7 List of publications

Original publications

Laggai, S., Kessler, S.M., Boettcher, S., Lebrun, V., Gemperlein, K., Lederer, E., Leclercq, I.A., Mueller, R., Hartmann, R.W., Haybaeck, J., and Kiemer, A.K. (2014) The *IGF2* mRNA binding protein p62/IGF2BP2-2 induces fatty acid elongation as a critical feature of steatosis. *J Lipid Res*, **55**, 1087-1097.

Kessler, S.M., **Laggai, S.**, Barghash, A., Helms, V., and Kiemer A.K. (2014) Lipid Metabolism Signatures in NASH-Associated HCC-Letter. *Cancer Res*, **74**, 2903-2904.

Laggai, S., Simon, Y., Ranssweiler, T., Kiemer A.K., and Kessler, S.M. (2013) Rapid chromatographic method to decipher distinct alterations in lipid classes in NAFLD/NASH. *World J Hepatol*, **5**, 558-567.

Kessler, S.M., Pokorny, J., Zimmer, V., **Laggai, S.**, Lammert, F., Bohle, R.M., and Kiemer, A.K. (2013) *IGF2* mRNA binding protein p62/IMP2-2 in hepatocellular carcinoma: antiapoptotic action is independent of IGF2/PI3K signaling. *Am J Physiol Gastrointest Liver Physiol* **304**, G328-G336.

Abstracts to short talks / poster presentations

Laggai, S. and Kiemer, A.K. (2014) The *IGF2* mRNA binding protein p62/IGF2BP2-2 induces fatty acid elongation as a critical feature of p62-induced steatosis. International PhD students meeting 2014 of the German Pharmaceutical Society (DPhG).

Laggai, S., Kessler, S.M., Gemperlein, K., Haybaeck, J., Mueller, R., and Kiemer, A.K. (2013) 1270 Altered fatty acid profile in livers overexpressing the *IGF2* mRNA binding protein p62: induction of fatty acid elongase ELOVL6 *via* IGF2-dependant SREBP1 activation. *Journal of Hepatology* **58**, S514. **Top 10% best abstracts.** EASL Young Investigator's Full Bursary for the International Liver Congress™ 2013, in Amsterdam, The Netherlands, April 24-28, 2013 offered by BMS, Gilead, MSD, and Roche

Laggai, S. and Kiemer, A.K. (2012) Regulation des Tumorsuppressors PTEN durch das *IGF2* mRNA bindende Protein p62. Kolloquiumsband der Graduiertenförderung der Hochschulen des Saarlandes: 1. und 2. Gesamtkolloquium der Graduiertenförderung am 14.10.2011 und 12.10.2012. *In*. Universitäts- und Landesbibliothek, Saarbrücken. *http://scidok.sulb.uni-saarland.de/volltexte/2014/5624/pdf/Kolloquiumsband_GraduiertenfArderung_2013.pdf*

Other publications

Kessler, S.M., Simon, Y., **Laggai, S.**, and Kiemer A.K. (2013) Erst schwillt sie, dann schrumpft sie-die Rolle von p62 in Lebererkrankungen. *Magazin Forschung*. *http://www.uni-saarland.de/fileadmin/user_upload/Campus/Forschung/forschungsmagazin/*

8 Acknowledgements

An erster Stelle möchte ich Frau Prof. Dr. Alexandra K. Kiemer danken. Sie gab mir die Möglichkeit mit einer Diplomarbeit in Ihrem Arbeitskreis zu beginnen und letztendlich mit einer höchst interessanten und anspruchsvollen Dissertation abzuschließen. Insbesondere möchte ich mich für Ihr Interesse, Ihr außergewöhnliches Engagement und das mir entgegengebrachte Vertrauen bedanken. Besonders in schweren Zeiten (bei plötzlich nicht mehr funktionierenden Kernisolierungen, p62 Überexpressionen oder bei den vielzähligen Stipendien-Anträgen und Veröffentlichungen) konnte ich immer, auch sehr kurzfristig, auf Sie zählen. Ohne die vielen interessanten Diskussion und die daraus resultierenden Ideen und Lösungen wäre meine Dissertation in dieser Form nicht möglich gewesen. Ich bedauere es sehr Ihre Gruppe zu verlassen und hoffe auf eine Tätigkeit in einem ähnlich angenehmen Arbeitsumfeld.

Weiterhin möchte ich mich bei Herrn Prof. Dr. Rolf Müller für die freundliche Übernahme des Zweitgutachtens und die verschiedenen Kooperationen mit seiner Arbeitsgruppe bedanken.

Herrn Prof. Dr. Christian Ducho möchte ich für die freundliche Übernahme des Prüfungsvorsitzes danken.

Herrn Dr. Stefan Boettcher gilt gleich zweifacher Dank. Zum einen für die Teilnahme als wissenschaftlicher Mitarbeiter in der Prüfungskommision und zum anderen für die unermüdliche Arbeit an der Optimimierung und Quantifizierung der Acyl-CoA Derivate.

Frau Dr. Sonja M. Kessler möchte ich als Betreuerin sowohl im Diplom als auch in der Promotion für Ihre Einführungen in fast alle praktischen Tätigkeiten, Ihre unermüdliche Geduld, Ihren Rat, die vielen Korrekturen und die tolle und früchtetragende Zusammenarbeit danken. Da wir die letzten 4 Jahre gemeinsam in unserem Labor so viel erlebt haben, werde ich sie sehr vermissen und hoffe dass sie einen adäquaten und ähnlich angenehmen Ersatz-Laborpartner findet.

Vielen Dank auch an Frau Dr. Jessica Hoppstädter und Susanne Schütz für die vielen anregenden Diskussionen und schönen Nachmittage/Abende in den gastronomischen Betrieben der UDS.

Ich möchte auch Frau Rebecca Hahn und Frau Dr. Yvette Simon für die schöne gemeinsame Zeit seit Beginn unseres Pharmaziestudiums danken.

Danke auch an die gesamte Arbeitsgruppe von Frau Prof. Dr. Kiemer. Durch Euch entsteht ein super Arbeitsklima und ich hatte eine sehr schöne Zeit. Vielen Dank Astrid Decker, Klaus Gladel, Dr. Britta Diesel, Theo Ranssweiler, Peter Schneider, Dr. Josef Zapp, Nina Hachenthal, Christina Schultheiß, Dr. Ksenia Astanina, Beate Czepukojc und Anna Dembek für die schöne gemeinsame Zeit, Eure Unterstützung und Hilfe.

Leider kann ich nicht jeden namentlich erwähnen, aber ich möchte mich bei allen die mich direkt oder indirekt bei den Publikationen und der Dissertation unterstützt haben, herzlich bedanken.

In diesem Sinne möchte ich mich auch bei der Graduiertenförderung der UDS bedanken, die meine Arbeit durch ein Promotionsstipendium über 3 Jahre gefördert hat und durch das jährlich stattfindende Gesamtkolloquium auch interessante Einblicke in die Arbeit anderer Doktoranden bietet.

Ganz besonderer Dank gilt meinen Eltern und meiner Großmutter, die immer hinter mir stehen, mich zu dem gemacht haben, was ich heute bin und ohne die weder mein Studium noch meine Abschlüsse erreichbar gewesen wären. An dieser Stelle möchte ich auch meiner Freundin Doreen Voetchen, „meinem Lebensmittelpunkt“, für ihre Unterstützung, Zerstreuungsversuche, ihre Energie und Liebe danken.